

University of Nottingham
UK | CHINA | MALAYSIA

The Development of a Low Carbon Prefabricated House

Zhang, Shihao

(BArch)

Thesis submitted to

The University of Nottingham

for the degree of Doctor of Philosophy

Nov 2021

Table of contents

Table of contents ii

Acknowledgement vi

Abstract viii

List of figures xi

List of tables xvi

List of acronyms xix

Nomenclature xxii

1. Introduction 1

1.1. Problem statement 1

1.2. Research aims 1

1.3. Contribution to knowledge 2

1.4. Research structure 4

2. Reviews on sustainable building and prefabricated sustainable technologies 6

2.1. Climate change 6

2.2. Demands for innovation in the building components.....7

2.3. The legislative context.....9

2.4. Sustainable and prefabricated buildings..... 13

2.5. Energy consumption patterns in building 19

2.6. Post construction assessment 26

2.7. Reviews of the prefabricated sustainable technology 31

2.8. Conclusion..... 56

3. Performance investigation of a novel heat recovery ventilator unit... 57

3.1. Introduction..... 57

3.2. Prototype description 58

3.3. Experimental rigs..... 62

3.4. Sound level measurements..... 63

3.5. Data acquisition 65

3.6. Experimental procedure and equation..... 68

3.7. Test results and performance analysis..... 69

3.8. Conclusion..... 72

4. The investigations on innovative photovoltaic vacuum glazing for building applications..... 73

4.1. Background..... 73

4.2. The design and system description..... 74

4.3. Using hot-box method for investigation of the PV VG-4L thermal performance..... 75

4.4. The studies of the performance of PV VG-4L under real conditions 81

4.5. The impact of solar transmittance of PV VG-4L..... 85

4.6. Conclusion..... 86

5. Theoretical analysis and evaluation of the Eco-house in Wuhan..... 88

5.1. Introduction..... 88

5.2. The requirements of the low-carbon building..... 89

5.3. The development process for the Eco-house in Wuhan..... 91

5.4. Testing the overall performance of the Eco-house..... 116

5.5. Computer simulation of the Eco-house..... 140

5.6. The construction experience of Eco-house in Wuhan..... 153

5.7. Limitations..... 154

5.8. Conclusion 155

6. Conclusions and future work 157

6.1. Conclusions 157

6.2. Future work 159

REFERENCES 161

APPENDIX 176

Acknowledgement

I would like to acknowledge the support from all the academic professionals who shared their intelligence and experience throughout my research. I could not manage all the research tasks without so many intelligent and experienced people. I would like to express my most heartfelt appreciation to

- My first supervisor, Professor Saffa Riffat, for his patience, motivation, and immense knowledge not only on my research and also on my life.
- My second supervisor, Dr Guohui Gan, for providing me with a lot of suggestions on my research.
- My internal assessor is Dr. Yuehong Su, for providing me with a lot of suggestions on my research.
- Zeny Amante-Roberts and Celia Berry, who helped me a lot during my research.
- Dr Hasila Jamiri and Dr Yate Ding, who guided me, giving me academic and moral support and continuous help in my thesis and more.
- The staff of the Department of the Built Environment, especially Tony Gospel, Andy Matthews, Daniel Cooper, and all the technical team.
- The wonderful friends from Nottingham, who shared their experiences with me and especially to Weihan Zhao, Yanan Zhang, Yixin Wang and Li Zhang for the constant supports to me.
- My friends in China, including Yongjie He, Jiawei Zhou, Jingbo Zhu, and many more friends who encouraged me even from far away, especially

for Hualiang Zhang, my best friend, who was there every step of my life with great support.

- Wei Zu, who believed in me long before I believed in myself and helped me all my life. I could not have imagined having a better advisor and mentor.
- My great parents, Junmou Zhang and Lixia Shi, parents in law, Fuchun Xu and Wenling Jiang, for their support, instructions, and wisdom.
- My wife, Qi Xu, accompany me all along the PhD research career. I am very grateful for the offering to me.

Abstract

Nowadays, due to the construction of new buildings, global warming becomes more serious every day. Thus, global governments are taking keen interests in the ways to reduce the building-related greenhouse gas (GHG) emissions. Considering the life cycle of a building, it consumes a vast quantity of energy, water, materials for construction, maintenance, and demolition effort. Improving building energy performance has great potential to meet the requirements above.

Through several years' study, the researcher has found that the prefabricated low carbon building would be the next revolution for building construction. The primary intention of the research is to investigate the applicability of prefabricated building technology and energy performance in the Eco-house of Wuhan. Laboratory testing for the prefabricated low-carbon building technologies including heat recovery ventilator and photovoltaic vacuum glazing were conducted. The heat recovery ventilator would be applied to the Eco-house.

In addition, the Eco-house provided an understanding of the exercise experience in China. Measurements such as airtightness tests, co-heating tests, thermographic images, and long-term monitoring were used to gain building performance data on the Eco-house. The data and experience gained from the project were combined to evaluate benefits of a low-carbon house in China.

PUBLICATIONS TO DATE

Shihao Zhang, Yate Ding, Saffa Riffat, 2017, A Review on Biomimicry Research for Low-carbon Building, The International Conference on Sustainable Energy Technologies 2017, BOLOGNA, Italy.

Shihao Zhang, Yate Ding, Saffa Riffat, 2017, Using Life Cycle Assessment to Analyse the Building Greenhouse Gas Reduction Policy, The International Conference on Sustainable Energy Technologies 2017, BOLOGNA, Italy.

Shihao Zhang, Yate Ding, Saffa Riffat, 2018, Reviews on Previous Work of Prefabricated Low Carbon Houses in the UK, The International Conference on Sustainable Energy Technologies 2018, WUHAN, China.

Shihao Zhang, Qi Xu, Saffa Riffat, 2018, Review on Prefabricated Low Carbon Technologies in Eco-house, The International Conference on Sustainable Energy Technologies 2018, WUHAN, China.

Shihao Zhang, Qi Xu, Saffa Riffat, 2019, Passive Design Method for Sustainable House, The International Conference on Sustainable Energy Technologies 2019, Kuala Lumpur, Malaysia.

Shihao Zhang, HASILA JAMIR, Qi Xu, Saffa Riffat, 2019, The Laboratory Testing for the Vacuum glazing, Double Glazing and Single Glazing, The International Conference on Sustainable Energy Technologies 2019, Kuala Lumpur, Malaysia.

Xu, Q., Riffat, S., & Zhang, S. (2019). Review of heat recovery technologies for building applications. Energies, 12(7), 1285.

List of figures

Figure 2.1 Energy consumption by final users in the UK (Department for Business, 2019) 21

Figure 2.2 The heat transfer approaches within dwelling 23

Figure 2.3 The contribution of heat loss for different approaches 25

Figure 2.4 Typical Air Leakage of the House 27

Figure 2.5 Air tightness testing process 29

Figure 2.6 Heat recovery ventilator system (Xu, Riffat and Zhang, 2019) 34

Figure 2.7 The arrangement of the three-heat exchanger (Baldini, Kim and Leibundgut, 2014) 39

Figure 2.8 The structure of VIPs 44

Figure 2.9 Window components showing glazing layers separated with spacers and sits 50

Figure 2.10 Schematic of a vacuum glazing 52

Figure 2.11 Comparison of U-value of triple vacuum glazing (Fang, Hyde and Hewitt, 2010) 55

Figure 3.1 Schematic of Novel WHRV system with Window Frame 58

Figure 3.2 The schematic of WHRV system 59

Figure 3.3 The photo of WHRV 61

Figure 3.4 Experimental Rigs 62

Figure 3.5 The schematic of testing rigs 66

Figure 3.6 The positions of 21 thermocouples 67

Figure 3.7 The temperature distribution while air velocity is 1.24 m/s 70

Figure 3.8 The temperature distribution while air velocity is 1.79 m/s 70

Figure 3.9 The temperature distribution while air velocity is 2.45 m/s 70

Figure 4.1 The photo of prototype 74

Figure 4.2 The schematic of PV VG-4L 75

Figure 4.3 The schematic of hot box 76

Figure 4.4 The schematic of the testing process on hot box 78

Figure 4.5 The measured temperatures 79

Figure 4.6 The hot box with the installed PV VG-4L 80

Figure 4.7 The photo of testing rigs 81

Figure 4.8 Variation in the outside glazing surface temperature (To-amb), inside glazing surface temperature (Tint), Outdoor ambient temperature (To-amb), indoor ambient temperature (Ti-amb) and solar irradiance (G) with time of the day. 83

Figure 4.9 The measured U-value of the prototype during night..... 84

Figure 4.10 The power generation (W, blue dots), the solar irradiance (W/m^2, orange dots)..... 85

Figure 5.1 The photo of Eco-house in Wuhan..... 88

Figure 5.2 The plans of the site 92

Figure 5.3 The screenshot of the 3D model in Revit..... 94

Figure 5.4 The layout of Eco-house..... 95

Figure 5.5 The photo of the prefabricated structure 96

Figure 5.6 The screenshot of PVGIS 98

Figure 5.7 The power generation of PV panel..... 99

Figure 5.8 The screenshot of setting on the exterior door in Revit 100

Figure 5.9 The photo of the WHRV system installed above the window frame 101

Figure 5.10 The schematic of the measurement on WHRV system in Wuhan 102

Figure 5.11 The schematic of summing thermal resistances..... 105

Figure 5.12 Summing thermal resistances on various glazing system 106

Figure 5.13 The photo of testing rigs 108

Figure 5.14 Schematic of Triple VG-Cavity 3L 110

Figure 5.15 The photo of the positions of thermocouples and heat flux sensor 111

Figure 5.16 The photo of VIP 113

Figure 5.17 The screenshot on the structure of SIPs in Revit 114

Figure 5.18 The photo of SIP 114

Figure 5.19 The photo of Co-heating testing rigs..... 122

Figure 5.20 The resulting of the Co-heating testing 124

Figure 5.21 The thermographic image photo of Eco-house from Front View 127

Figure 5.22 The thermographic image photo of exterior door..... 128

Figure 5.23 The thermographic image photo of window..... 129

Figure 5.24 Thermographic image of the junctions between the wall and floor 130

Figure 5.25 Thermographic image of the joint between wall and roof..... 130

Figure 5.26 The schematic of positions of sensors 132

Figure 5.27 The temperature distribution for April to mid of May 133

Figure 5.28 The temperature distribution for June..... 134

Figure 5.29 The temperature distribution of July.....135

Figure 5.30 The temperature distribution of August.....136

Figure 5.31 The temperature distribution of September.....137

Figure 5.32 The 3D model in Revit.....142

Figure 5.33 The zones of Eco-house in Revit.....143

Figure 5.34 The distribution of interior and exterior temperature.....146

Figure 5.35 The average fabric gains for various months at 0 am.....147

Figure 5.36 The average fabric gains for various months at 12 pm.....147

Figure 5.37 The heating loads for three cases.....149

Figure 5.38 The cooling loads for three cases.....149

Figure 5.39 The Lifecycle of building.....151

Figure 5.40 Carbon emission per square metre under various parameters.152

List of tables

Table 2.1 the climate target of various government 6

Table 2.2 The requirements on the thermal transmittance of building components on different standards 11

Table 2.3 The requirements on the thermal performance for various regions of China (Ministry of Housing and Urban-Rural Development in China, 2015) .. 12

Table 2.4 The research on the prefabricated building om environment impact 16

Table 2.5 The common passive strategies 17

Table 2.6 The common requirements on the airtightness of various building 28

Table 2.7 Recent achievement on the different types of heat recovery 35

Table 2.8 List of the common insulation materials..... 41

Table 2.9 the list of floor material..... 47

Table 2.10 Parameters for Passivhaus Standard certified glazing products.. 51

Table 2.11 Parameters for SPACIA-21 vacuum glazing..... 53

Table 3.1 The testing rigs on sound level measurements 63

Table 3.2 The information about the measurement tools 65

Table 3.3 The air velocity under different voltage supply 67

Table 3.4 The temperature difference under various air velocity 71

Table 3.5 The thermal effectiveness under air velocity..... 71

Table 4.1 Experimental results for the glazing surface temperature and U-value using the calibrated hot box..... 80

Table 4.2 Measured parameters and accuracy..... 82

Table 5.1 The requirements on the building components on various regulations 90

Table 5.2 The optimal angle (°) for the adjustable PV panel 97

Table 5.3 The summary on the effectiveness of WHRV system under various temperature gap 103

Table 5.4 The surface resistance values (MCRMA, 2006).....105

Table 5.5 The coefficient of thermal conductivity W/(mK) of unventilated air cavities (MCRMA, 2006) 106

Table 5.6 the U-value of the various glazing 109

Table 5.7 The measured U-value of SIP and VIP.....115

Table 5.8 The summary of device during airtightness testing.....119

Table 5.9 The temperature difference between inside and outside against daily energy consumption.....123

Table 5.10 Parameters for FLIR C2 Compact Thermal Imaging System 126

Table 5.11 The retrofit plan on Eco-house.....138

Table 5.12 Air conditioning energy saving level (National Energy Fundamentals and Management Standardization Technical Committee, 2010) 140

Table 5.13 The summary of the thermal parameters and structure of ‘refence house’.....141

Table 5.14 The summary of size for different zones 143

Table 5.15 The summary of the parameters for Eco-house and ‘reference house’.....144

Table 5.16 The expected daily energy consumption of appliances 145

Table 5.17 The annual space cooling/heating of three cases.....150

List of acronyms

A

A - Air Cavity

B

BIPV - Building-integrated Photovoltaics

C

CfSH - Code for Sustainable Homes

COVID -19-Coronavirus disease 2019

G

G - Glazing

GDP - Gross Domestic Product

GFP - Gas Filled Panel

GHG - Green House Gas

GWP - Global Warming Potential

H

HDD - Heating Degree Day

HLC - Heat Loss Coefficient

HVAC - Heating, Ventilation, and Air Conditioning

I

IAQ - Indoor Air Quality

L

LCA - Life Cycle Assessment

M

MMC - Modern Methods of Construction

MHRV - Mechanical Heat Recovery Ventilator System

P

PE - Primary Energy

PV VG-4L - Integrated Semi-transparent Thin-film PV Vacuum Glazing with Four Layers of Glass

PV - Photovoltaic

PWF - Present Worth Factor

V

V - Vacuum Cavity

VG - Vacuum Glazing

VIP - Vacuum Insulation Panel

VIPs - Vacuum Insulation Panels

W

WHRV - Window Heat Recovery Ventilator

Nomenclature

A

$A_{s/a}$ -The angle of the PV panel in spring and autumn, °

A_{su} -The angle of the PV panel in summer, °

A_w -The angle of the PV panel in winter, °

A_G -The total area of the individual glazing, °

C

$C_{A,exist}$ -Annual heating cost with existing U-value, £

$C_{A,impro}$ -Annual heating cost with improved U-value, £

C_f -Cost of fuel, £

C_{ins} -Cost of insulation material, £

G

$G_{internal}$ – The energy gains through occupancy body temperature, lighting, appliances, kWh

G_{solar} – The energy gain through solar irradiance, kWh

G_s -Solar irradiance, W/m^2

H

H – The heating gains for overall building, kWh

L

L_{trans} – The heat transfer through the building fabric via conduction, kWh

L_{vent} – The heat exchange through ventilation between inside and outside, by air leakage or fenestration, kWh

R

R_{se} -External surface resistance, K/W

R_{si} -Internal surface resistance, K/W

T

$T_{ambient}$ -Two points of thermocouples of ambient air, °C

T_{box} -Three points of thermocouples in the test insulated box, °C

T_{e1} -The temperature measured inside the glazing, °C

T_{e2} -The environmental temperature measured outside the glazing, °C

T_{ein} -Four points of thermocouples in the exhaust air inside the box, °C

T_{eout} -Four points of thermocouples in the exhaust air outside the box, °C

T_{i-amb} -Indoor ambient temperature, °C

T_{int} -Internal glazing surface temperature, °C

T_{o-amb} -Outdoor ambient temperature, °C

T_{sin} -Four locations of thermocouples in the supply air inside the box, °C

T_{sout} -Four points of thermocouples in the supply air outside the box, °C

U

U -Average heat loss, W/(m^{2}K)

Greek symbols

ε_s -The heat recovery effectiveness

η -Heating system efficiency

φ -The heat flux though the prototype, Watts

1. Introduction

1.1. Problem statement

The energy and material consumption by buildings accounts for about 40% of annual global consumption(Glass, Dainty and Gibb, 2008)(Zhao *et al.*, 2015). The efficiency of energy consumption becomes an key concern for the whole world (ZHANG, MO and CHENG, 2015). Additionally, it is a major cause of carbon emissions. Governments are making efforts to develop low-carbon building technologies (Zhao *et al.*, 2015). With the rising demands to achieve an environmentally friendly situation around the world, an increasing interest in the sustainability of buildings has been shown. In recent years, various low-carbon devices and technologies have been promoted to support the sustainable revolution in the global building industry, such as passive design strategies (Zhang, Platten and Shen, 2011) and low waste technologies (Zhang, Wu and Shen, 2012).

1.2. Research aims

This research intends to investigate the applicability of prefabricated building technology and energy performance in the Eco-house of Wuhan. Based on this, three key points have been identified below:

- Develop effective prefabricated low carbon technologies.
- Specific low-carbon design, construction, and operation of the Eco-house.
- On-site thermal performance of the Eco-house in Wuhan.

The thesis aims to explore the following contents:

- Identify and review the energy consumption patterns in the dwellings, and the investigation methods that could be used to assess the built house.
- Literature review on the technologies and devices which can be integrated into the building units, including fabrics, fenestrations, and heat recovery ventilation devices.
- Laboratory investigation on the prefabricated low-carbon building technologies including window heat recovery ventilator-WHRV device and photovoltaic vacuum glazing.
- Discuss the architectural design process of the Eco-house in Wuhan.
- Investigate the thermal performance of the Eco-house based on several on-site tests.
- Simulate the energy consumption of Eco-house.

1.3. Contribution to knowledge

This research promotes two prototypes of prefabricated technologies, including a window heat recovery ventilator unit and photovoltaic vacuum glazing. These prototypes were tested under laboratory conditions in the UK. Furthermore, the design of the Eco-house in Wuhan is described, with overall thermal measurements on components, airtightness, co-heating, thermographic images, long-term monitoring.

The novel window heat recovery ventilator-WHRV system can be integrated into the window frames of a building/room to provide a comfortable

environment. The prototype integrates heat pipe/heat exchanger to recover sensible heat loss and uses this heat to warm the incoming air. The effectiveness of prototype is about 43% to 59%. The WHRV system provides 100% fresh air to interior space and exhausts the stale air.

Vacuum glazing is a novel solution to reduce heat transfer through fenestration which would limit the amount of air particles within the middle gap. The proposed PV VG-4L does not only have much better thermal insulation performance than conventional glazing but also has the ability to generate direct current (DC) power. As the solar irradiance at about 500 W/m^2, the PV VG-4L can generate electricity at a level of 12 W/m^2. The results indicate that prototype can not only generate electricity but also has high insulation performance compared to a conventional single-film PV glazing.

Based on the cognition of the author, the Eco-house is the first attempt to utilize the Building Information Modelling (BIM) for budget low-carbon houses in Wuhan. The exercise of the Eco-house introduces not only a set of low-carbon technologies for China but also several practical experiences. A number of methods for investigating the performance of a low-carbon house are first applied in Wuhan. Ultimately, the Eco-house developed here can provide new insights into the Chinese low-carbon housing market. The practice above has value on both a research dataset and policy basis.

1.4. Research structure

The research was conducted in different steps and covered several tasks. The work contains six chapters, and a summary is described as following:

Chapter 1: Relevant information has been quoted to explain the present situation and background about the topic. The aims and structure of the thesis have also been illustrated.

Chapter 2: Literature reviews on the prefabricated low-carbon houses and low-carbon technologies are included. Relevant building energy consumption patterns and governmental targets are explained as well as the evaluation methods on the sustainable house, including airtightness test and co-heating test. Furthermore, the review also includes heat recovery ventilator system, insulation material as well as various glazing systems.

Chapter 3: This chapter presents the design and testing procedure of the novel window heat recovery ventilator (WHRV) under laboratory scale.

Chapter 4: Thermal performance of novel vacuum glazing is investigated. The design of the hot chamber in the University of Nottingham is covered as well as the assessment of the novel photovoltaic vacuum glazing is presented. Additionally, the testing procedure of PV VG-4L in hot chamber is presented.

Chapter 5: The passive design of the Eco-house in Wuhan is described, with an overview of the design details, components performance, material, and devices. A detailed evaluation of its thermal performance is presented. Data gained from several different tests (airtightness, co-heating, thermographic

images, long-term monitoring) is used to assess the post-construction quality. Furthermore, a detailed retrofit plan for the Eco-house, based on the flaws identified in the previous testing, is promoted to enhance the energy-saving performance of Eco-house in the future.

Chapter 6: Conclusions of the research are presented here. And future work on current research is stated, including further investigations on the Eco-house.

2. Reviews on sustainable building and prefabricated sustainable technologies

2.1. Climate change

With the increasing evidence that greenhouse gas (GHG) absorbs emitted radiant energy and causes the greenhouse effect, taking urgent measures to prevent greenhouse effect in the future has become crucial (Taleb and Sharples, 2011). To mitigate the impact, the United Nations Framework Convention on Climate Change (UNFCCC) has been published (Bodansky, 1993). And many governments have made the promise on reducing carbon emission (shown in Table 2.1).

Table 2.1 the climate target of various government

Area	Targets	Reference
European Union	The reduction of greenhouse gas emission in 2030 should account for at most 55% of 1990 levels.	(European Commission, 2020)
China	China will reduce its 2050 carbon emissions to a level that is 42% below the country's 2010 carbon emissions.	(Zhou *et al.*, 2019)
United Kingdom	UK will reduce its emissions by at least 68% by 2030, compared to 1990 levels.	(Business, 2020)
United States	US establishes GHG reduction targets below 2005 emissions levels of 28% by 2025 and 45% by 2030.	(Damassa, Ge and Fransen, 2014)

The building sector has an instrumental role in climate changes. The building-related industry has become the primary contributor to GHG emissions. In cities, there are thousands of buildings. They need to be constructed, maintained, and demolished, each of which consumes a vast amount of energy and materials during the life cycle. With the development of real estate in Asia and Mideast area, total GHG emissions would increase greatly in the next 40

years. As for China, the situation is more urgent. The growth rate of energy consumption in buildings is about 10% since the past decades(Chang *et al.*, 2014). In fact, Chinese people suffer from the High Emission Economy.

At the same time, the building construction industry enjoys great potential to reduce carbon emissions up to 1.35 billion tonnes of carbon emissions (Tzikopoulos, Karatza and Paravantis, 2005). Therefore, climate remediation is currently necessary for reducing power consumption and carbon emissions (Tzikopoulos, Karatza and Paravantis, 2005). To accomplish it, one of the practical ways is to develop the prefabricated building system and integrate as many as possible sustainable technologies into building units.

2.2. Demands for innovation in the building components

Shortage of affordable housing in China

Because of the policy of Economic Reform and Open Up in China in the last 40 years, China has become the 2nd largest economy after the USA. The Gross Domestic Product (GDP) has increased 8% every year. More than 850 million people in China have lifted themselves out of extreme poverty (Kinmond, 2019). Although China has made an impressive 'economic miracle', its market reforms have not finished like those in other developed countries. The rapid development in China also brought several challenges, such as an imbalanced economic status, ageing population and so on. The high house price is a concern of everyone in China and it is also one of the major social contradictions. The Chinese house price grew about 10% every year from 1999-2019 (Ren, Xiong and Yuan, 2012). In 2010, the house price is 25%

higher than in the previous year (Ahuja *et al.*, 2010). The high house price has caused several social issues. In Beijing, the average price of high-end apartments has reached over CNY 96,000 (about US$ 13,700) per square metre in 2019. The high house price in Chinese cities forces a large number of people to go back to rural areas for a living. Those well-educated people need more comfortable and modern houses rather than the conventional and outdated house, which provides opportunities for developing the low-carbon house in Chinese rural area.

The status of current building construction in Chinese rural areas

The Chinese building-related industry in rural area is very conservative, possibly due to the low labour and energy cost and insufficient innovation intentions. The high upfront cost is one of the most important issues facing investors. Under the current environment in Chinese rural area, it is difficult to convince people to inject extra investment on sustainable features to their house (Zuo and Zhao, 2014). (Paul and Taylor, 2008) states that the thermal comfort of novel sustainable buildings is not significantly different from that of conventional buildings which are equipped with heating, ventilation, and air conditioning systems. This idea is also the consensus of many people in China (Zuo and Zhao, 2014).

The traditional approaches of house design and construction is irrational without any reasonable analysis before construction. The design and construction are decided by the construction members. There is little contribution from specialist suppliers in design, structural analysis, cost

estimation and so on which leads to rough construction with extra energy costs and conflicts in the future (Wang *et al.*, 2019). Modern construction methods such as prefabricated components, are widely used in urban areas. The traditional methods, such as brick walls, are still widely used in Chinese rural areas. However, with the development of the Chinese economy, side effects of development have appeared. The rising labour cost and energy shortage are forcing the building-related industry away from conventional methods and closer to modern approaches, prefabricated construction.

2.3. The legislative context

After several energy crises in recent decades, the global governments have promoted comprehensive legal systems for energy saving. The building regulations limiting the energy using are most complex.

The passivhaus standard

The Passivhaus Standard, also named as Passivhaus Standard, promoted by Germany refers to a construction requirement for domestic building. A passive house is regarded as an energy-saving and comfortable house. The passive house can maintain a comfortable temperature during winter and achieve a cool temperature with little energy consumption in summer (Feist, 2009). The Passivhaus Standard includes three key specifications, including limits on heating and cooling loads, a comfortable thermal environment, and a series passive device or system. In other words, the passive house should include good insulation, minimized thermal bridges and air infiltration, an efficient heat recovery system and well-insulated building components.

(Feist, 2007) states the current Passivhaus standards below,

- The average annual heating or cooling loads for one square metre should be less than 15 kWh.
- The Renewable Primary Energy Demand for all appliances including heating, household electricity, should be less than 60 kWh
- The air leakage of the passive house should not exceed 0.6 ACH@50 Pa
- The interior room temperature should be maintained at more than 20°C

Code for sustainable homes

The Code for Sustainable Homes (CfSH) was promoted in England in 2007 as a compulsory national regulation to reduce the energy consumption of dwellings. Before the CfSH, the environmental rating scheme for buildings in the UK was the EcoHome rating. It was replaced by the CfSH in 2008. The CfSH is a standard to evaluate the thermal performance of a building throughout its life. Its objective is to provide general information on the overall thermal performance of buildings and a measure for comparison between various houses. Currently, all new-built house in the UK should satisfy the requirement of the Code 6 on zero carbon emission. Code 6 means that not just the combination of traditional passive solar energy devices but also a reduction in the heating requirement of interior rooms.

(Department for Communities and Local Government, 2010) clearly listed all the requirements on different codes as well as the Passivhaus Standards, as in Table 2.2 below.

Table 2.2 The requirements on the thermal transmittance of building components on different standards

	Code 1	Code 2	Code 3	Code 4	Code 5	Code 6	Passive House
External Wall W/(m^2· K)	0.30	0.30-0.26	0.26	0.20	<0.1	<0.1	0.15-0.1
Floor W/(m^2· K)	0.22	0.22-0.19	0.19	0.14	<0.1	<0.1	0.15-0.1
Window W/(m^2· K)	2.0	2.0-1.6	1.6	1.2	<0.8	<0.8	0.8
Roof W/(m^2· K)	0.22	0.22-0.19	0.19	0.14	<0.1	<0.1	0.15-0.1
Airtightness M^3/(h· m^2) @ 50Pa	<3.0	<3.0	<3.0	<1.0	<1.0	<1.0	0.6/h @50Pa

From Table 2.2, the overall requirements of CfSH Code 6 on building fabric are higher than the Passivhaus Standard. The Passivhaus Standard is born for central Europe, especially Germany.

Chinese Legislation

In 2015, the Ministry of Housing and Urban-Rural Development promoted the 'Technical Guidelines for Passive Ultra-low Energy Green Buildings (Trial)' (Ministry of Housing and Urban-Rural Development in China, 2015). The regulation defines the ultra-low energy consumption house with the following characteristics:

- Well insulated building fabric
- Well insulated glazing system
- High airtightness

- Efficient heat recovery ventilator system
- Make full use of renewable energy

Table 2.3 presents the technical requirements on the thermal performance for ultra-low energy consumption houses in China.

Table 2.3 The requirements on the thermal performance for various regions of China (Ministry of Housing and Urban-Rural Development in China, 2015)

Regions	**Unit**	**Ultra-cold**	**Cold**	**Hot Summers, Cold Winter**	**Hot Summer, Warm Winter**	**Mild**
Building Fabric	W/(m^2·K)	0.10-0.20	0.10-0.25	0.20-0.35	0.25-0.40	
Windows	W/(m^2·K)	0.70-1.20	0.80-1.50	1.0-2.0	1.0-2.0	≤2.0
Heating Load	kWh/m^2	≤18	≤15		≤5	
Air Tightness	N_{50}		≤ 0.6/h			

Compared with the conventional house in China, the ultra-low energy consumption house has several advantages, listed below:

- More energy saving. The demand for heating and cooling loads of buildings throughout the year is significantly reduced, up to 90%.
- More comfortable. The indoor temperature and humidity of the building are more suitable for occupants.
- Better air quality. The heat recovery ventilator system provides enough fresh air in the room.
- Higher quality assurance. High-quality building components make the building quality higher and give a longer life.

2.4. Sustainable and prefabricated buildings

Because of long-term efforts, the stakeholders of buildings seek to introduce intelligent technologies into the built environment. The passive design applied by architects responds to climate conditions and requirement (Ahmad, Thaheem and Anwar, 2016). The stakeholders aim to reduce energy consumption and meet the requests from regulations promoted by governments.

Low-carbon house or eco-house are terms used to describe such houses by architects and engineers. Prefabricated houses use specific choices to mitigate the impacts from buildings on the natural environment. Compared with conventional houses, a prefabricated house has better energy and thermal performance (Energy and Sources, 2009). Compared with the conventional cast-on-site technology, prefabrication technology reveals a series of potentials in Environment Impact-EI (Cao *et al.*, 2014). The prefabricated components with high thermal performance are utilized in these houses (Energy and Sources, 2009). Furthermore, because of the massive production runs, the price of the prefabricated unit would be lower than the cast-on-site building. It would be more popular in the future.

Prefabricated building

The conventional method of building a house is to transport bricks, concrete, or other raw material to the site. Then, build the house on site using these materials. The process from raw material to building components are all finished on site. A prefabricated building, in which most of the building

components were produced in a certain place and transported to the construction site, and finally, assembled together, has become popular around the world (Zhang, Skitmore and Peng, 2014). Compared with the traditional construction method, this approach is very different from a lot of field construction, for instance, the raw processed materials are transferred to the factory rather than for construction on the site directly. From the academic field, there are several terms used to describe the prefabricated building or technology, such as preassembly, modularization and off-site construction (Song *et al.*, 2005). In the USA, the prefabricated house is also named modular housing (Song *et al.*, 2005), off-site production in EU countries (Song *et al.*, 2005) and in mainland China the name is industrialized housing (Zhang and Skitmore, 2012).

After decades of development, the prefabricated building has been extensively utilized in EU countries. And in mainland China, It just takes its own first step (Zhang and Skitmore, 2012) (Zhang, Skitmore and Peng, 2014). With the rising of consciousness in low-carbon house, the prefabricated house has been spread rapidly in China, especially in Beijing and Shanghai for satisfying the requirement of housing needs and reducing pollution during the construction. Compared with traditional methods, this kind of factory control and industrialization is also believed to improve the environmental performance of building (Steinhardt and Manley, 2016). (Hong *et al.*, 2018) states the benefits of the prefabricated house in China as listed below

- 75% of on-site labours can be saved compared with previous construction methods

- Less skilled labour required on site
- Duration of on-site construction can be reduced by about 50%
- Factory manufacture can promise high accuracy and quality of components and reduce the risk of infiltration or exfiltration through building fabric
- On-site pollution and waste can be reduced greatly
- Fewer demands on material storage
- Less dependence on weather conditions during construction
- A more prefabricated construction scheme
- Smaller risk of on-site construction faults

Several benefits of the prefabricated house have been addressed from the academic field(Liu and Ying, 2009). With the rising need to accomplish a low-carbon society around the world, various green technologies have been promoted by sustainable practice in the global building industry, such as the passive building strategies (Zhang, Platten and Shen, 2011) and sustainable technology (Zhang, Wu and Shen, 2012). Technology is also regarded as a new approach to sustainable construction to save energy and raw materials (Zhang, Skitmore and Peng, 2014). The environmental impacts of the prefabricated building can be significantly reduced. Thus, it is very important to know how to integrate sustainable technology into building components. Several studies have been proposed about the environmental benefits of off-site production building in China.

Table 2.4 lists the summary of studies.

Table 2.4 The research on the prefabricated building om environment impact

Reference	Application of Prefabricated	Environment Impacts
(Liu and Ying, 2009)	prefabricated concrete	Reduce solid waste
(Chen, 2010)	material and energy use	20% reducing
(Zhang, Skitmore and Peng, 2014)	timber shuttering	87% reducing
(Cao *et al.*, 2014)	Prefabricated concrete column	62% reducing

Prefabricated technology demonstrated a great advantage in environmental impact over traditional building. (Cao *et al.*, 2014) state that the combination of the prefabricated building with prefabricated-sustainable technology is the key point to improve the performance of prefabricated houses. This project is trying to integrate low-carbon technology into a building.

The common passive strategies in a prefabricated house

Concerning the low-carbon prefabricated house, the other part of the topic is the sustainable house. Nowadays, many governments encourage low-carbon design, the passive design referred to the architectural strategies applied by the architect and engineers to respond to the climate conditions and requirements (Ahmad, Thaheem and Anwar, 2016). Low-carbon houses are intended to decrease the environmental impacts of the building. With help of a suitable architecture design, a comfortable interior environment can be achieved, which means the needs for energy on cooling or heating can be reduced. In the most stressful season, summer or winter, the interior temperature should be the primary consideration of the building design (Ochoa and Capeluto, 2008).

Besides the mechanical improvement through innovation in ventilation, such as power fans or heat pumps, the natural heat transfer approach is also available.

Table 2.5 summarises references for architecture design which covers common passive strategies for the components in prefabricated buildings:

Table 2.5 The common passive strategies

Passive Strategies	Reference	Statement
Orientation on building	(Morrissey, Moore and Horne, 2011)	The easiest approach in achieving thermal comfort is the adherence to the oriented buildings
	(Bekkouche *et al.*, 2011)	Positioning the house in the right direction is entailed in the central principle during building design
	(Haase and Amato, 2009)	Solar irradiance can be determined by the orientation
	(Olgyay, 1967)	Building alignment corresponds to local climatic conditions to maximize the natural benefits
Building layout (Shape)	(Okeil, 2010)	Ventilation dependents on the building shape
	(Capeluto, 2003)	Self-shading has significant impact on the interior spaces
Building envelope	(Capeluto, 2003)	The cooling or heating systems can be economized by adequately sealing the building
	(Radhi, 2008)	Residential buildings with decreased window/wall ratio were observed to have reduced energy demand
Walls	(Christian *et al.*, 2006)	The impact of thermal insulation has significant effect on the heat conservation in the building.
Window	(Kamal *et al.*, 2000)	The heat loss from the window account for the one fourth of the overall energy loss from the building.
	(Cuce and Cuce, 2016)	The glazed window not just limited to being more tough, but also the impact of heat transmittance, thermal bridging via glazing, and direct solar gain

Building colour	(Asimakopoulos, 1996)	Envelope colour leads for convective heat transfer, leading to quicker cooling down of the textured surface
Solar controls/Shading elements	(Bouchlaghem, 2000)	A decrease in the heat obtained by the building is favoured through passive shading systems.
	(Graves *et al.*, 2001)	Using more natural light is more comfort than artificial lights. Reduction in use of artificial lights also leads to decrease in heat generated within the building
	(Capeluto, Yezioro and Shaviv, 2003)	Adjustable shading devices can reduce the energy consumed for the heat and cooling.
Thermal Mass	(Sidanius *et al.*, 2000)	It is highly advised to use material with thermal mass to maintain the internal condition.

The acceptance and applicability of prefabricated construction

In 2005, the Buildoffsite conducted a survey about how prefabrication has been applied in the UK (Pan, Gibb and Dainty, 2005). The survey shows that the most obvious barrier to achieving prefabricated low-carbon house includes higher capital cost, long-term payback period and random design changes during construction. The result also reports that when the constructor considered the prefabricated house, 71% of them were not satisfied with its on-site performance. From the survey, the main drivers for prefabricated application were skilled labour shortage, high quality, and minimal on-site time. Another side effect of the prefabricated house is inflexible design during construction, which means higher requirements on the designer and civil engineer. Although prefabrication can reduce time and money consumption, the funding mechanism should adjust to accommodate the higher cost of the designer as it requires a much longer design period and also more skilled

designers. It seems there will still be a long-term period to spread prefabricated houses. Therefore, in order to achieve any innovation in the industry, the first thing is to increase the knowledge among the stakeholders. The designer and constructor can share the same experience and build prefabricated low-carbon houses.

2.5. Energy consumption patterns in building

Energy consumption patterns in buildings rely heavily on local climate conditions, the behaviours of occupants and the regulations of the country. The developed counties are developing energy conservation in the building sector in general and in residential buildings. Additionally, these countries have systematic GHG emission reduction policies and criteria defining the space heating or cooling loads with the unit-kWh/m^2. For example, the Passivhaus Standard defines the annual heating and cooling loads of buildings as being less than 15 kWh/m^2.

About 40% of energy use is consumed by building-related industry (Gong and Song, 2015). Moreover, the building industry accounts for almost half of the global energy consumption (Ghiaus and Inard, 2004) and produces 33% of global GHG emission (Berardi, 2016). The energy for cooling and heating in the interior space is around 40% of the global annual consumption, with a great amount of GHG emissions (Omer, 2013). In the last decades, the development of air conditioning demands a considerable increase in electricity use (Chiesa, Simonetti and Grosso, 2014) (Omer, 2013). To release the pressure on GHG emissions and energy crises, there are considerable common interests in the

world, promoting environmental protection. All the governments in the world are raising awareness of sustainable development by producing environment-friendly designs which can use the least energy to satisfy the most comfortable interior environment. Because of the needs for reducing energy consumption, the researchers have proposed several sustainable approaches and energy-efficient technology(Berardi, 2016).

China has become the world's largest consumer of energy. Compared with 2000, the energy consumption in 2035 is expected to increase by two fifths per unit (Zhang and Liao, 2015). In 2009, China has proposed several policies to reduce Chinese carbon emissions per unit GDP by 50%. And in the 12th five-year plan-2010, the total energy consumption in China was 7% greater than that in 2010(NBS, 2012). According to the Ministry of Housing and Urban-Rural Development, the construction industry consumed 27.8% of the total energy consumption in China. And the heating, ventilation, and other domestic appliances contribute more than half of the energy consumed by the building(Yang *et al.*, 2010).

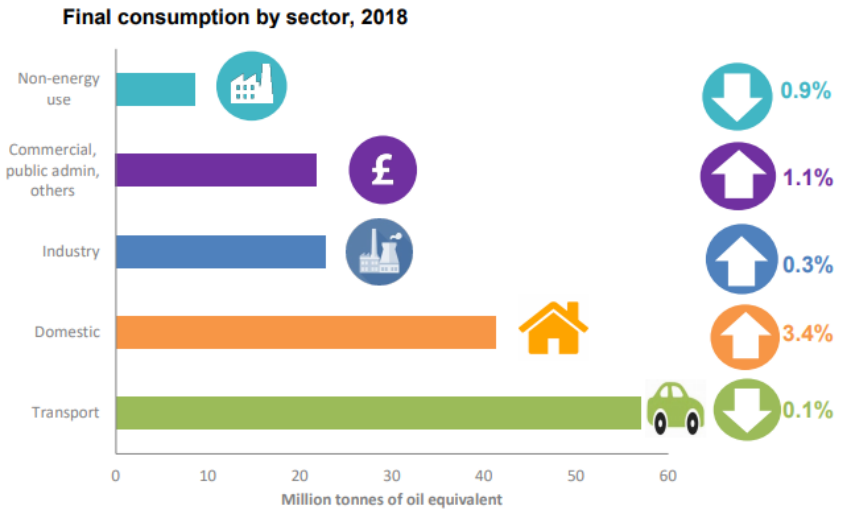


Figure 2.1 Energy consumption by final users in the UK (Department for Business, 2019)

According to the report (Department for Business, 2019), as Figure 2.1 shows, energy consumption in the domestic sector was increased by 3.4%, while the service part was up by 1.1% in the UK. The consumption in transportation experienced a fall of about 1%, as Figure 2.1 shows. The domestic sector is the most responsive to temperature changes as a larger proportion of energy is consumed for space heating. The energy consumption for industry experienced significant drops from 62 to 22 million Tonnes of Oil Equivalent-M toe. The most notable element is the growth in transport consumption and domestic use.

UK is facing a significant but exciting infrastructure challenge. Therefore, energy efficiency in buildings is essential to improve the local environment-friendly level and decrease the energy requirement. To reduce the carbon emission from buildings, the British government required that certain new buildings are energy efficient and require all the new buildings to be zero carbon from 2016. They also introduced the low-carbon approaches to encourage people to pay for home improvements using savings on their regular energy

bills and improve the certificate for the energy performance to be more user-friendly.

Active and passive measures can help to improve energy-saving performance. Active approaches include upgrading the appliances with higher efficiency units. The passive measures cover the improving thermal performance of building components and proper airtightness. For example, replacing the ordinary double glazing with vacuum glazing can reduce the heat transfer coefficient from 2.8 to 1 W/($m^2 \cdot K$), which allows the interior temperature to remain for a longer time and enables one to reduce the energy bills.

Principles of heat flow in buildings

The main heat-loss channels are though convection, conduction, and radiation. The heat energy would transfer from the hot side to the cold side and cannot flow backwards without the help of other devices such as heat pumps. To evaluate the thermal performance of the house, it is necessary to investigate the principles of heat flow within the buildings. It can provide guidance on minimizing the building heat loss. It is also important to consider the thermal comfort within the interior environment since the main purpose of a house is to provide a comfortable interior environment for occupancy. The current regulation suggests that the internal temperature should range from 18°C to 24°C (Park and Oh, 2014).

The thermal performance of the fabric components such as fenestration, wall, roof and airtightness would have a great impact on the temperature, humidity and ventilation (Ormandy and Ezratty, 2016). As the increase of airtightness

and insulation performance of the fabric, the energy consumption would decrease greatly. However, the possibility of overheating and increasing CO_2 proportion increases (Patidar *et al.*, 2011), which would have a negative impact on the occupants' health.

There are several approaches in which energy transfers from the building fabric to the environment. Figure 2.2 shows the main heat loss or gain routes for dwellings.

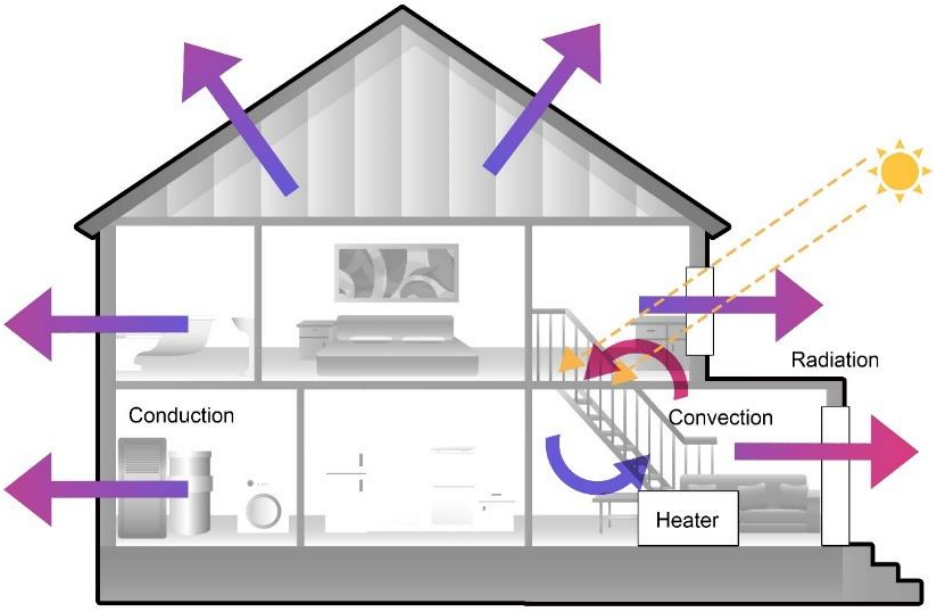


Figure 2.2 The heat transfer approaches within dwelling

Presuming that a house with an internal temperature similar to the external temperature, there will not be energy transfer through the building fabric. But under most situations, there would be a temperature difference between inside and outside, since the distribution of internal temperature is smaller than the ambient temperature for comfort. The common heat losses and gains are summarised below:

- Transmission heat loss (L_{trans}) – the heat transfer through the building

fabric via conduction

- Ventilation heat loss (L_{vent}) – the heat exchange through the ventilation between inside and outside, by air leakage or fenestration
- Solar heat gains(G_{solar}) – the energy gain through the solar irradiance
- Internal heat gains ($G_{internal}$) – the energy gains through occupancy body temperature, lighting, appliances.

(Feist *et al.*, 2007) states that the heating equation for a dwelling is as below, as the H is the heating gains for overall building:

$$H = (G_{solar} + G_{internal}) - (L_{vent} + L_{trans}) \quad \text{Equation 1}$$

(Baehr and Stephan, 2011) states that the main heat transfer approach for building is conduction. The conduction would happen with temperature differences between inside and outside. The convection always happens in the internal air. The warm air expands and rises while the cold air sinks because of the density difference. The convection would introduce the air circulation within rooms. Due to the solar irradiance transmitted through windows and other building components, solar irradiance is the simplest method for heat transfer. Infiltration is the air leakage through the joints of building components. With the air leakage, the heat would be transferred to the air. Under a high level of airtightness, the contribution of heat loss through infiltration will reduce greatly.

Preventing heat transfer

This section is to investigate the main approaches of heat loss. By reducing the heat transfer through building fabric, the heating or cooling loads will be greatly

decreased. (Chris Woodford, 2019) states that the heat transfers in three different ways within dwellings.

- Heat flows down directly into soil or rock through foundations
- Energy transfers by conduction through building fabric, such as wall, roof, and windows.
- Large amounts of energy can flow in/out of the building via infiltration or exfiltration.

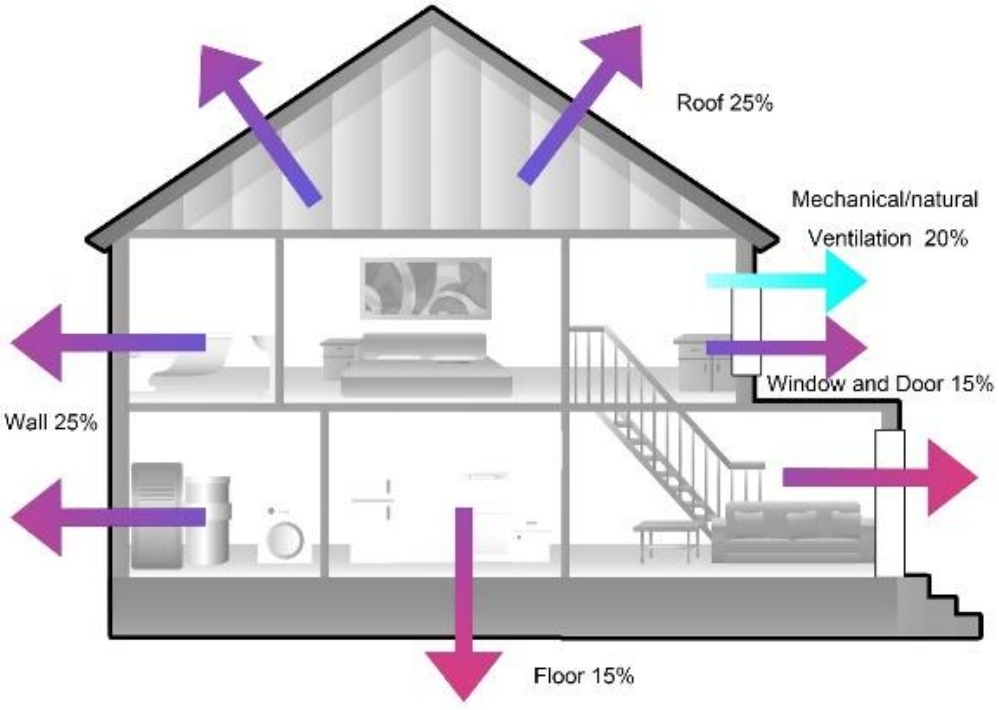


Figure 2.3 The contribution of heat loss for different approaches

Figure 2.3 shows the contribution of energy loss to a building. The building fabric accounts for more than 85% of the heat loss of a building, as the roof, walls, and fenestrations account for about 25%, 35% and 25%, respectively. Pareto's principle states that, for many events, roughly 80% of the effects come from 20% of the causes (Bunkley, 2018). Therefore, the key to reducing the heat transfer is to increase the thermal performance of building fabric.

Specifically, reducing the thermal transmittance of material and the thermal bridge between inside and outside is the main way. Furthermore, increasing the airtightness of the building is also important as the infiltration or exfiltration accounts for a great amount of energy transfer.

2.6. Post construction assessment

Normally, the estimation on the building energy consumption before the construction stage are essential. At the same time, the post construction assessment of the building is also necessary to investigate the actual performance. However, the systematic post construction assessments on the low-carbon house have not been promoted among the building related industries in China. For the EU, there may be a policy change in the building evaluation process, that is, the energy consumption of a building is defined by on-site evaluation rather than modelling at the design stage (UKGBC, 2019).

The post construction assessment is not only based on a qualitative analysis of the occupancy review. Furthermore, the assessment is used to refer to the systematic assessment of thermal performance and indoor environment (White, 2014). The assessment approach provides a comprehensive evaluation tool for post construction. It is certain that the information obtained from the evaluations is invaluable to designers and other stakeholders as the performance of the completed building can be compared to that at the design stages. It would help to locate the factors leading to gaps between reality and expected performance.

Reviews on the air tightness testing

Buildings require a suitable level of ventilation to maintain the health and well-being environment. However, the uncontrolled air infiltration through the voids or gaps of building fabric can cause heat loss or gain, leading to excess or inefficient energy consumption. The heat loss through air leakage can account for about 30% of total energy loss in existing buildings. For various types of buildings and structures, the typical air leakage pathway is different. Figure 2.4 shows the typical air leakage way in a house.

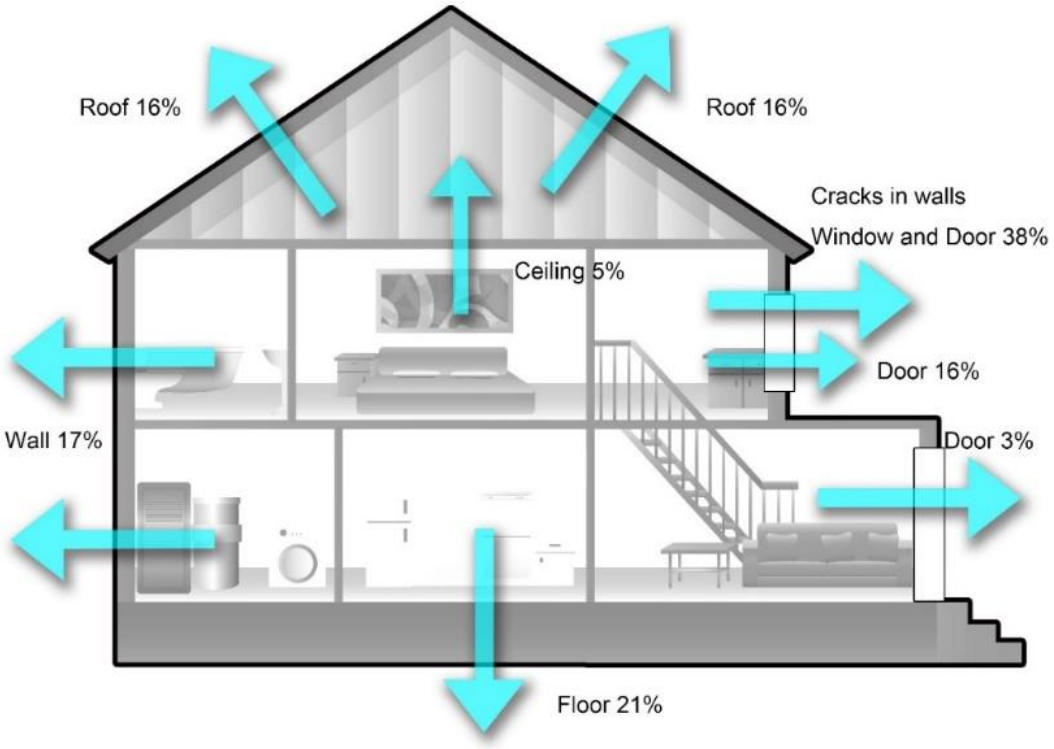


Figure 2.4 Typical Air Leakage of the House

The majority of obvious air infiltration is caused by the combination of cracks, and joints of building components rather than through the centre of a single component. For various types of buildings and structures, the typical air leakage

pathway is different. (Infiltration and Centre, 2012) states leakage typically occurs at the following locations on the building envelope:

- Junctions between walls and floors
- Junctions between window frames and walls
- Electrical equipment
- Wall penetrations

According to the different building types, the recommended airtightness standards have been established in Table 2.6.

Table 2.6 The common requirements on the airtightness of various building

Type	**Air permeability $m^3/(h \cdot m^2)$ @ 50Pa**	
	Best Practice	Normal
Offices		
Naturally ventilated	3.0	7.0
Mixed mode	2.5	5.0
Air conditioned/low energy	2.0	5.0
Factories/warehouses	2.0	6.0
Superstores	1.0	5.0
Schools	3.0	9.0
Hospitals	5.0	9.0
Museums and archival stores	1.0	1.5
Cold Stores	0.2	0.35

In all new housing developments, the British regulations request that the minimum of air permeability should be not over 10 $m^3/(h \cdot m^2)$ @ 50 Pa. As a compulsory standard, the testing on airtightness is the first stage of the post

construction assessment. The most admired approach to investigate air leakage rate is the blower door test. The basic process of the evaluation is installing a certified blower fan at the gate of the building and sealing all obvious vents within the dwelling. Figure 2.5 below shows the air-tightness testing process.

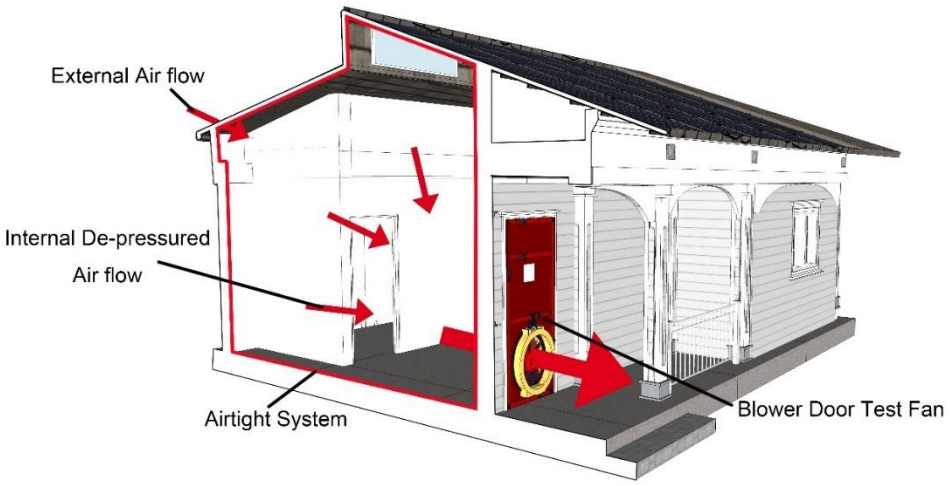


Figure 2.5 Air tightness testing process

When the blower fan is exhausting or intaking the air, there would be a slight positive or negative pressure difference between inside and outside. Once the pressure gap reaches about 50Pa continuously, the air flow through the blower fan would be the rate of air leakage of the dwelling at 50 Pa (DCLG, 2015). The main terms used to describe the air tightness parameters are $q50$ and $n50$ (Sinnott and Dyer, 2012). $q50$ is most commonly used in the UK. It means that the volume of air passing every m^2 of building fabric every hour, expressed in $m^3/(h \cdot m^2)$ @ 50 Pa. $n50$ represents the volume of air leakage divided by the overall volume of interior space, expressed in air change rate.

Reviews on thermographic images

In order to visually investigate the thermal bridge between the interior and outside, the infrared thermographic survey can provide visible and direct results using a thermographic camera. The thermographic camera provides the visible evaluation of the quality of construction, such as the joints between the building components. The thermographic camera is also used in air pressure testing, which can identify the air leakage area and reduce the energy transfer (Balaras and Argiriou, 2002).

Reviews on co-heating testing

The evaluation of the overall heat loss or gain for dwellings is necessary for low-carbon house. The development of the co-heating test methodology began in the late 1970s (Bauwens and Roels, 2014). The Co-heating test is widely used in Europe to investigate the total heat transfer through the fabric of buildings (Jack *et al.*, 2018). The primary method on evaluation for overall heat loss in the UK is the co-heating test (M. Taylor; L. Morgan, 2011).

To undertake the co-heating testing, heat flux sensors may be applied with the datalogger to gain the parameters of conductive heat transfer current of building envelope. The heat flux sensor which mounts on building walls or other building components can record the amount of heat energy lost or gained through that component.

This method utilizes several electric heaters to maintain a constant intemal temperature. The on/off operation of fan heaters can be controlled by the

thermostat under a specific set temperature. Normally, the interior temperature should be over 10°C higher than the outside temperature. And the total power supply to the heater is measured by a power consumption meter. The circulation fan is employed to accelerate air flow and mixing. A pyranometer is used to measure solar irradiance. The duration of the testing more than 5 days is recommended. The result from the co-heating test, heat loss coefficient (HLC), is a measurement of total heat loss current through the envelope and divided by the temperature difference, expressed as W/K.

From the above measurement, the on-site assessment of the constructed building can be analysed. Such assessments can provide valuable information on the actual thermal performance of the constructed building and identify the gaps between the designed and as-built thermal performance.

2.7. Reviews of the prefabricated sustainable technology

The global temperature increased by 0.2°C in the past 100 years. The researcher predicts that the average temperature in China would increase about 5°C, which would have great impacts on the peak temperature during summer in Wuhan. According to the statement (Roberts, 2008), the average carbon consumption per square metre in domestic buildings would be much higher than in industrial or public buildings. Roberts (Roberts, 2008) also mentioned that most of the houses in the UK were built between 1930-1970s. Previous occupants did not consider energy saving at that time. Because of historical restrictions, those old buildings do not have good thermal performance. However, the annual replacement rate for new homes in the UK

is about 1%. Thus, there would be a very long time to reduce the overall building-related carbon consumption. In China, the situation is similar. The wide application of low-carbon houses starts from 2010s. Previously built houses did not consider energy saving.

The prefabricated components can satisfy the high accuracy requirements of low-carbon technologies. In this chapter, the reviews also cover the recent achievements of prefabricated low-carbon technologies, including fabric, fenestration, and heat recovery.

Mechanical heat recovery ventilator system

Reducing the energy demand not only includes the application of more efficient devices or equipment but also increases the airtightness of buildings. Increasing airtightness means lower air infiltration (Gendebien, Bertagnolio and Lemort, 2013). However, the increasing airtightness has side-effects on the indoor air quality-IAQ of buildings. It has a negative impact on the health of occupants. Necessary frequent ventilation would help to improve air quality but would cause more energy uses than normal. Hence, the ventilation of buildings must be undertaken under controllable level to satisfy the requirements from thermal conditions and IAQ. It is necessary to recover energy by utilizing heat recovery ventilator systems. Common ventilation devices are difficult to achieve the above requirements. The mechanical heat recovery ventilator (MHRV) system provides an optimal solution for the dilemma. MHRV can offer several functions, including air freshness, climate control and energy recovery.

Heat recovery is a method that is used to reduce the heating and cooling loads of buildings. Normally, there would be a temperature difference between inside and outside. The exhaust air can be used as a heat source or heat sink for the inlet air (Li, Wild and Rowe, 2019) (Gendebien, Parthoens and Lemort, 2019). The heat energy of exhaust air can be transferred to inlet air. The temperature of pre-heated or pre-cooled air can increase or decrease close to the interior temperature. Thus, the heat loads of the building can be reduced.

Definition and concept of heat recovery ventilator

The heat recovery ventilator is referring to the air-to-air heat recovery system in this section. The system transfers the energy from an air stream with a higher temperature to the other air stream with a lower temperature, which is effective to run (Gan and Riffat, 1998). (Qi Xu, Saffa Riffat, 2019) defines the device as a unit operating between two air flows with temperature gaps and transfers the energy from one flow to the other flow. It is based on preheating the incoming air to the interior through recycled waste heat of exhaust air.

As Figure 2.6 shows, a representative heat exchanger system in buildings usually is composed of a heat exchanger unit, ducts for the fresh and exhaust air and a fan (Mardiana-Idayu and Riffat, 2012). At present, the heat recovery system can recover about 60-95% of the waste energy, which is very promising (Qi Xu, Saffa Riffat, 2019). Besides the energy saving, the MHRV system also enjoys other advantages such as supplying efficient ventilation, air filtration, reducing the moisture in the toilets and so on.

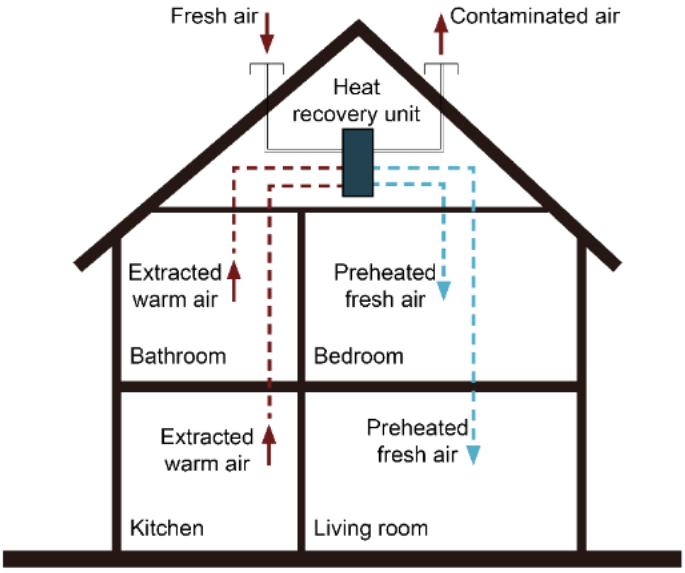


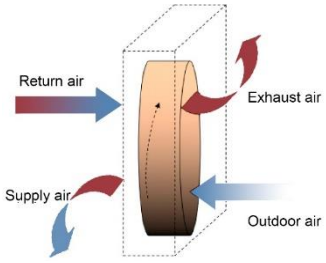
Figure 2.6 Heat recovery ventilator system (Xu, Riffat and Zhang, 2019)

The heat exchanger is the place where energy or heat is transferred. In the heat exchanger, the fresh air gains or loses the heat automatically from the exhaust air and introduces it to the inside environment. There is heat transfer between inlet air and outlet air without the air mixture. The MHRV system is always installed in the attic as Figure 2.6 shows.

Classification of heat recovery

Heat recovery can be categorized into several types, especially for air-to-air heat recovery systems. There are four different heat recovery devices that can be installed in the building (Xu, Riffat and Zhang, 2019). The main difference between these MHRV systems is the heat exchanger type. (Cuce and Riffat, 2015) provides a classification of heat exchanger based on the below properties, including heat transfer method, air flow direction and so on. The primary types of heat recovery system cover fixed plate, heat pipe, rotary wheel, and run-around coil. Recent achievements of the different types of heat recovery are analysed and compared for suitability for integration into passive ventilation systems (shown in Table 2.7). In Table 2.7, the thermal efficiency of the heat recovery has been summarized.

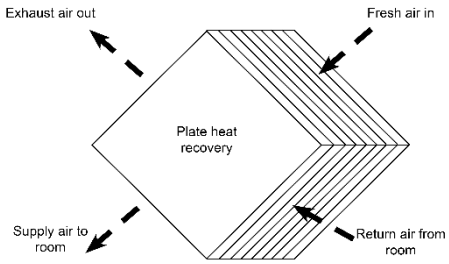
Table 2.7 Recent achievement on the different types of heat recovery

Rotary thermal wheels
• Rotary wheel heat recovery system is a motor-driven rotating porous wheel. • The speed of rotors usually low, ranging from 3 rpm to 15 rpm. • The total efficiency of rotary thermal wheels is generally above 80% (Juodvalkis *et al.*, 2011). 
• The heat wheel heat recovery barely recovers 40% of the available enthalpy. • In terms of the performance of rotary wheel heat recovery, atmospheric conditions (Nóbrega and Brum, 2009), air mixing rate (Tu, Liu and Jiang, 2013), rotation speed (Ruivo, Angrisani

and Minichiello, 2015) and wheel materials (Jani, Mishra and Sahoo, 2016) take a significant place.

Fixed plate

- Plate exchangers are made of thin plates stacked together.
- The plates may be smooth.
- Most common type of heat recovery system.
- The typical efficiency of sensible heat transfer is from 50% to 80% and air flow can be counter-flow, cross-flow or paraleel flow.

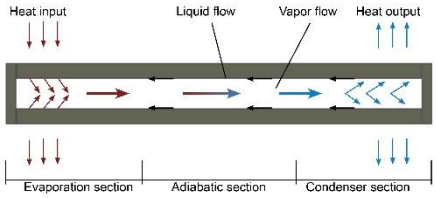


- (Kragh *et al.*, 2007) (Kragh, Rose and Svendsen, 2005) has promoted a counter-flow heat recovery system with efficiency almost 90% in ventilation system in cold climate.
- (Cuce and Cuce, 2017) states efficiency of polycarbonate heat exchanger can achieve about 50–80%.
- (Nasif, 2015) found that air-to-air fixed plate energy recovery heat exchanger utilizing porous paper and Mylar film can save 78% energy.
- (Al-Waked *et al.*, 2013) confirmed that the fixed plate heat recovery is most effieiency.
- (Nasif *et al.*, 2010) states the efficiency of membrane fixed plate is about 75% for sensible and 60% for latent.

Heat Pipes

- A sealed self-contained, fluid evaporating condensing system.
- The unit is divided into two sections for inlet air and outlet air where the working fluid is evaporator and condenser
- No flexible part
- No need for external power supply
- No cross contamination

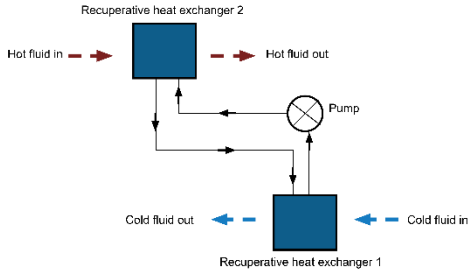
- Wide range of applications
- Easy for clean



- Typical heat pipe exchangers could achieve thermal efficiency at around 50%
- Shao and Rifat's experiments proved that, with the pressure loss every 1 Pa, the efficiency of a heat pipe recovery system in naturally ventilated house could achieve 50%.
- (Gan and Riffat, 1998) showed that the efficiency of het pipe heat recovery system would decrease with the increase of velocity and poor thermal contact between fins and heat pipe

Run-around

- Run-around heat recovery system consists of two individual heat exchangers and a coupling liquid
- liquid to transfer absorbed heat from one stream into the other side



- run-around system does not require the supply and exhaust air duct side by side.
- thermal efficiency of run-around is normally from 45% to 65%.
- (Dhital, Besant and Schoenau, 1995) stated a run-around heat recovery system can allow the ventilation airflow rate to be increased without the increasing the energy consumption.

Applications of heat recovery system in ventilation system of buildings

The application of heat recovery in buildings can significantly increase the energy efficiency of the building. The combination of heat recovery and different energy-efficient systems could contribute to reducing heat loss, stabilizing the heat flux of buildings. The mechanical ventilation system is used for creating the desired airflow and maintaining indoor comfort. However, mechanical ventilation devices consume large amounts of electricity for circulating fresh air. And sometimes, it would increase the energy consumption by up to 50% (Manz and Huber, 2000). Several researchers have tested the performance of heat recovery unit with decentralized ventilation systems based on different outdoor conditions.

Baldini has tested a decentralized cooling and dehumidification system, as Figure 2.7 shows, which is suitable for humid climates with high temperatures. The experimental result reported that within air temperature around 30°C and 20 g/kg humidity ratio, the air coming from outdoors could be treated to the required conditions, supply air at 14–15°C and 8–9 g/kg (Baldini, Kim and Leibundgut, 2014).

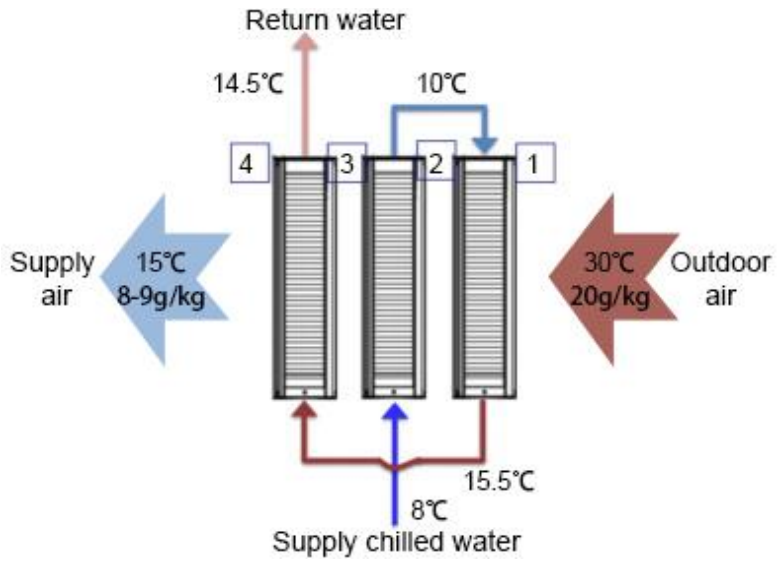


Figure 2.7 The arrangement of the three-heat exchanger (Baldini, Kim and Leibundgut, 2014)

The combination of heat recovery with ventilation systems could obviously reduce heat loss. Compared with fixed-plate type heat recovery, the integration of heat pipe and rotary wheel heat recovery with a wind tower enjoys the advantage of being more compact (Zeng, Liu and Shukla, 2017). However, unexpected noise from the DC motor for the rotary wheel heat recovery unit (rotating regenerator) during its operation could be an issue. The effects of air pollution on decentralized ventilation, heat recovery and indoor air quality lack investigation.

Fabric technology

The study for the envelope of buildings has become the main field of low-carbon house research as two thirds of the energy loss in buildings is through the facades (Granadeiro *et al.*, 2013).

Walls are the main part of the building envelope and thermal transmittance have a significant impact on the capacity of heat conservation in buildings. Thus, increasing the thermal resistance is the main approach for the low-carbon building envelope.

Insulation material

The building components, such as, windows, walls, floors, skylights, and roof, through which the living space is protected from exterior elements are referred to as the “building envelope”. Certain supplementary facilities, for instance, shielding a home’s structure from a difficult climate, blocking outside noise, and improving indoor air quality are the services delivered by an effective building envelope. Current cooling or heating systems can be economized or they can be switched to low-energy substitutes for the purpose of saving maximum energy upon the implementation of passive thermal control, besides adequately sealing the building (Iyengar, 2015). The thermal comfort of occupants largely depends on the thermal performance of the building envelope (Khampom and Chaiyapinunt, 2014). Insulation material must provide acceptable performance which means not only the thermal performance. Other factors include sound insulation, resistance to fire, water vapor permeability and impact on human health.

Table 2.8 summarizes the list of common insulation materials analysed in the market.

Table 2.8 List of the common insulation materials

Conventional		
Insulation material	**Thermal conductivity (W/m · K)**	**Statements**
Stone wool	0.033–0.040	• The water vapor condenses has negative impact on thermal insulation performance of stone wool (Karamanos, Hadiarakou and Papadopoulos, 2008). • Stone wool has several advantages, such as good performance of sound absorber and easy to recycle during demolition. • Stone wool is typically classified as a non-combustible material, which means it has minimal or zero contribution to the spread of fire (Pereira *et al.*, 2016).
Glass wool	0.031–0.037	• Thermal insulation performance of glass wool can be not affected by high temperature and moisture conditions (Tatematsu et al., 2014). • Glass wool can be recycled for secondary use. • Glass wool is extremely low spread of flame, non-emission of dense smoke and toxic gases, on depletion of oxygen (Zhang *et al.*, 2017).
Expanded polystyrene	0.031-0.038	• The thermal performance depends on the density of material. The higher the density, the better thermal performance. • Expanded polystyrene is easily flammable and can release hazardous gases for occupants. • Polystyrene is highly flammable and ignites at relatively low temperatures, which requires brominated flame retardant to improve its fire resistance.
Extruded polystyrene	0.032-0.037	• Extruded polystyrene has similar characters to Expanded polystyrene. • The water vapor condenses has negative impact on thermal insulation performance. • Polystyrene foam is combustible.

Cellulose	0.037–0.042	• Cellulose is produced by recycled papers, wood fibres (Hurtado et al., 2016). • The thermal conductivity of cellulose is between 0.037 and 0.042 W/m K. • The density of cellulose is between 30 and 80 kg/m3 • These materials can be recycled. • Cellulose insulation is naturally flammable. But, with help of phosphorus based flame retardants, the cellulose would be suitably flame retarded (Gaan and Sun, 2007) (Salimova, Gaan and Nazarov, 2008).
Wood fibre	0.038–0.050	• The water vapor condenses and increasing temperature has negative impact on thermal insulation performance (Troppová et al., 2015). • Wood fibre-based insulation material is flammable. Thus, the fire resistance should be improved by treatment with a retardant reagent.
Mineralized wood fibre	0.060–0.107	• Mineralized wood fibre could be recycled.
Vermiculite	0.062-0.100	• It can be used in bricks (Sutcu, 2015) and lightweight concretes (Maderuelo-Sanz et al., 2016), or mixed with a binder (Schackow et al., 2014). • Vermiculite could be recycled after demolition. • Vermiculite is ideal for non-combustible material (Hezhev *et al*, 2018).
		Alternative
Hemp	0.034-0.043	• During application, hemp needs to be protected away from moisture, rodents and insects (Zach et al., 2013). • Hemp based walls are fireproof and enjoy advantages on acoustic performance.
		Advanced
Vacuum Insulated Panel-VIP	0.0035-0.008	• VIP consists of a core material installed with getters, desiccants and opacifiers and enveloped by air-tight fabric. • The core is usually made of a porous material with low thermal conductivity. • The thermal conductivity can reach down to 0.004 W/(m·K).

		• The life span is up to 160 years (Baetens, Jelle, Thue, et al., 2010). • Although the core material of VIPs can achieve excellent fire resistance, the enclosing membrane can be a fire risk (Kontogeorgos *et al.*, 2016).
GFP (gas filled panel)	0.010-0.035	• The gas can be air or other gases with lower thermal conductivity (Baetens, Jelle, Gustavsen, et al., 2010).
Aerogel	0.013-0.015	• Aerogel is defined as a porous structure with pores ranging from 2 to 50 nm in diameter. • The density can reach down to 3 kg/m^3 • Unique binary network microstructure endows aerogel with excellent fire resistance.

Besides the conventional insulation material, the innovative insulation such as Vacuum Insulation Panel-VIP, Gas Filled Panel-GFP and aerogels present ultra-low thermal conductivity with physical advantages that are becoming commercial these years (Jelle, 2011). In addition, the application of Phase changing material (PCM) in building fabric can provide significant energy savings (Kalnæs Simen Edsjøand Jelle, 2015).

Vacuum insulation panels

Vacuum insulation panel (VIP) is one of the most promising building insulation material. Typical VIPs include a porous core enveloped by an airtightness cover, usually aluminium foil. The porous structure of the core would allow the air to exhaust. The most common materials are core cover fibreglass, polyurethane, cork, perlite, aerogels and so on. The radiation heat transfer is reduced by the use of opacifier.

As Figure 2.8 shows, the envelope material should be airtight and vapour-tight in order to reduce the side effect from air and vapour on the thermal insulating

properties (Villasmil, Fischer and Worlitschek, 2019) (Alam *et al.*, 2017). The common thermal conductivity is about 0.004 W/(m·K).

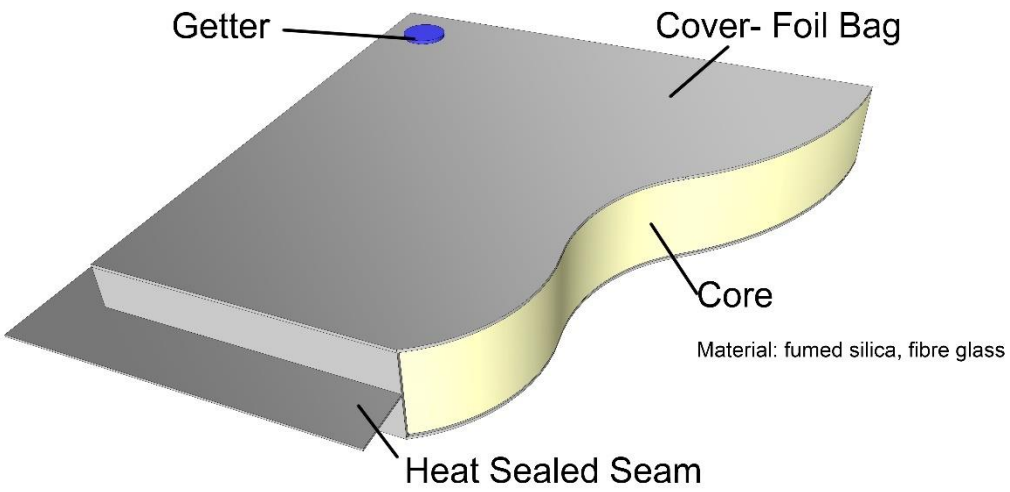


Figure 2.8 The structure of VIPs

However, the thermal insulating properties would increase after long-term application due to the air and moisture infiltration through the envelope (Kalnæs Simen Edsjøand Jelle, 2014). Stabbing the VIP envelope would also cause a great increase in the thermal conductivity to about 0.020 W/(m·K). It is the major drawback of all types of VIPs. Thus, the VIP is not suitable for construction without detailed design. It is suitable for the prefabricated low-carbon house as prefabricated components are manufactured in the factory (Jelle, 2011). The lack of flexibility and the risk of perforation will be the main barriers for wider application of VIPs.

The application of VIPs requires extra additional supporting components. The thermal insulating property of these supporting components is not the same as the VIPs. Thus, there would be a thermal bridge through the components. (Lorenzati *et al.*, 2016) promoted a model for estimation of the performance of

VIPs with supporting components. (Mujeebu, Ashraf and Alsuwayigh, 2016) suggests replacing the traditional insulation panel with VIPs to reduce the heat loss through the building fabric. They used Autodesk Revit to simulate energy consumption for houses. The result shows the VIPs application would reduce energy consumption by 18%.

The major drawback is the irreversible increase of thermal conductivity. Regular maintenance is required due to its fragile nature. In case a VIP is punctured, the thermal conductivity increases greatly. It must be considered that the metalized film around the VIP will form a thermal bridge. A special structure is required to protect the VIP without damaging the surrounding materials. Thus, the cost of the building with VIPs is four and eight times more than the same building with EPS and UPR (Villasmil, Fischer and Worlitschek, 2019).

To reach the same thermal resistance, the VIPs can be constructed thinner which saves space. (Liu, 2012) suggested that VIP materials have better performance in terms of insulation and space-saving. But the cost is still high due to its nature. Thus, the VIP is suitable for the building with high cost, as its space-saving capacity would mitigate the impact of high capital cost.

Structural insulated panels

Structural Insulation Panel-SIP is one of the prefabricated components and has become a topic concern for researchers in recent years. The concept of structural insulation boards was first proposed in 1935 in the Forest Products Laboratory in Madison, USA, which provides a flexible, cost-effective solution for highly insulated and energy efficient houses. SIPs enjoy advantages of

minimal material wastage, less site material, controlled quality, faster project completion, labour-savings, and lower total construction costs (Whitmore II, 2015). Furthermore, lower weight of SIPs compared to the conventional wall systems, such as brick, leads to the lower total weight of constructure.

SIPs are a sandwich panel used as building components such as walls, roofs, and floors. The main difference between various SIPs is the thickness of the two layers of skin material and the thickness of core layer, which can be made of various materials according to its application.

The core of SIPs is usually non-structural and ridged. The foam is commonly Extruded Polystyrene and Expanded Polystyrene or Polyurethanes. (Frostig and Thomsen, 2011) stated that the Polyurethanes enjoys better performance against fire, flaming, and against loads. Injected Polyurethanes foam can be easily adhered to all SIPs. Furthermore, there are several SIPs skin materials including Oriented Strand Board-OSB, fibre cement, cement, calcium silicate, and metal. Oriented Strand Board is the most widely used skin material because of its low cost (Panjehpour, Abang Ali and Voo, 2013). However, that kind of board is flammable and vulnerable to moisture. In order to alleviate the above shortcomings, SIPs made of OSB can be utilised as partition wall that are not exposed to moisture. Among the skin materials, the cement board is more convenient to use as SIPs (Panjehpour, Abang Ali and Voo, 2013). However, there is need for future research to improve its brittle failure and its high density.

Floor material

The term ‘floor’ refers to the lower enclosing surface of spaces within buildings. Table 2.9 below summarized the statements on common floor materials.

Table 2.9 the list of floor material

Floor Type	Statement
Timber	1. Timber floor can be very durable although it may scratch and is prone to movement. 2. It can be unsuitable for use in rooms that may be exposed to humidity or moisture. 3. Timber floors should be well ventilated to reduce the risk of timber rot and musty smells, which would cause heat loss (Harris and Dudek, 1997).
Laminate	1. Laminate flooring is a versatile and resilient flooring type. 2. It is a compressed fibreboard plank. 3. Laminate wood flooring exhibited the highest thermal conductivity over the other floorings (Seo *et al.*, 2011). 4. Air can escape through the joints.
Vinyl	1. Vinyl flooring is generally fixed by gluing. 2. It is easy to maintain and keep clean.
Bamboo	1. Bamboo can be compressed into a floor material. 2. Bamboo has been considered one of the most promising building materials for decades (Zea Escamilla *et al.*, 2018). 3. Bamboo flooring is easier to catch fire than timber flooring, and the risk of flashover is higher, and the carbon dioxide content produced by early combustion is higher (SHU and Chen, 2007). 4. The heat loss can escape from gaps between bamboo flooring.
Cork	1. Cork is water-resistant. 2. Cork materials are composites. 3. Cork is a natural thermal and acoustical insulator.
Ceramic	1. Ceramic is difficult to scratch or dent and is also suited to wet environments.
Carpet	1. Carpet is a multi-layer mixture of different polymers and inorganic fillers. 2. By 2025, carpet waste will be banned from landfill in the UK, because they are non-biodegradable (Sotayo, Green and Turvey, 2015).
Rubber	1. The rubber floor is made of natural or synthetic materials, including recycled rubber tires.

2. Rubber flooring is suitable for the applications that often require moisture and dirt resistance, sound absorption, and temperature stability.
3. Rubber flooring enjoys advantages on excellent elastic performance and high thermal insulation (Zhang *et al.*, 2019).

Floor insulation brings a lot of comfort and leads to energy savings. Commonly used floor insulation materials include:

- Cellulose.
- Cork board.
- Hempcrete.
- Woodfibre.
- Mineral wool.
- Extruded Polystyrene.
- Expanded Polystyrene.

Fenestration

When heating is considered, 10-25% of heat loss is due to windows, whilst for cooling, the heat penetrating glass could result in considerable heat gain which also depends on the outdoor temperature (Robinson and Hutchins, 1994). Thus, windows and glazing have much significance on energy savings when modelling buildings to determine thermal comfort and total energy consumption (Pal 2009). There is a significant impact of window to wall ratio on energy saving for the purpose of heating and cooling within buildings. As window to wall ratio increases, so does solar heat gain. Heat loss through building fabric will also increase since windows have a bigger area in comparison to solid wall (Robinson and Hutchins, 1994).

Purpose of developing high performance window systems

Glazing systems are regarded as the primary heat transfer bridge in the building envelop. Comparing with the thermal performance of insulated wall, the U-value of the window hardly approached that of the wall as the fenestration is primarily for ventilation and illumination. The purpose of ventilation and illumination limits the thickness of windows. Windows can account for about 40% of the heat loss during summer and winter while the area of windows just 10% of building fabric. Under more strict building regulations, the new build house tends to utilize the low thermal conductivity window system to reduce the heat loss. To cope with the energy-saving requirements, window glazing systems has been developed with several options and double glazing has been applied world-wide (Corgnati, Perino and Serra, 2007).

The most advanced window system has much better physical configurations and optical properties. The novel state-of-art glazing system is not only limited to increasing the thermal performance but also integrating other devices to satisfy other purposes, such as photovoltaic, phase changing material and so on. The glazing system aims to provide several properties, such as high thermal performance, solar energy collection or daylighting control (Sadineni, Madala and Boehm, 2011). This section will review the current development of glazing systems.

Components of windows

Window systems might be the most complicated components in a building. It should satisfy the requirements for airtightness, ventilation, daylighting, and solar energy insulation. The requirements above are contradictory. As Figure 2.9 shows, the window system is an assembly of glazing, frame, spacer, and sash. Fenestration refers to the design of doors and windows in houses. The thermal performance of a window depends on many factors, such as the number of layers of glass panels, frame materials, and the airtightness of joints. The material selection of the window frame has a significant influence on the thermal transmittance value. Wood, vinyl, or PVC frames have higher heat resistance than metal. Furthermore, metal frames, especially aluminium, can be improved by adding thermal isolation or thermal fracture between the inside and the outside. The U-value of ordinary single glazing is about 6 W/(m^2K). While the heat conductivity is the centre of the glazing, it does not consider the energy transfer through frames and edges of glazing. The low emittance coatings can reduce the U-value of the window system.

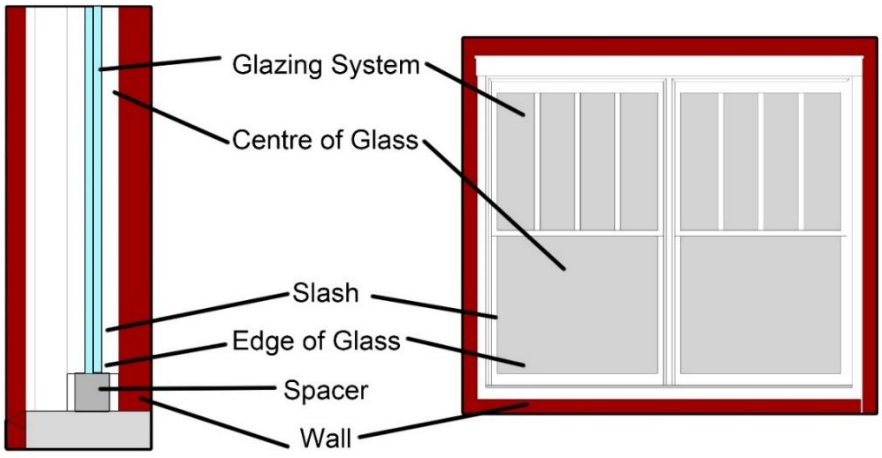


Figure 2.9 Window components showing glazing layers separated with spacers and sits

Multilayer glazing system

The multilayer glazing system is the most used and developed product in market. The cavity between the two glass sheets is filled by air or another gas. The key advantages over single glazing are energy-saving, solar and acoustic shield properties. Normally, the glazing system can achieve better thermal system by increasing the number of layers. Once the cavities between the sheets are filled with argon or krypton, the thermal conductivity and weight of windows can reduce rapidly. In Table 2.10, the properties of samples are summarised. It can be noticed that krypton is most common inert gas applied in multilayer glazing systems. The cost of argon filled insulated glazing systems is lower than krypton. However, the lowest U-value for multilayer glazing filled with argon is about 0.6 W/(m^{2}K).

Table 2.10 Parameters for Passivhaus Standard certified glazing products

Manufacturer	Product name	U-value W/(m^{2}K)	Visible Transmittance	Direct Energy Transmission	Shading coefficient	Reference
Pilkington	Optifloat 4mm single	5.8	0.89	0.83	0.98	(Pilkington OptifloatTM Clear, no date)
	energiKare 2·16mm argon Triple	0.6	0.71	0.64		(Pilkington energiKareTM Triple, no date)

INTERPANE GLASs	iplus 3CE	0.8	0.71		0.47	(Institute, 2017)
Guardian Glass	ClimaGuard N	0.5	0.71	0.45	0.53	(ClimaGuard ® N: insulating glass by Guardian Glass, no date)

Vacuum glazing

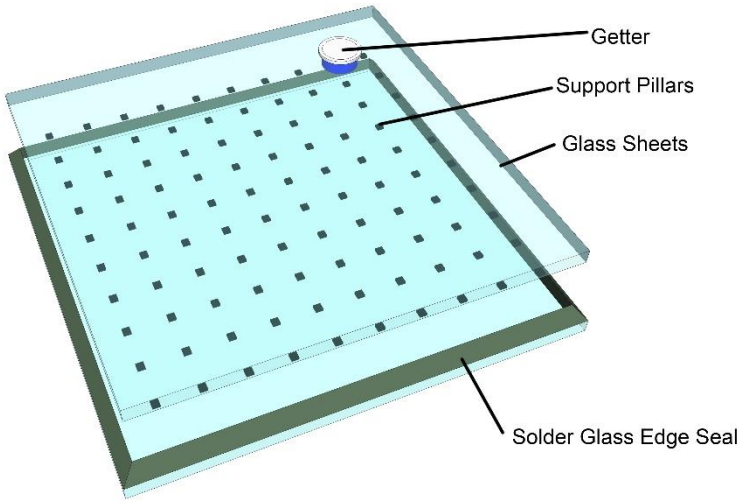


Figure 2.10 Schematic of a vacuum glazing

In vacuum glass, the evacuated chamber prevents the conduction and convection of the gas to reduce the heat transfer between the inside and the outside. As Figure 2.10 shows, a high vacuum gap, normally less than 1Pa, is maintained in the vacuum cavity by support pillars, normally solder material or indium. The tiny support pillars keep the two sheets of glass apart from each other. Furthermore, when combining a low emittance coating, the solar-radiation heat transfer between the glass sheets can be reduced greatly. (Jelle *et al.*, 2012) found that the common thickness of double vacuum glazing

product is in half thickness of a typical triple glazing with same U-value 0.70 W/(m^{2}K), as Table 2.11 shows.

Table 2.11 Parameters for SPACIA-21 vacuum glazing

Manufacturer	Product name	U-value W/(m^{2}K)	Visible Transmittance	Direct Energy Transmission	Shading coefficient	Reference
Pilkington	SPACIA-21	0.7	0.533	0.228	0.32	(*Pilkington Spacia^{TM}*, no date)

In recent years, the concept of triple vacuum glazing has spread. Some researchers state that the triple vacuum glazing can significantly reduce the U-value compared with the typical double vacuum glazing (Memon, 2019) (Serajian Tehrani *et al.*, 2019). According to the research, a U-value less than 0.20 W/(m^{2}K) can be achieved by triple vacuum glazing.

Photovoltaic glazing

Solar energy devices such as the Photovoltaic (PV) panel, or solar collector can reduce the carbon emissions. Nowadays, the PV device is not limited to mounting on the roof, the vertical PV device is also promoted. The PV glazing is the main development trend. Photovoltaic glass can both shade and generate electricity. Most PV glass is made of mono-crystalline silicon wafer solar cells. (Qiu, Yang and Zhang, 2019) found that the solar cells has significant impacts on the overall heat gain for interior environments. (Remes *et al.*, 2019)(Cho *et al.*, 2019) states that the semi-transparent amorphous silicon solar cells have been developed and commercially applied in markets. The semi-transparent amorphous silicon cells are produced thin by dividing a regular tiny gap for

visibility. The solar transmittance of the PV glazing can be adjusted by controlling the area and distance of the gaps. Thus, the electric generation of PV glass is influenced by its transmittance. After suitable adjustment, the PV glazing can be a desirable application for offices, houses and so on. The normal generation performance of PV glass is about 4.3%, which is relatively low for normal PV panels. However, 54.2% of heat gain can be reduced and also 56W electric generation can be achieved because of the PV glass. (Bambara and Athienitis, 2019) found that photovoltaic glass may replace all the electricity in the greenhouse to supplement the lighting and reduce by about 23% the life cycle cost of greenhouses. Therefore, the PV Glazing is suitable for greenhouse applications.

Low-emissivity coating

Low-emissivity (low-e) coatings can be used in order to reduce energy usage in transparent areas of a building (Jelle, Kalnæs and Gao, 2015). The largest part of solar energy can be found in visible light (380-780 nm) and near infrared (780-3000nm). In general, solar gain is the major contributor to interior overheating. Controlling the solar irradiance transmittance and utilizing the solar daylight is one of the key factors to accomplish a sustainable house.

Low emissivity refers to a surface with low radiant heat energy emission. Normally, the emissivity of specific material would be affected by the temperature, wavelength, and surface roughness. The low-emissivity coating is to reduce the radiative heat transfer. The near-infrared light would be reflected by the low-e material to reduce the solar gain. Low-e coatings can be applied

to the surface of glazing by sputtering or pyrolytic coating processes (Mardiana-Idayu and Riffat, 2012).

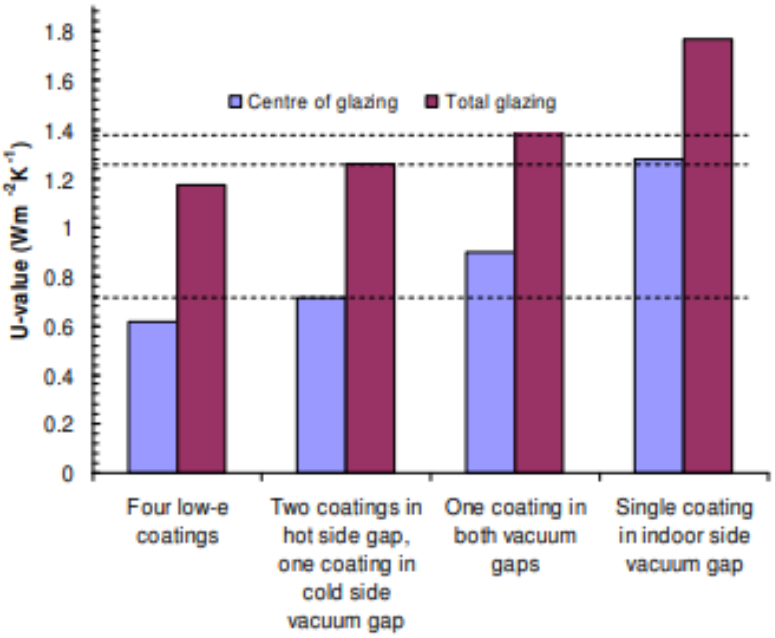


Figure 2.11 Comparison of U-value of triple vacuum glazing (Fang, Hyde and Hewitt, 2010)

The number of low-e glazing coatings has a significant impact on the thermal performance of low-e coating glazing (Fang, Hyde and Hewitt, 2010), as Figure 2.11 shows. The U-value of the glazing increases with the decrease of low-e coating layers. This means that increasing the number of coatings on the glass surface will reduce heat transfer.

State-of-art glazing systems are aimed to provide high performance insulation, solar gain control or daylighting. Several current commercial thermal glazing types are reviewed in this section. However, there are several side effects of these glazing systems such as heavy weight, relatively low solar transmittance, high capital cost, and complicated manufacturing processes. In the later part, the novel PV VG-4L-photovoltaic vacuum glazing is promoted and tested.

2.8. Conclusion

Low carbon buildings are the main contributor for reducing carbon emissions in the future. The promising way is to reduce heating and cooling loads as well as minimizing the material consumption during construction. The prefabricated components can promise high quality and accuracy of low-carbon house.

The thermal performance of a building is complex and multidimensional. The design and construction of a low-carbon building should consider the majority of heat loss approaches and try to prevent the pathways. The post-construction analysis, including co-heating test, thermographic analysis, air tightness test, provide the on-site data of whole building thermal performance. These results are invaluable for the existing building retrofits in the future and provide real inspiration for the design and construction of a future energy-saving house.

The low-carbon house introduces significant challenges to the building industry. Energy-saving cooling or heating systems have contributed to achieving ultra-low carbon emissions.

Significant energy saving for cooling or heating loads can be achieved by the application of heat recovery ventilators, insulated walls, and vacuum glazing systems. Due to the lower thermal conductivity, VIPs and vacuum glazing would be a more energy efficient alternative to other conventional building components.

3. Performance investigation of a novel heat recovery ventilator unit

3.1. Introduction

The heat recovery ventilator can reduce energy consumption from the HVAC systems (Dodoo, Gustavsson and Sathre, 2011)(Zhong and Kang, 2009). The energy in the exhaust gas can be transferred to the fresh air. Therefore, increase the temperature of the fresh air, and reduce the heating demand in winter. The previous review has investigated the effectiveness of various types of heat recovery devices. In addition, they also have great potential for integration into passive ventilation systems. (Sauer and Howell, 1981) concluded that heat recovery devices were suitable for both passive and mechanical ventilation. The heat recovery units with heat pipes were proved to be the most effective for passive ventilation due to the fixed components except for fans.

This section is about the thermal performance of the novel window heat recovery ventilator (WHRV) unit. In this report, an evaluation on the performance of WHRV unit has been conducted. The unit was tested in an insulated box to evaluate the impacts of various factors on the performance of the heat recovery unit.

3.2. Prototype description

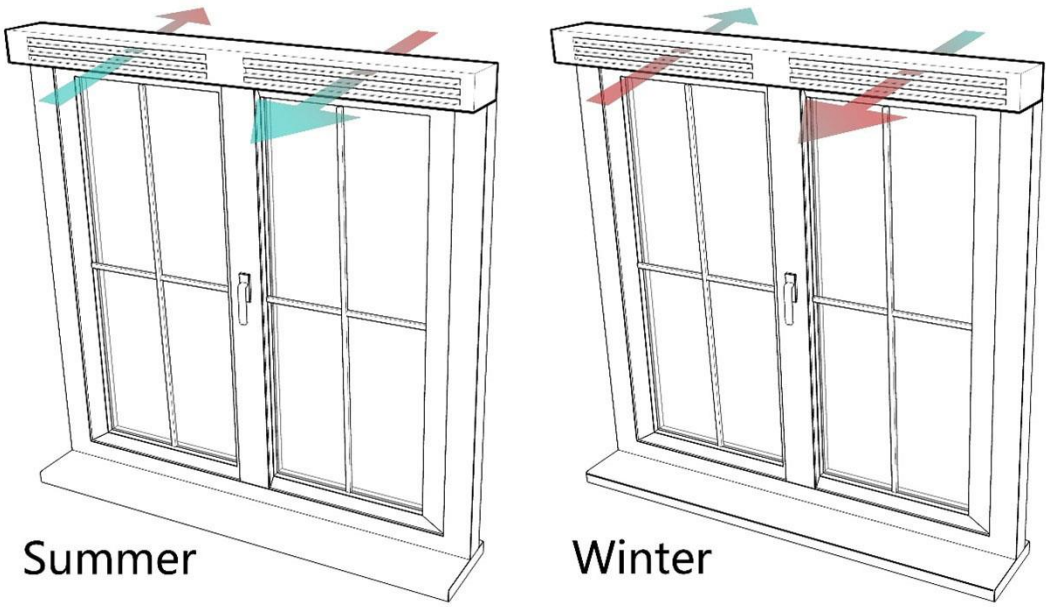


Figure 3.1 Schematic of Novel WHRV system with Window Frame

This project proposes a unique innovative compact and uncomplicated design of WHRV. The proposed technology can provide both efficient heating and cooling ventilation systems in various seasons. As Figure 3.1 shows, the proposed WHRV unit could be prefabricated into a building/room window frame and automated with advanced intelligent control systems which could provide a promising solution in providing the thermal comfort for heated/cooled buildings, while minimizing heat losses through ventilation. Horizontal installation of unit is recommended. Through the pre-test, the system could only work with a vertical position when the heating section was on the top. The thermal transfer performance of heat pipes will be limited by operation orientations. Moreover, the vertical application would take a longer time to heat up the air than horizontal scheme. Therefore, all the later lab-scale investigation was conducted based on the horizontal scheme.

Additionally, the proposed system is designed to be compact and easy to install due to its small size and light weight compared to the integration of a typical heat recovery system with conventional heat pump. There are some advantages in terms of two separated air flows, such as no moving parts to transfer heat, high reliability, no cross contamination, compact, fully reversible for preheating or precooling and easy for cleaning. Furthermore, a large cross-section can transfer a large amount of heat over a relatively long distance without inputting additional power to the system to transfer energy (BROWN, KOSSON and UNGAR, 1991).

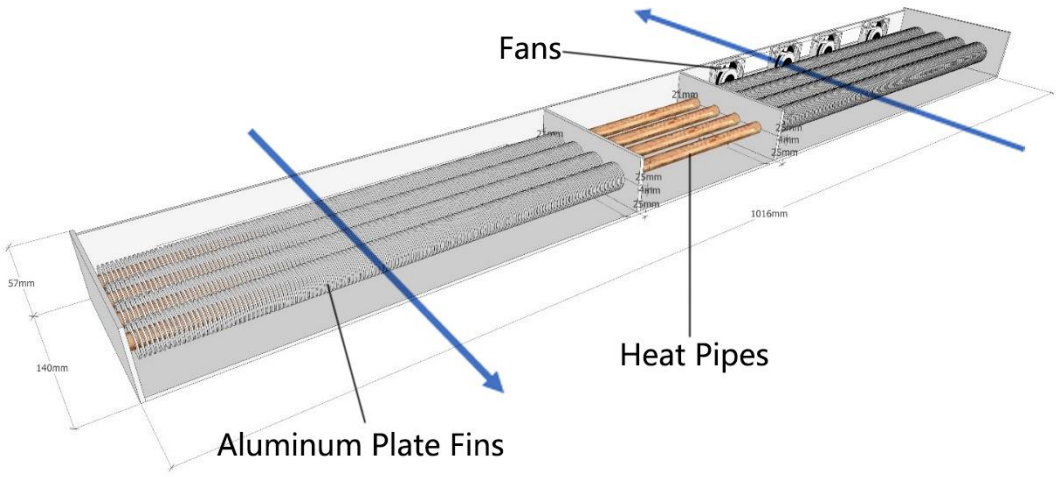


Figure 3.2 The schematic of WHRV system

A window-based unit should be much easier to fit for real application following discussion with window installation companies. The size of window frame can provide enough space for the unit. As Figure 3.2 shows, the common height and depth of frame is 6 cm and 10 cm, respectively. It will not stick out beyond the windowsill due to the current outer size. Thus, the height and depth of unit should shorter than window frame. The widths of window frames are various, commonly in 1 m, 0.915 m and 0.63 m (POINT, 2015). In order to install in the

window frame, the unit should be slim with a low profile. The length of unit should be less than the width of window frame. Therefore, the size of the WHRV is 1 m · 0.14 m · 0.057 m.

Heat pipes are used for heat transfer between air flows. The heat pipe is made of grooved copper tube with 0.0125 m in outside diameter, a wall thickness of 0.5 mm and 0.95 m in length. There are 130 continuous plain fins on both the condenser and evaporator sections. The outside diameter of each fin were 0.025 m and 1 mm in thickness. There were four 0.02 m dividers on the outside of the heat pipes and at the middle of the bank to prevent cross-contamination of return and supply air. Overall, four heat pipes were used in this experimental work, each filled with same amount of methanol with operating temperature ranges from -40°C to 100°C. At the thermal interface of the heat pipe, the liquid in contact with the thermally conductive solid surface becomes vapor by absorbing heat from the surface. Then, the steam travels along the heat pipe to the cold end, and then condenses back to the liquid, releasing latent heat. Then, the liquid returns to the thermal interface by capillary action and repeats. Since the heat transfer coefficient of boiling and condensation is very high, the heat pipe is a very effective heat conductor.



Figure 3.3 The photo of WHRV

The majority of the system has been constructed from lightweight aluminium sheet with thickness 1.5 mm. As Figure 3.3 shows, there are four fans to pump the air out. In the middle space of the unit, there is a power bank named *Power Traveller Powergorilla Multi-Voltage Portable Charger*. It can provide different DC current to power the axial fans and provide various air velocities. The maximum voltage for the fans, 12 V, 8.4 V, 9.5 V and 12 V, are applied to fans separately to get different air velocity. Furthermore, the unit can work with PV panels. The PV panels can provide DC power direct to the fans or charge the power bank without the need for DC-AC converters during daytime. During night, the power bank can supply the power to the fans. According to the testing, the fully charged power bank can power the fans for over 4 hours without extra power supply.

3.3. Experimental rigs

The evaluation was conducted using a controllable insulated box located at the Laboratory of the Department of Architecture and Built Environment, University of Nottingham. The test box was made of expanded polystyrene insulation to reduce the influence of surroundings, as Figure 3.4 shows. The test box is in size of 1.8 m·0.7 m·0.7m. The prototype was placed on one side of the test box with two separate air flow vents (supply and exhaust). The gaps between box and WHRV were sealed by aluminuim tape from the top to the bottom. The air supply fans introduce the air intake into the insulation box through the air inlets and the heat pipes. The exhaust fan exhausts the air and blows it out of the box through the air outlets. A heater fan with 2 kW capacity was placed to simulate warm condition in the test room.



Figure 3.4 Experimental Rigs

3.4. Sound level measurements

Conventional centralized mechanical heat recovery ventilator-MHRV systems are usually noisy, require pipeline transportation, are complex to install, and costly maintenance, so they are not widely used in buildings (Balvers *et al.*, 2012) (Cuce and Riffat, 2015). (Harvie-Clark *et al.*, 2019) states that the noise from the ventilation system should be less than 25 dB according to the Passivhaus Standards. According to (HM Government, 2010), noise from continuously running systems should not exceed 30 dB in living rooms and bedrooms. However, the most heat recovery ventilators can generate sound level at 45-55 dB (Seagren, 2019). Zero Carbon Hub in the UK states that the occupants interviewed by the them prefer to turn off their ventilation systems because of noise (Zero Carbon Hub, 2016).

In order to investigate the noise level of the promoted unit, the sound power level has been measured by sound level meter. Table 3.1 below summarized the devices for measurement.

Table 3.1 The testing rigs on sound level measurements

Device	Type	Description
Sound Level meter	RS PRO RS-95 Sound level Meter	Range: 30 to 130 dB
Sound Level Calibrator	Castle 01GA612 Sound level Calibrator	Accuracy: ±0.4 dB

Before the measurement, the sound level meter should be calibrated by sound level calibrator. Here are the steps to calibre the sound level meter:

1. Carefully place the calibrator on the microphone of meter

2. Activate the calibrator at the desired tone, which normally start from 94 dB, then 104 dB.
3. Keep the calibrator on until the procedure is complete and check the meter.

From the calibration, the sound level meter used enjoy the accuracy ±1.2 dB. According to the testing result, the noise level of the WHRV is 38 dB, which is much lower than other normal ventilators as mentioned in previous section.

3.5. Data acquisition

Thermocouples are common temperature measurement device, as shown in Table 3.2. However, thermocouples measure temperature based on voltage, not directly within the temperature range. As a result, the thermocouple needs to be calibrated to produce interpretable measurement information. Using water in ice and steam points to calibrate temperature is the easiest option. It can be seen from Appendix 1 that the laboratory has calibrated all thermocouples used. It can be noticed that the accuracy of the selected thermocouple is about ± 0.4°C.

Table 3.2 The information about the measurement tools

Measurement Tools	Details	Description
Datalogger	DT80 series 3	Linearization errors < 0.1°C
K-type Thermocouple	K-type	Accuracy: ±0.4°C
testo 405i Hot-wire anemometer wireless Smart Probe	0 to 30 m/s	Accuracy: ± 0.03 m/s

As Figure 3.5 shows, the DataTaker (DT85 series 3) was used as an interface between a computer and the thermocouples. The datalogger is used for the data collection. The data were collected over a period for each test. The datalogger collects the data every five seconds.

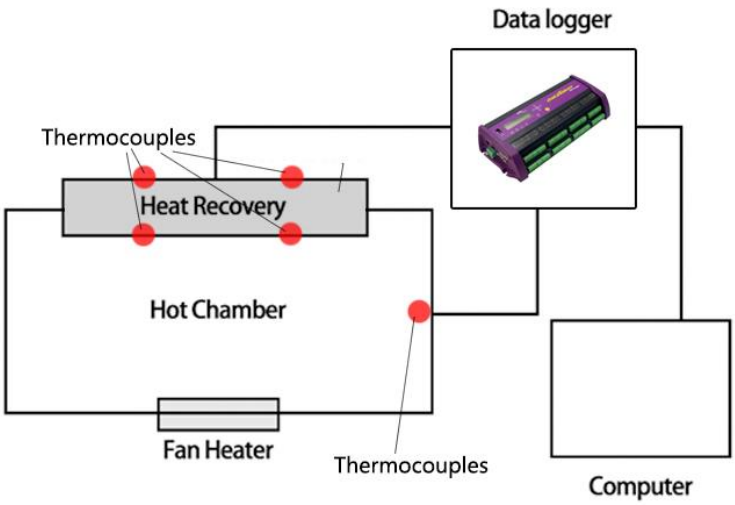


Figure 3.5 The schematic of testing rigs

In order to measure the air velocity, a hot-wire anemometer with an accuracy within 0.03m/s was used. The anemometer was used to measure the air velocity at the inlet and outlet at the same locations. The velocity readings were averaged. According to the measurement, the average air velocity of WHRV unit under 8.4 V power supply is about 1.24 m/s. And average air velocity of WHRV unit under 9.5 V power supply is about 1.79 m/s. Average air velocity of WHRV unit under 12 V power supply is about 2.45 m/s. ASHRAE Standard 62.2-2016 stated that the minimum ventilation volume is 15 Cubic Feet per Minute-cfm per person in a house with mechanical ventilation (ASHRAE, 2016). The 15 cfm equals to 25.5 m^3/h.

As shown in Table 3.3, it can be noticed that the minimum air flow rate of prototype is higher than the requirements for single room.

Table 3.3 The air velocity under different voltage supply

Power supply to fans (Voltage)	Air velocity (m/s)	Air flow rate (m^3/h)
8.4	1.24	28.12
9.5	1.79	40.6
12	2.45	55.6

Figure 3.6 states the positions of thermocouples in the testing rig. The positions of the thermocouples are listed below:

- Four locations of thermocouples in the exhaust air outside of box, T_{eout} (A, B, C, D)
- Four locations of thermocouples in the supply air outside of box, T_{sout} (E, F, G, H)
- Four locations of thermocouples in the supply air inside of box, T_{sin} (I, J, K, L)
- Four locations of thermocouples in the exhaust air inside of box, T_{ein} (M, N, O, P)
- Three locations of thermocouples in the test box, T_{box} (Q, R, S)
- Two locations of thermocouples of ambient air, $T_{ambient}$(T, U)

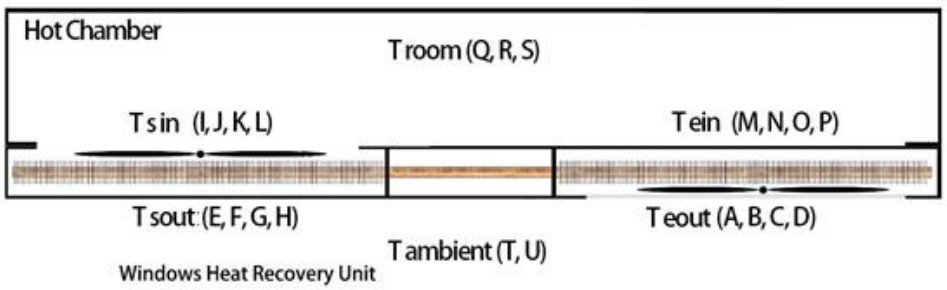


Figure 3.6 The positions of 21 thermocouples

3.6. Experimental procedure and equation

The evaluation on the thermal performance of the WHRV unit requires measurement of air velocity and air temperature of inlet air and exhaust air. Measurement for WHRV system was carried out with different air velocities under the following steps.

- Set the insulated box under high temperature environment (29 ºC), while the ambient temperature is about 22 ºC.
- Turn on the fans. And the air velocity under 8.4 V power supply is 1.24 m/s. While the ambient air was pumped into the unit from the inlet, the air inside the test room were pumped into the unit from the other side. Measure the temperature of the air flow from the two outlets.
- Then, switching the power supply from 8.4 Voltage to 9.5 Voltage, measure the temperature of the air from the two outlets.
- And finally, switching the power supply from 9.5 V to 12 V, measure the temperature of the air from the two outlets.

Effectiveness equation

According to the ASHRAE Standard, the effectiveness of heat recovery is expressed by the following Equation 2, the temperature change of supply air divided by the temperature difference between the exhaust air and the supply air (ASHRAE, 2013). The effectiveness of the heat exchanger is defined as the ratio of actual rate of heat transfer by the heat exchanger to the maximum possible heat transfer rate between the two air flows.

$$\varepsilon_s = \frac{T_{sin} - T_{sout}}{T_{ein} - T_{sout}}$$ Equation 2

While ε_s is the heat recovery effectiveness.

3.7. Test results and performance analysis

The tests were carried out to investigate the performance of WHRV unit including four heat pipes by measuring temperature and air velocity at the supply and exhaust flows. According to the evaluation results, the following parameters were calculated using equation abovementioned.

- Temperature changes under different air velocities
- Effectiveness under different air velocities

Temperature data

The tests were carried out with an ambient temperature between 22°C to 23°C and test room temperature 29°C to 31°C. It should be noticed that the unit has been sent to Wuhan in April of 2018 to install in Eco-house in Wuhan. There was only 1 weeks to test the unit in the UK. The testing condition was unsatisfactory because of limited time. The ambient temperature was about 21°C while the testing was undertaken. I am suggested to increase the temperature in box to reach about 10°C difference between inside and outside. Thus, the interior temperature of box is 30°C.

Figures 3.7, Figure 3.8 and Figure 3.9 are the temperature results while the air velocity is 1.24 m/s, 1.79 m/s and 2.45 m/s, respectively.

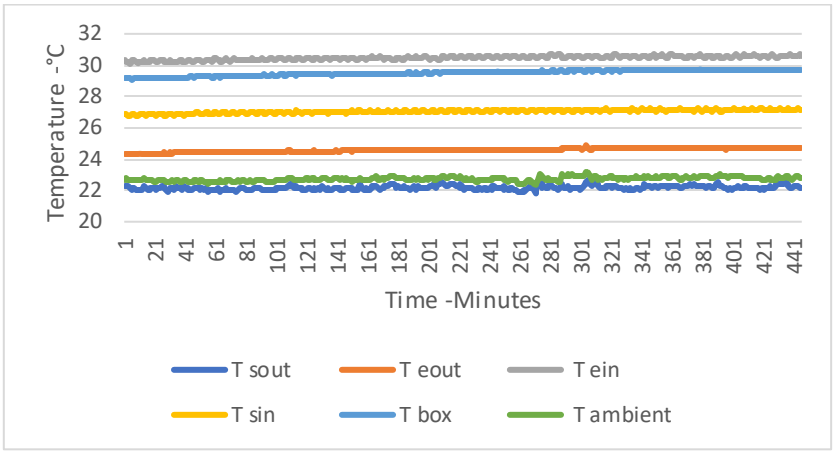


Figure 3.7 The temperature distribution while air velocity is 1.24 m/s

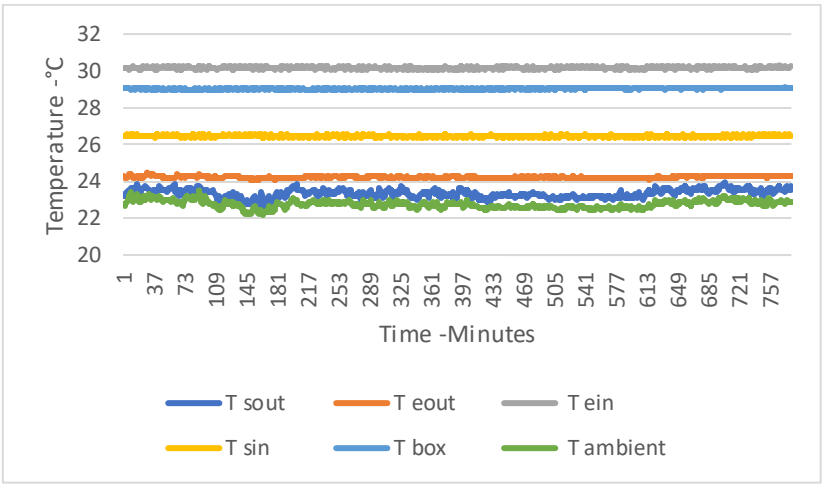


Figure 3.8 The temperature distribution while air velocity is 1.79 m/s

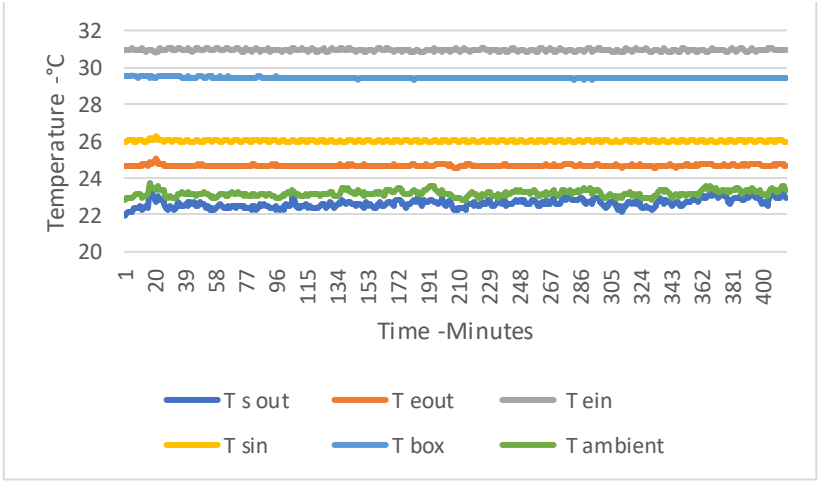


Figure 3.9 The temperature distribution while air velocity is 2.45 m/s

The temperature difference for the supply air, T_{sin}-T_{sout} was collected. The temperature difference presents the changes between supply air to the box and ambient fresh air. From Table 3.4, it should be noticed that the temperature difference will increase when air velocity decrease.

Table 3.4 The temperature difference under various air velocity

Air velocity (m/s)	Average Temperature changes (°C)
1.24 m/s	5.26
1.79 m/s	4.92
2.45 m/s	4.04

Heat recovery effectiveness

Different tests were conducted to investigate the impacts of air velocity on the heat recovery effectiveness under a stable airflow rate. The effectiveness of the crossflow arrangement heat recovery is calculated by Equation 2 based on the collected data. Table 3.5 illustrated the results of sensible effectiveness, ranging from 43% to 59%. The effectiveness of WHRV system would increase with the decrease of air velocity.

Table 3.5 The thermal effectiveness under air velocity

Air flow rate (m^3/h)	Effectiveness
55.6	43%
40.6	49%
28.12	59%

3.8. Conclusion

This chapter discussed experimental evaluation on WHRV unit performance. The unit was tested in an environmental control insulated box with various air velocities. Compared with complicated tubes and vents of traditional MHRV system, WHRV is more compact, and easier to install. Due to the current situation with coronavirus, adequate ventilation by either opening windows or mechanical ventilation devices is essential to avoid suffering from diseases (Bhagat *et al.*, 2020). This technology may play an important role in reducing the impact of the spread of COVID-19 in poorly ventilated residential/commercial buildings. Such a system will be able to effectively capture pollutants in the air and kill viruses entering the building.

Some conclusions could be conducted from the results, as shown below:

- As the air velocity increase, the effectiveness air velocity would decrease.
- When the air velocities ranged from 1.24 to 2.45 m/s, the effectiveness ranged from 43% to 59%.
- This unit is a small and light device which can achieve high effectiveness, low in noise and could be prefabricated into a window frame.
- The proposed prototype can provide both efficient heating and cooling ventilation system on various seasons.

4. The investigations on innovative photovoltaic vacuum glazing for building applications

4.1. Background

Vacuum glass has great potential to reduce heat transfer through the building fabric. Furthermore, it is a feasible approach to reduce the carbon emissions. This chapter is about the design and development of an integrated semi-transparent thin-film PV vacuum glazing with four layers of glass, named PV VG-4L.

The main aim of this testing is to investigate the high-performance PV-VG window technology. In order to evaluate the performance of PV VG-4L, prototypes were manufactured and studied under laboratory and actual conditions. At the laboratory scale, the experiments were conducted under steady-state conditions using a TEC-driven hot box in the Sustainable Energy Research Laboratory at the University of Nottingham, UK.

4.2. The design and system description

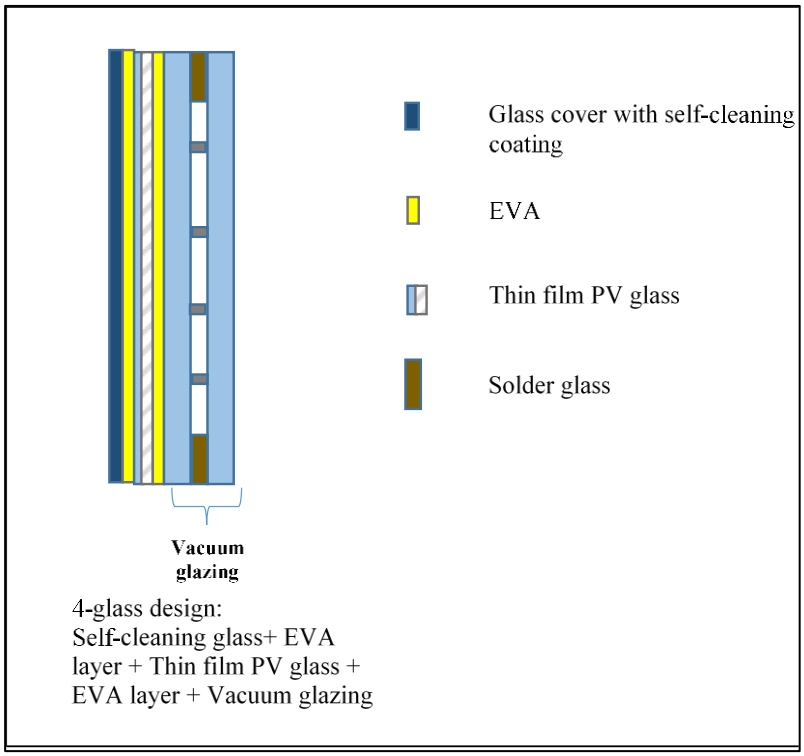


Figure 4.1 The photo of prototype

The design of PV VG-4L is illustrated in Figure 4.1. PV VG-4L integrate a thin-film PV glass window with double layers vacuum glass and extra self-cleaning coated glass layer, which has thickness about 28.5 mm. The use of a self-cleaning coating on the glass surface will increase PV lifetime, enhance efficiency by 1-3%, and reduce cleaning requirements. The layers are combined through an ethylene vinyl acetate (EVA) film. For this research, a thin film PV glazing with 40% transparency was used.

The novel PV VG-4L was made by the combination of a conventional vacuum glazing and PV thin film glazing system. The PV VG-4L has sandwich structure with the polyvinyl butyral. The transmittance of the PV laminated glass is about 35%.

The PV VG-4L is shown in Figure 4.2. The dimension of the PV VG-4L prototype is 300 mm · 300 mm · 28.5 mm, much thinner than conventional triple glazing. The novel glazing technology can produce power as well as offering the highest thermal insulation performance. Additionally, the novel glazing system is suitable for the building integrated Photovoltaic-BIPV applications.



Figure 4.2 The schematic of PV VG-4L

4.3. Using hot-box method for investigation of the PV VG-4L thermal performance

An affordable small hot box suitable for thermal performance measurement on glazing unit

This section presents a small affordable hot box built in the Department of Architecture and Built Environment, the University of Nottingham. Whilst no specific European Standards are available for the small hot box, at a cost of approximately GBP 10,000, the design, development and utilisation of the hot box were performed by taking into account almost all the requirements outlined in the ISO 8990 and ISO 12567 standards (Klems, 1979). As Figure 4.3 shows,

the hot box comprises three components, including the metering box, the prototype panel, and the cold/hot box. The box is designed by considering the minimum requirement for the metering area according to ISO 8990 (1 m · 1 m) and the maximum size of the window that can be tested is 1.2 m · 1.2 m. In order to ensure uniform air circulation at the air speed requirement specified in ISO 12567, a baffle with a series of 12 V Direct-Current fans was installed in each of the cold and hot areas. Innovative heating and cooling elements were introduced in the design of the hot box using two separate units of thermoelectric (TEC) air to air heat pumps at 102 W capacity, capable of achieving 3°C to 45°C in the cold and hot enclosure respectively.

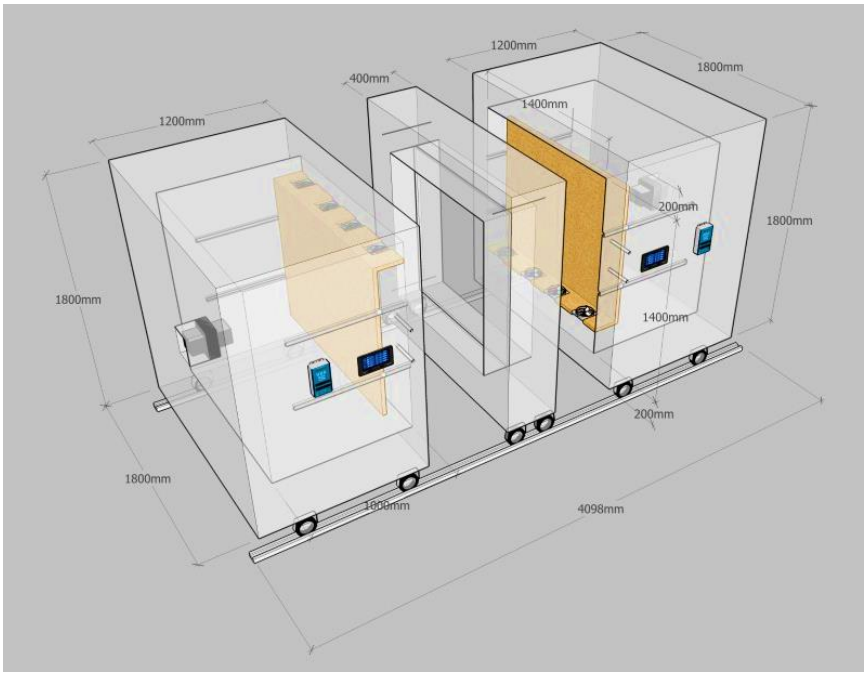


Figure 4.3 The schematic of hot box

The box which provides warm air and represented indoor conditions, is called the metering box; meanwhile the box which provides cool air and represents outdoor conditions is the cold box or the environmental chamber. The panel

that holds the prototype is called the prototype panel. In the design of the hot box, the following important requirements should be satisfied,

- Good wall insulation. The heat flow rate through the wall must be small enough to be neglected.
- High airtightness. The gaps between the components should form an air- and water-vapour-tight enclosure to avoid unexpected heat or moisture transfer.
- The prototype panel is a critical component, and lateral heat flow is minimized by edge insulation.

The small hot box was constructed using Polyisocyanurate (PIR) insulation core from EcoTherm of 0.022 W/(m·K) and at 150 mm thick which gives a heat flow rate through the metering box at a temperature difference of approximately 0.18 W/(m^2·K). In order to minimise the heat loss through the perimeter of the specimen, the edges of the metering and cold box that meet the specimen panel are fitted with a rubber tape. The assembly is closed tightly using a clamp mounted on the frame of the boxes.

An air-to-air thermoelectric heat pump (TEC-HP), AA PowerCool Series AA-100-24-22, at capacity of 102 W was used to provide heating and cooling environment to the space. The heat pump is environmentally friendly since no compressor or refrigerants are involved in the heating and cooling process. An easy-to-use PC software is included for programming and visual review of output parameters. The temperature sensor which controls the output of the controller uses T type thermocouples which is located between the baffle and the specimen. It is noticed that, to monitor the heat flux rate from the metering area, a total of 16 thermocouples were placed on the inner surface of the metering wall as Figure 4.4 shows.

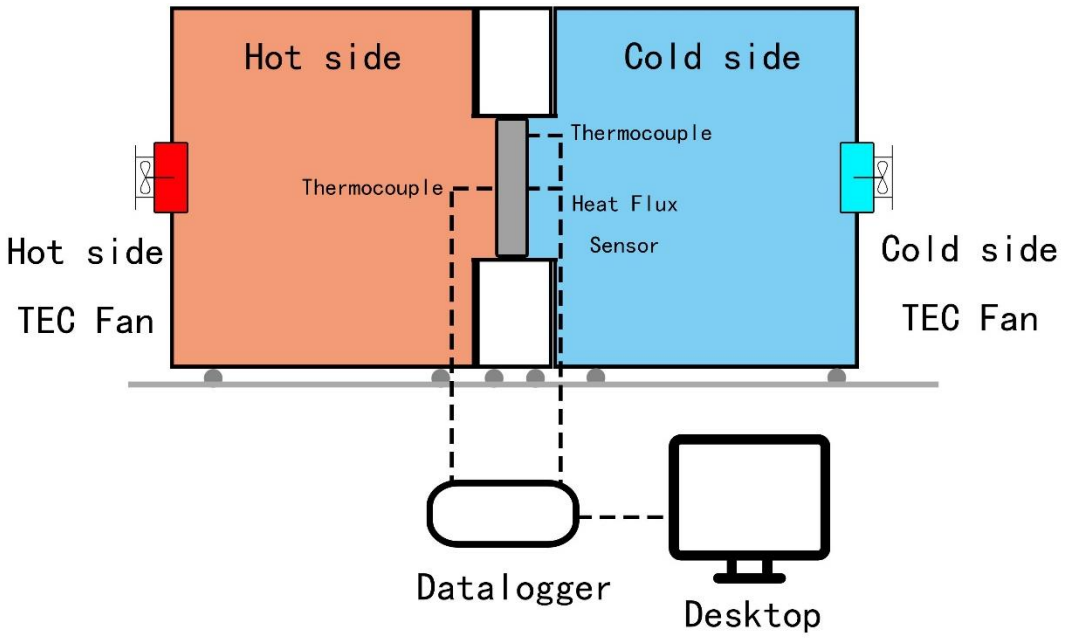


Figure 4.4 The schematic of the testing process on hot box

Since different materials have different thermal mass values, the temperature should be steady state. To check the temperature variation within the hot box, an insulation sample at 150 mm thickness has been used for verification. From the analysis, the measured U-value of the sample is 0.020 W/(m^{2}K) meanwhile the value given by the manufacturer is 0.022 W/(m^{2}K). Figure 4.5 presents the measured temperatures on the insulation layer at steady state condition for about 6 hours.

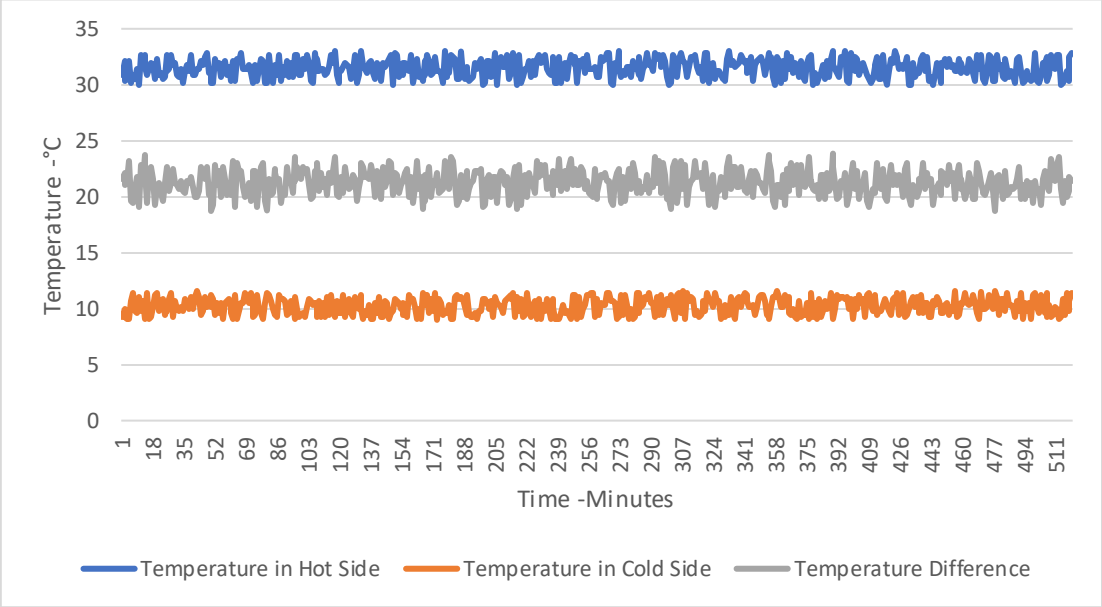


Figure 4.5 The measured temperatures



Figure 4.6 The hot box with the installed PV VG-4L

A PV VG-4L prototype, as Figure 4.6 shows, was manufactured. By following closely ISO 12567 standards, the PV VG-4L was installed at the prototype area of the hot box. As Table 4.1 shows, the test was performed under three different temperature conditions. However, the air velocities on the hot and cold sides are fixed at 0.3 m/s and 1.5 m/s, respectively. Using a hot box, the total heat transfer coefficient can be estimated from the hot and cold surfaces of the PV VG-4L prototype. Based on the Equation 4, the measured U-value of PV VG-4L was presented in Table 4.1.

Table 4.1 Experimental results for the glazing surface temperature and U-value using the calibrated hot box

Surface temperature on the hot side °C	Surface temperature on the cold side °C	U-value W/(m^2· K)
33.4	19.6	0.58
26.76	14.62	0.56
25.32	9.91	0.56

4.4. The studies of the performance of PV VG-4L under real conditions

The on-site performance of PV VG-4L under real sky conditions was investigated for the power generation performance. This section first discusses the thermal performance of the PV VG-4L under real conditions. The prototype was installed at the E. ON House at the University of Nottingham, United Kingdom. The PV VG-4L was set up horizontally 0.9m above the floor on stilts so that the solar condition of the prototype is like the common glazing of a house.

During the testing, various parameters were measured, including the ambient air temperature, the exterior solar irradiation, the outside and inside surface temperature of the prototype as well as the I-V curve and the power generated by the prototype. Figure 4.7 shows the installation of the PV VG-4L.

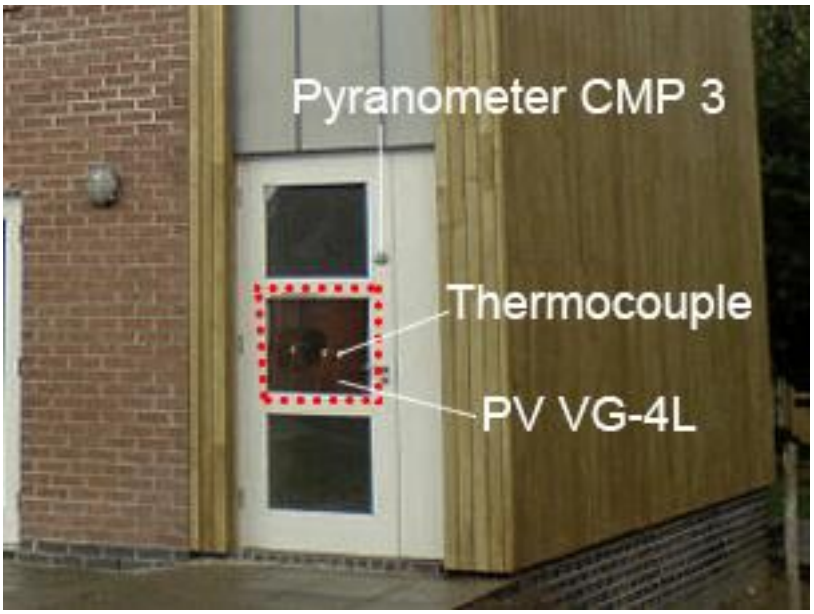


Figure 4.7 The photo of testing rigs

It is important to note that the pyranometer to measure the incident solar irradiance was placed parallel to the surface of the PV VG-4L. The thermal and electrical characteristics of PV VG-4L under real conditions were monitored using the sensors summarized in Table 4.2. It is worth noticed that the outdoor monitoring of PV VG-4L is carried out under two conditions: daytime and night-time. In the daytime, the thermal transmittance reading of PV VG-4L given by the heat flux sensor can get the heat gain value. A 1 kW convective heater was used as the heat source.

Table 4.2 Measured parameters and accuracy

Parameters	Sensor	Accuracy
Heat flux	Hukesflux Thermal Sensors	± 1.9 x 10-6 V/(W/m2)
Solar irradiance	CMP3 Pyranometer	Temperature dependence of sensitivity: ±5%
Maximum power produced by the PV VG-4L	RO4 Handheld Digital Multi-meter	Electric current (±1.5 μA)

Hukesflux heat flux sensor is made of ceramics and plastic combined as flat plate. It is installed on the cold side of the wall to measure the heat flow from the hot side of the wall. It generates a small amount of voltage, which will be recorded by DataTaker, and then divided by the sensitivity of the HF01 heat flux to calculate the heat flow. Thus, it was used to measure the heat flow from the hot side of the wall to the cold side of the wall. It has been proved by ISO 9869 and ASTM C1046 to be used to calculate R-value and U-value. CMP3 Pyranometer is proved by ISO 9060 spectrally flat Class C.

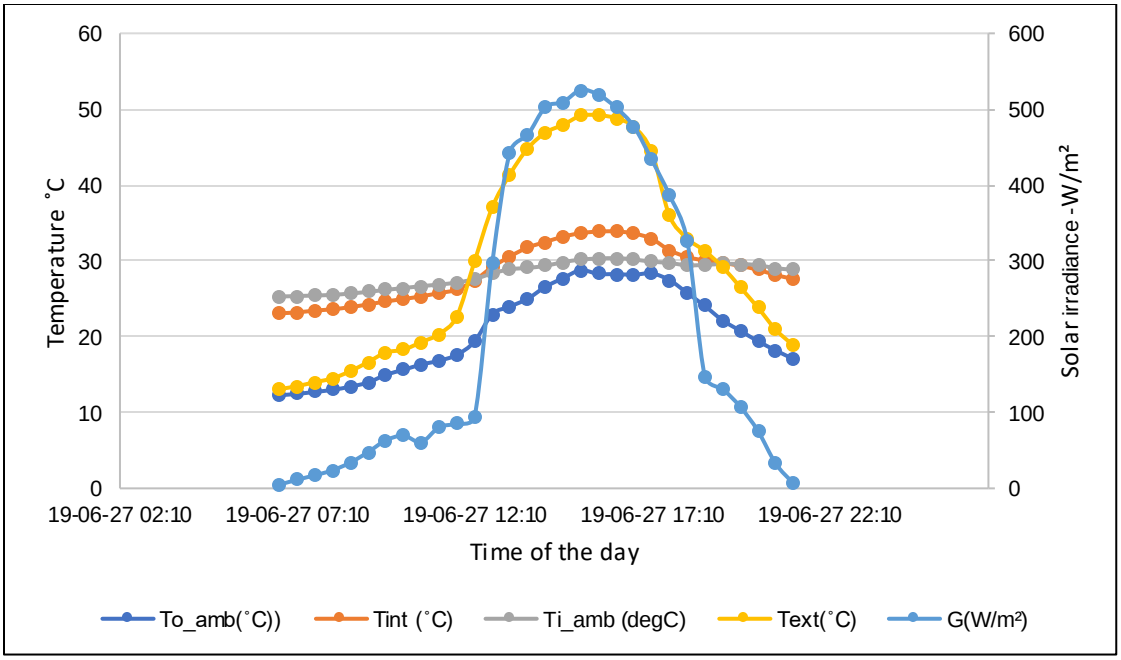


Figure 4.8 Variation in the outside glazing surface temperature (To-amb), inside glazing surface temperature (Tint), Outdoor ambient temperature (To-amb), indoor ambient temperature (Ti-amb) and solar irradiance (G) with time of the day.

Figure 4.8 shows the changes in the surface temperature of the outer glazing, the surface temperature of the inner glazing, the outdoor ambient temperature, the indoor ambient temperature, and the solar irradiance during the day. All the data below are collected in June of 2019, the average interior temperature was heated up to 30 ˚C by a convective heater. At night, the internal temperature of the prototype is higher than its external surface temperature. However, as the incident solar irradiance increases, the outer surface temperature also increases. As the prototype absorbs the solar irradiance, some of the radiation was converted into heat energy. The heat energy would increase the temperature of the outside glazing surface. Therefore, the external surface temperature became higher compared to its internal surface temperature of the prototype. Compared with conventional single thin film PV glazing, the vacuum layer behind the PV component can act as an insulation layer to reduce the heat transfer though the prototype.

As Figure 4.9 shows, the overall U-value of the PV VG-4L was measured to be as low as 0.6 W/(m^{2}K), which is similar to the laboratory test result.

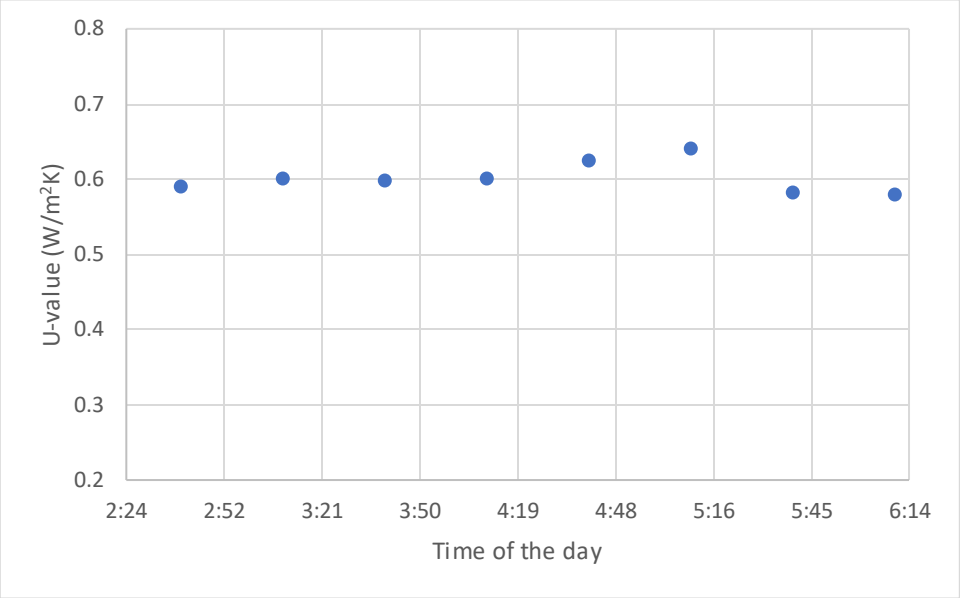


Figure 4.9 The measured U-value of the prototype during night

(Waichal, 2018) stated that any exposure to the conditions outside the specifications, such as direct sunlight, rain or wind will certainly have adverse effect on the output from Hukesflux sensor. During testing, the Hukesflux sensor is attached on the outerior side of PV VG-4L. The sensor would be affected by the direct sunlight. In order to mitigate the impact from sunlight, the measurement on the thermal transmittance should be undertaken during night-time.

The investigation on the thermal performance of PV VG-4L has been presented. The power generation performance of the prototype is provided below. From Figure 4.10, it can be concluded that the maximum power generated at average solar irradiance of 500 W/m^2 is approximately 2 W for 0.4 m x 0.4 m PV VG-4L made of amorphous silicon solar cells. Thus, the PV output rate is about 12 W/m^2.

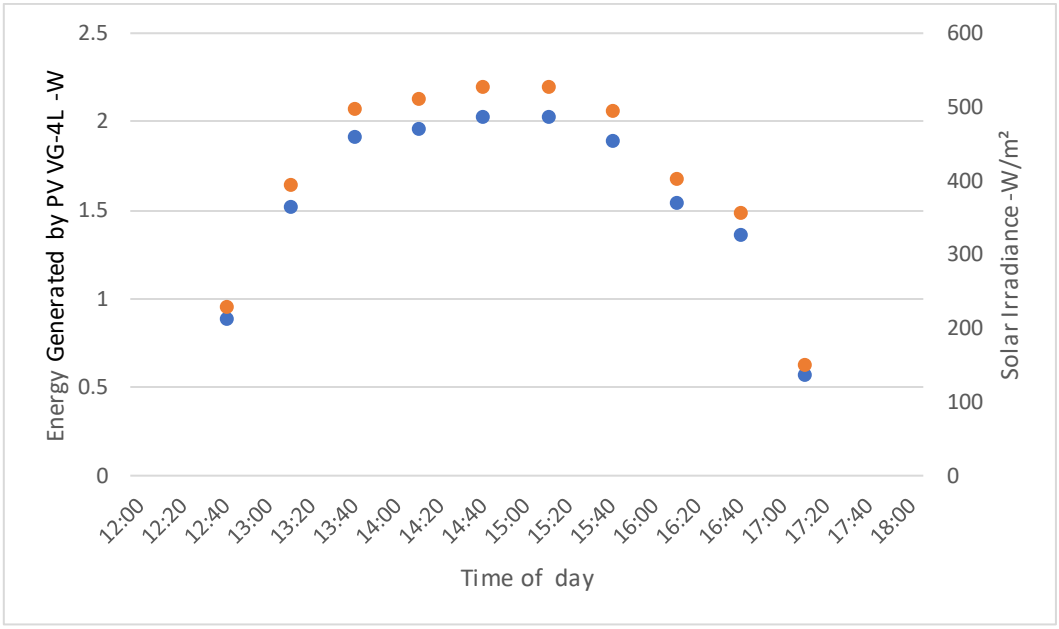


Figure 4.10 The power generation (W, blue dots), the solar irradiance (W/m^2, orange dots)

4.5. The impact of solar transmittance of PV VG-4L

During winter, the PV VG-4L can effectively conserve the heating energy. During summer, the vacuum PV glazing provides the most energy-saving for cooling. From the measurement of project partner, the solar transmittance of PV VG-4L is about 36%. Solar gain is a particularly effective form of passive heating as the radiation from the sun is mainly short-wave infrared radiation, which can pass through the glazing and heat the internal structure of the building. The low solar transmittance can result in the low level of solar energy

gains. Thus, the application of the prototype requires additional heating energy in winter because of its solar transmittance. Furthermore, the low solar transmittance would affect the daylight in the room. (Qiu and Yang, 2020) stated that vacuum PV glazing can provide more useful than daylight illumination in room and avoid the daylight glare for the interior space. The PV VG-4L reduce the unwanted solar illumination, and the power generated can supply to the artificial lights.

4.6. Conclusion

From the indoor analysis, the U-value of the proposed glazing system is about 0.58 $W/(m^2 \cdot K)$. Meanwhile, when investigated under real conditions (field testing), the overall U-value of the PV VG-4L was measured down to 0.6 $W/(m^2 \cdot K)$. As the solar irradiance increases, the solar heat absorbed by the thin film PV glazing layer, has led to the increase temperature of the external glazing surface. The vacuum layer of the prototype could help to reduce the heat transfer from outside to inside. At average solar irradiance of 500 W/m^2, the PV VG-4L can generate maximum 2 W energy. Thus, the PV output rate is about 12 W/m^2.

Clearly, the vacuum layer introduced in the PV VG-4L glazing presented in this paper is better in thermal performance as an additional benefit. The results show that PV VG-4L not only can generate electricity, but also has high insulation performance compared to a single-film PV glass with a typical U value of about 5 $W/(m^2K)$. The U-value of PV VG-4L has improved by almost 90% over single-film PV glass. The performance of the PV VG-4L promises a

wide range of potential applications. Furthermore, the proposed PV VG-4L is a combination of the conventional vacuum glazing and thin film PV glass. There is no manufactural difficulty in factory. The factory even does not need to change the production line and just combine two parts together. Thus, the current manufacture factory would prefer to produce the PV VG-4L products over other novel vacuum PV glazing system as almost no need for the cost on design and research.

It should be mentioned that the design and sample of PV VG-4L was proposed and manufactured in 2019. Thus, the PV VG-4L was not installed and tested in Eco-house.

5. Theoretical analysis and evaluation of the Eco-house in Wuhan

5.1. Introduction

In China, there are over 600 million people living in rural areas. However, less than 1% of the houses in Chinese rural areas are sustainable buildings. The previous conventional house with several disadvantages, such as poor daylighting and bad sound insulation, cannot satisfy the modern requirements on house. People would prefer to purchase new-built property with modern characteristics. There would be a massive market opportunity and potential to promote the new-built sustainable house which can minimise the requirements on the grid power supply and energy loss through constructions.



Figure 5.1 The photo of Eco-house in Wuhan

As Figure 5.1 shows, the Eco-house is an innovation building designed to handle the challenges discussed in the Chapter 2. This house is the first attempt on construction and operation of budget low-carbon house in the central area in China. The project partner had an agreement with the local government that

this building would be an important attempt to the *China Council for the construction of new socialist countryside Policy* in Hubei Province. In addition, the property provides an opportunity to evaluate the feasibility of sustainable prefabricated houses for low-income families.

This chapter demonstrates the design process and experience to minimise the energy consumption of Eco-house. A substantial investigation into the performance of a budget sustainable house is covered as well.

5.2. The requirements of the low-carbon building

Sustainable design is regarded as the particular way to construct and operate a building by using as much as possible natural resources, such as heat, air, passive solar gain, and cooling. Through the passive design, the use of mechanical systems can be reduced by about 80%. The laws limiting the energy using of buildings are most complex, covering the requirements on heating/cooling loads, thermal performance of building components and air infiltrations.

Table 5.1 summarizes the requirements from the various building regulations.

Table 5.1 The requirements on the building components on various regulations

Regulations	Hot Summers, Mild Winter (Ministry of Housing and Urban-Rural Development in China, 2015)	Passivhaus Standard	CfSH-Code 5	CfSH-Code 6
Building Fabric W/m^{2}K	0.20-0.35	0.15-0.1	0.2	0.1
Windows W/m^{2}K	1.0-2.0	0.8	1.2	0.8

The requirements of CfSH Code 6 on building fabric are higher than the Passivhaus Standard, and they have more demanding requests on airtightness. However, the above standards might not be suitable for Chinese climate conditions, especially in Wuhan, and are needed for extra adjustments. Wuhan is located in the area named' Hot Summers and Cold Winter'. 'Hot summer and cold winter' areas mean that the average temperature of the coldest month is about 0~10°C, and the average temperature of the hottest month is about 25~30°C. The buildings in this area must consider the requirements of the well-insulated building fabric for winter and summer. Based on the 'Passive ultra-low energy consumption green building-Technical guidelines' and above other standards, the energy performance of the Eco-house in Wuhan should satisfy the following requirements.

- The annual heating/cooling demand must not be more than 15 kWh/m^2 per year.

- The maximum air tightness level should less than 0.6/h at 50 Pascals pressure
- The interior room temperature should be maintained between 20°C to 26°C as required by building regulation in China

The operation schedule of the house in a rural area is listed in Appendix 4. The occupants spend their time in the Bedroom during the night and about 5 hours in the Livingroom during the daytime. The schedules for weekdays and weekends are also different.

5.3. The development process for the Eco-house in Wuhan

Nowadays, many governments encourage low-carbon design, which refers to the architectural strategies applied by the architect and engineer to respond to the climate conditions and requirements (Ahmad, Thaheem and Anwar, 2016). In order to obtain a clear process of sustainable design, the Eco-house in Wuhan would use sustainable design with the help of the Building Information Model. The design procedure for the Eco-house is summarized below.

1. Analysis the site of Eco-house in Wuhan
2. The Eco-house designs
3. Design and investigations on the thermal performance of components
4. Testing the overall performance of the Eco-house
5. Computer simulation on Eco-house
6. The construction experience of the Eco-house in Wuhan

Analyse the site of the Eco-house in Wuhan

Wuhan is located in the centre of China. The climate of Wuhan is a subtropical monsoon climate, which is warm and moist humidity in summer, cold and dry in winter. The summer precipitation is about 1000 mm, which accounts for about three quarters of the annual precipitation. Thus, evaporative cooling is not suitable for applications in Wuhan. Furthermore, the Chinese government has forbidden the application of city-level central heating supply for Wuhan urban area since the 1950s. The insulation performance of Eco-house is necessary, as the average temperature during winter is much lower than the comfort temperature for humans.

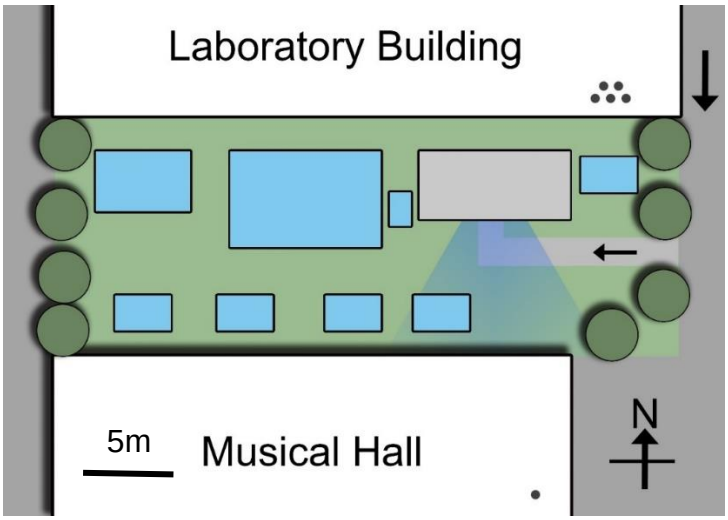


Figure 5.2 The plans of the site

The construction site is located in the Hubei University of Technology-HBUT, Hongshan District, Wuhan. The size of the site is about 120 m · 35 m, alongside a boulevard. As Figure 5.2 shows, a music hall is located on the south side of the site. The height of the music hall is about 8 metres. And, on the north side, there is a five-storey experiment building. Furthermore, on the northeast side

of the site, there is a photovoltaic car-parking experimental structure. Through the lighting and ventilation analysis from the computer programme, the best choice of the site is chosen, the grey area. The existing buildings, the white rectangles, have not considered the quality and visibility of human life and other existing factors for the Eco-house. The construction site used to be a grassland for relaxation and entertainment. Furthermore, the height of the music hall would have negative effects on the illumination and visibility quality. The narrow space for the new-built house would cause insufficient sunlight to be received by the building.

The new-built house has a chance to get the direct wind blowing from the western side of the building. In order to get better ventilation movement and sunlight angle, it is required that the Eco-house be far away from other existing buildings. It aims to avoid the negative effects of other buildings and give more 'free' spaces.

The Eco-house design with BIM

The concept of the Building Information Modelling-BIM is a life-cycle platform merging design, construction, energy analysis and cost analysis. It enables all parties to work on a project with a shared platform. The building component has been utilising various information and visualisation technologies to support construction activity. Compared with the Computer Aided Design (CAD), the BIM is increasing the visibility in three dimensions, especially when designing and representing complex areas or complex elements. The most common BIM software is Autodesk Revit. The software allows users to design a building with

structure and its components in 3D. In addition, the software would set the properties of the building performance, such as thermal resistance, structure and so on.

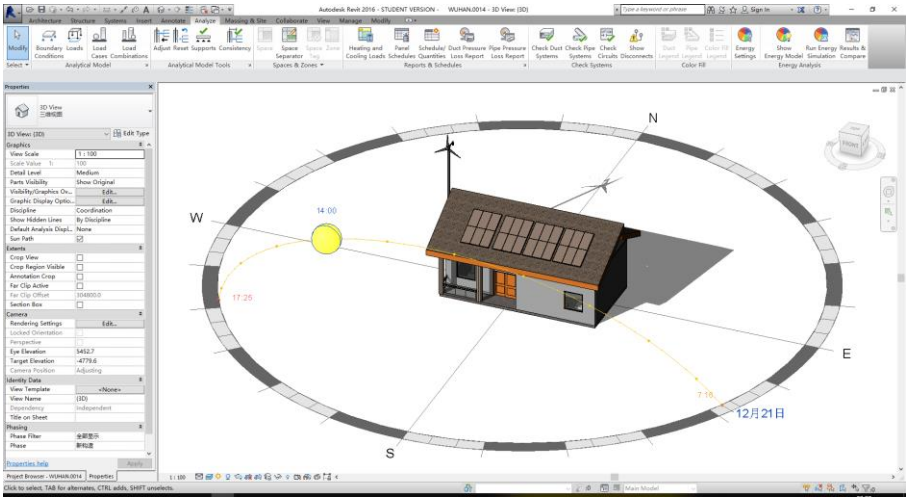


Figure 5.3 The screenshot of the 3D model in Revit

As Figure 5.3 shows, the shape of the building should not be complicated to reduce the capital cost of construction, and to make all the technology integrated easily into the component of the building.

This Eco-house is for the people who lived in the rural area in Hubei Province. Most of the families are extended families. Extended families include at least three generations: grandparents, married offspring, and grandchildren. Normally, the labours of the family are always away from their hometown and work in the city for higher income. Thus, the most common family in the Chinese rural area includes the grandparents and grandchildren. The common number of family members is about 3-4 people. Currently, the new-built house in rural area only has two or three bedrooms with one living room.

As Figure 5.4 shows, the layout of this building includes two bedrooms with one living room. The north-south orientation can make full use of the natural sunlight and ventilation. Both living room and bedroom can get direct sunlight all day. The rooms will be more likely to gain the maximum solar irradiance during winter.



Figure 5.4 The layout of Eco-house

In order to make the building easy to manufacture, the building components are designed in the module concept. From Figure 5.5, the size of all the building fabric is 3 m · 3.9 m and are easy to prefabricate in the factory. Besides the careful layout of the building envelope, the structure was designed for better performance.



Figure 5.5 The photo of the prefabricated structure

Because of the application of PV panels on the pitched roof, the angle of the roof should consider being the optimum angle of PV to get the best performance. The optimal angle of the PV panel could be determined by the latitude and longitude of Wuhan. The latitude and longitude coordinates for Wuhan (China) is 30.58333 °, 114.26667 °. For different seasons, the angle of the adjustable PV panel is shown below,

$$A_{su} = L_W * 0.92 - 24.3 \quad \text{Equation 3}$$

$$A_{s/a} = L_W * 0.98 - 2.3 \quad \text{Equation 4}$$

$$A_w = L_W * 0.89 + 24 \quad \text{Equation 5}$$

While,

the A_{su} is the angle of the PV panel in summer,

the $A_{s/a}$ is the angle of the PV panel in spring and autumn,

the A_w is the angle of the PV panel in winter,

The L_W is the latitude of Wuhan.

Based on the above equations, the optimal angle for the adjustable PV panel for various seasons is listed below in Table 5.2. The average angle of the above gable solar panel is 27 °.

Table 5.2 The optimal angle (°) for the adjustable PV panel

Jan	Feb	Mar	Apr	May	Jun
43	35	27	19	21	4
July	**Aug**	**Sep**	**Oct**	**Nov**	**Dec**
11	19	27	35	43	50

However, most of the BIPV panels on the roof have fixed angles. Without the adjustable PV panel, less power would be generated. As for the city latitude between 25° and 50°, this equation 11 is used to calculate the best angle for fixed PV panel,

$$A_{city} = L_W * 0.76 + 3.1 \quad \text{Equation 6}$$

The A_{city} is the angle of the PV panel where the latitude of the city is between 25° and 50°. The optimal angle of the fixed PV panel is about 26°, which is

similar to the average adjustable angle above. Thus, the angle of the pitched roof is about 26° in order to maximise the PV generation performance.

To access solar energy potential in different areas, PVGIS (Photovoltaic geographical information system) developed by European Commission Joint Research Centre as an online tool could be friendly to estimate the solar power generation capacity of PV systems (Ghazi and Ip, 2014). The general efficiency value, 14% for the polycrystalline panel, is suggested by PVGIS, as Figure 5.6 shows.

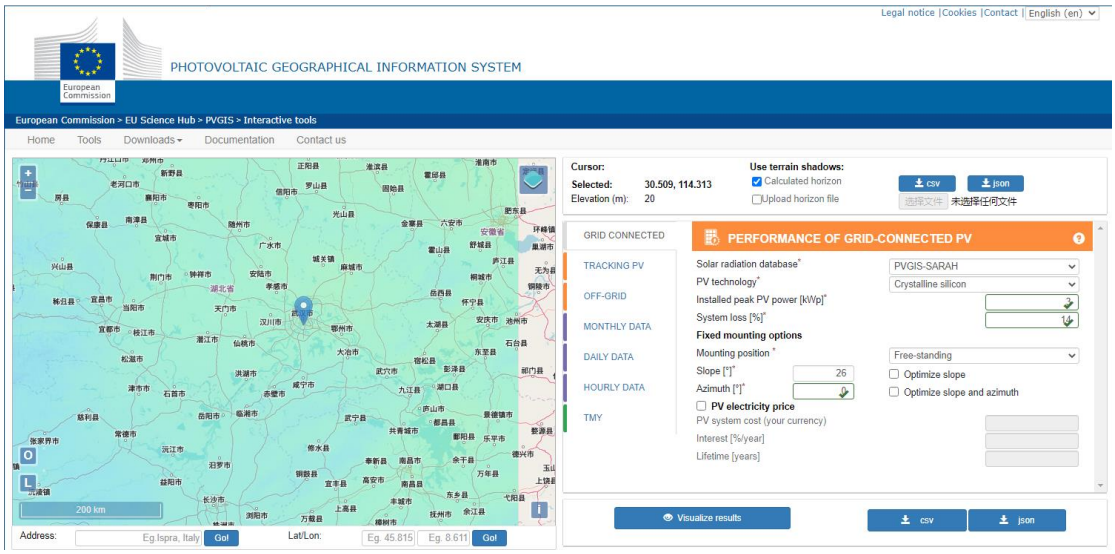


Figure 5.6 The screenshot of PVGIS

The estimated annual power generation from PV panels is 3259.61 kWh. The monthly energy generated by the PV panel has been presented in Figure 5.7.

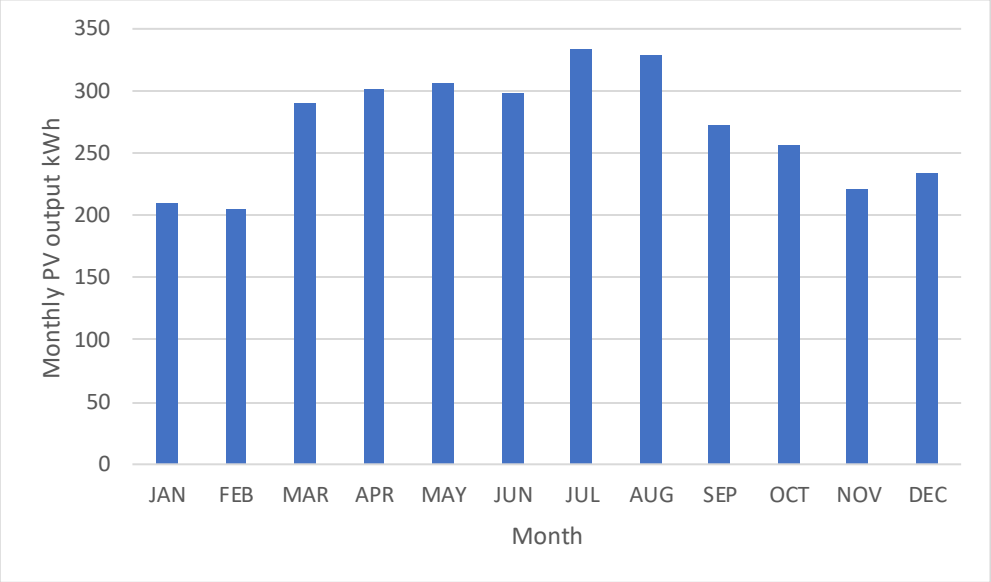


Figure 5.7 The power generation of PV panel

Design and investigations of the thermal performance of building components

Prefabrication of windows, doors, kitchen cabinets, and roof has become an important role in Eco-house construction. Recent innovations have resulted in an even wider variety of prefabricated components. This section is to evaluate these prefabricated building components. The thermal performance of the wall, WHRV, door and vacuum glazing system was also investigated.

Exterior door

Door is usually used for the entrance and provides effective protection against external temperature, noises, or other factors. A well-insulated door should have several characteristics, such as a highly insulated body and air tightness. The cost of the insulated door is much higher than the normal door. But there is no clear regulation defining the thermal performance of the exterior door in Wuhan. In order to reduce the capital cost of the building, the constructor would prefer the normal door rather than the insulated door.

The 'Technical Specification for Door and Windows of Residential Buildings DB11/1028-2013 in the Beijing Area' requires that the U-value of the door should be less than 1.8 W/(m^2K). The climate in Wuhan is much warmer than in Beijing. The regulations in Beijing can satisfy the requirements for an exterior door in Wuhan. Figure 5.8 shows the details about the designed hollow core wooden door with a U-value of 1.87 W/(m^2K) in Revit.

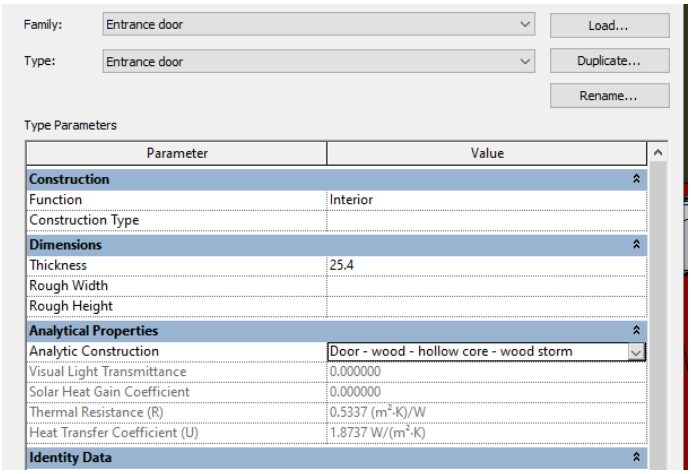


Figure 5.8 The screenshot of setting on the exterior door in Revit

However, the measured U-value of the door is about 3.46 W/(m^{2}K). The performance of the exterior door is far away from the demands. In the future, the project partner would replace and retrofit the door with better thermal performance.

Windows heat recovery ventilator



Figure 5.9 The photo of the WHRV system installed above the window frame

In Eco-house, the experimental investigation was carried out by placing the WHRV unit above the window frame, as shown in Figure 5.9. This section investigates the on-site performance of the novel Window Heat Recovery Ventilator (WHRV) installed in the Eco-house, especially the impacts from the temperature difference between inside and outside. The proposed WHRV unit has been tested in the UK under laboratory conditions as Chapter 3 states. Then, in 2018, the unit was delivered to Wuhan by air.

As in the previous chapter, the measurement for heat recovery effectiveness was carried out with different temperature differences between inside and

outside. Most of rigs are the same as with previous testing. The testing required extra anemometer, RS PRO AVM-01 Vane, with an accuracy of ±3%.

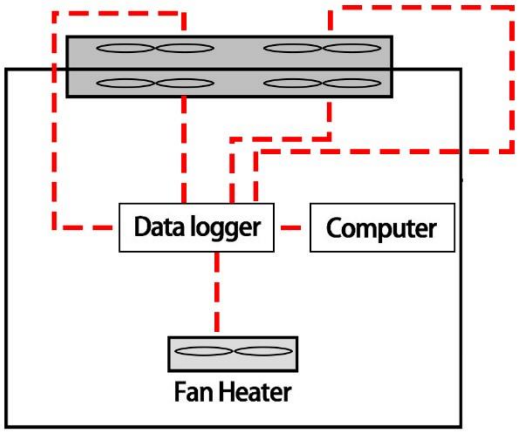


Figure 5.10 The schematic of the measurement on WHRV system in Wuhan

As Figure 5.10 shows, the measurement steps on the WHRV system have been listed below. The DC power supply for the fan was set to 8.5 V. The measured air velocity is 1.24 m/s.

- Turn on the fan heater. Set the inside temperature at about 21°C, while the outside temperature is about 18°C. Measure the temperature of the air flow from the two outlets by thermocouples and record the data every 3 seconds by datalogger.
- Then, switch the fan heater to a higher power to adjust the internal temperature. At this time, the internal temperature is 9°C higher than outside. And measure the temperatures of the air flow.
- Finally, adjust the temperature gap to 15°C and take the measurement.

Based on Table 5.3, the heating effectiveness of the WHRV system is about 55% under various temperature gaps between inside and outside. The testing result is slightly lower than the laboratory testing results, 59%. It is noticed that

the temperature difference between inside and outside almost has no impact on the effectiveness of the WHRV system than the air velocity.

Table 5.3 The summary on the effectiveness of WHRV system under various temperature gap

Exterior Temperature °C	Interior Temperature °C	Temperature gap °C	Effectiveness
18	21	3	57%
18	27	9	56%
18	33	15	54%

The measurements on Eco-house were undertaken in May of 2018. The exterior temperature in Wuhan is about 17°C to 37°C. There was no satisfactory testing environment in Wuhan. Thus, we and our project partner decided to adjust the interior temperature to simulate the hot weather in Wuhan. And the exterior temperature is to simulate the interior temperature. Through above the method, the operation condition during the summer of WHRV has been simulated.

The glazing system for Eco-house

The most common glazing types for domestic buildings are single glazing, multilayer-insulating glazing, and vacuum glazing. Currently, single glazing is becoming a thing of the past, and is being replaced with more durable and efficient counterparts, double glazing, and vacuum glazing. Air-filled double glazing is the most common fenestration products in the market as a consequence of their well-documented manufacturing process and considerably better thermal insulation feature compared to conventional single glazing (Cuce, 2016). Double glazing has been widely used in the EU and China. The unit price of the double glazing is not like before because of massive manufacture. A conventional vacuum glass window is composed of two flat glasses separated by a vacuum cavity and small pillars.

This section investigates the thermal transmittance of three types of glazing above mentioned. The main aim of the research is to find the best glazing type compatible with the higher level of the Code for Sustainable Homes and Passivhaus Standards.

Mathematical analysis of the heat transfer process

BS EN ISO 6946 and CIBSE Guide A quote standard values for the thermal resistance of unventilated cavities providing a function of the thickness of the cavity and the direction of heat flow, which are shown in Table 5.4, Table 5.5, and Figure 5.11.

Table 5.4 The surface resistance values (*MCRMA*, 2006)

Surface Resistance	**Direction of the heat flow**		
$m^2 \cdot K/W$	Upwards	Horizontal	Downwards
R_{si}	0.1	0.13	0.17
R_{se}	0.04	0.04	0.04

· Rsi: internal surface resistance, Rse: external surface resistance

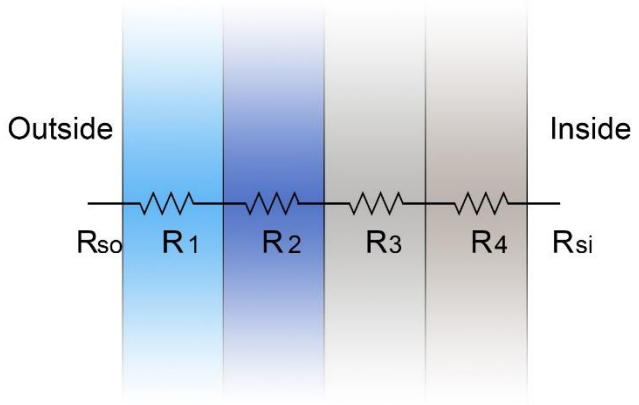


Figure 5.11 The schematic of summing thermal resistances

$$R_G = R_{so} + R_1 + R_2 + R_3 + R_4 + R_{si} \quad \text{Equation 7}$$

Table 5.5 The coefficient of thermal conductivity W/(mK) of unventilated air cavities (MCRMA, 2006)

Thickness of the air cavity (d)	**Direction of the heat flow**		
	Upwards	Horizontal	Downwards
5	0.045	0.045	0.045
7	0.054	0.054	0.054
10	0.067	0.067	0.067
15	0.094	0.088	0.088
25	0.156	0.139	0.132
50	0.313	0.278	0.238
100	0.625	0.556	0.455
300	1.875	1.667	1.304

The values in above Table 5.5 are directly proportional to the thickness of the layer, ***d*** in metres, and can be expressed as:

- Upwards heat flow: $\lambda = 0.00511 + 6.227 \cdot \boldsymbol{d}$ W/(mK).
- Horizontal heat flow: $\lambda = 0.00858 + 5.518 \cdot \boldsymbol{d}$ W/(mK).
- Downwards heat flow: $\lambda = 0.0247 + 4.268 \cdot \boldsymbol{d}$ W/(mK).

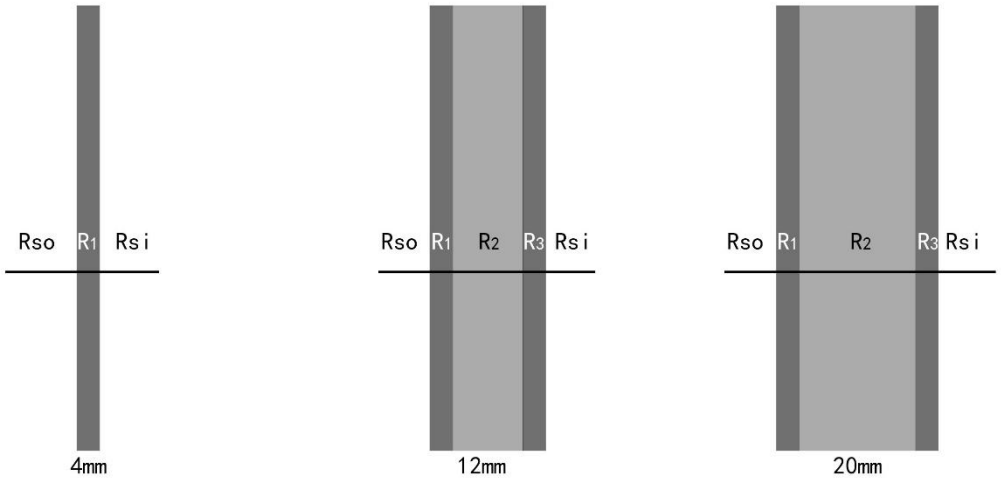


Figure 5.12 Summing thermal resistances on various glazing system

1. Based on above references, for 4 mm single glazing, $\lambda_{glass} = 1.05$ W/mK, $R_{glass} = 0.0038$ m^{2}K/W. $R_{so} = 0.04$ m^{2}K/W, $R_{si} = 0.13$ m^{2}K/W.

$R_{Single} = R_{so} + R_{GLASS} + R_{si} = 0.172\ m^2K/W$

2. Based on above references, for 28mm double-glazing, $\lambda_{air} = 0.12$ W/mK, $R_{air\text{-}20mm} = 0.17\ m^2K/W$. For the glazing, $\lambda_{glass} = 1.05$ W/mK, $R_{glass} = 0.0038\ m^2K/W$. $R_{so} = 0.04\ m^2K/W$, $R_{si} = 0.13\ m^2K/W$.

$R_{28mm} = R_{so} + R_{GLASS} + R_{air} + R_{GLASS} + R_{si} = 0.34\ m^2K/W$

3. For the 20mm double-glazing, $\lambda_{air\text{-}12mm} = 0.075$ W/mK, $R_{ver} = 0.16\ m^2K/W$. For the double glazing with air gap in 12mm, $\lambda_{glass} = 1.05$ W/mK, $R_{glass} = 0.0038\ m^2K/W$. $R_{so} = 0.04\ m^2K/W$, $R_{si} = 0.13\ m^2K/W$.

$R_{20mm} = R_{so} + R_{GLASS} + R_{ver} + R_{GLASS} + R_{si} = 0.338\ m^2K/W$

Therefore, the theoretical U-value of single glazing is:

$U_{Single} = 1/R_A = 5.8\ W/(m^2K)$

The theoretical U-value of double glazing in 28 mm is:

$U_{20mm} = 1/R_B = 2.88\ W/(m^2K)$

The theoretical U-value of double glazing in 20 mm is:

$U_{28mm} = 1/R_C = 2.96\ W/(m^2K)$

Experimental set up and procedure

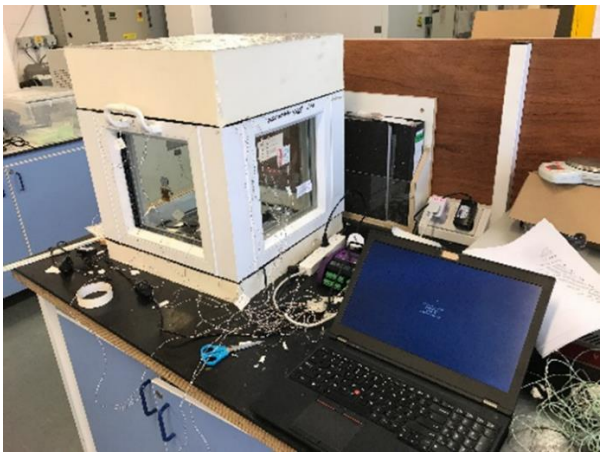


Figure 5.13 The photo of testing rigs

In the laboratory in Nottingham, four types of glazing are used for testing with a size of 300mm · 300mm and designed for evaluations of the overall U-value. The test rigs were the same as the testing rigs, as shown in Figure 5.13. Temperature gaps between inside and outside glazing surfaces were collected by K-type thermocouples, with ±0.4 °C accuracy. HFP01-05 heat flux sensors were used to measure conductive heat transfer through the window surface with a sensitivity of 63.6 μV/(W/m^2). A 200W mini heater was applied as a constant heating power supply for the glazing box. The data was collected by DT85 data logger.

The U-value of the various glazing has been measured and listed in Table 5.6. When the rigs reach equilibrium, data collecting by DataTaker is taken, and the test lasts 1.5 hours.

Table 5.6 the U-value of the various glazing

Glazing	U-value – W/(m^{2}K)
Vacuum glazing	1.056
28mm double glazing	2.675
20mm double glazing	2.78
Single glazing	6.245

From Table 5.6, it could be deduced that vacuum glazing takes a major place due to its better thermal resistance performance. The expected U-value of various glazing is similar to the test results. From Table 2.2, the thermal transmittance required by CfSH Code 6 and Passivhaus Standard should be less than 0.8 W/(m^{2}K). Theoretically, the seven layers of air-filled glazing system can provide thermal transmittance lower than 0.8 W/(m^{2}K). In practical applications, it is impossible to apply eight layers of glazing on the window. Based on the above statement, vacuum glazing enjoys the best potential to achieve the requirements from CfSH Code 6 and Passivhaus Standard, as the performance gap between vacuum glazing and standards is most narrow. Thus, in the Eco-house, Novel Triple VG-Cavity 3L has been applied.

Novel triple VG-Cavity 3L

The design and structure of VG-cavity 3L, is illustrated in Figure 5.14. Triple VG-Cavity 3L involves the integration of 12mm air cavity with an 8mm vacuum glazing, low-E coating, and an additional layer of 4mm self-cleaning glass. The total thickness of the three-layer glass unit is 24 mm.

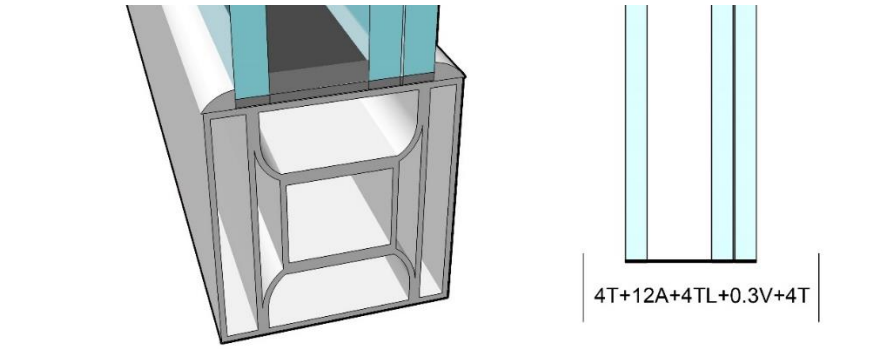


Figure 5.14 Schematic of Triple VG-Cavity 3L

From the website on Passive House Institute, the most of certified glazing products is triple glazing filled with argon (Institue, 2021). The U-value of the products ranges from 0.6 W/(m^2K) to 1.19 W/(m^2K) with a thickness of 44 mm. Compared with air filled glazing, the thermal conductivity of argon, 0.016 W/(mK), is much lower than air, 0.026 W/(mK). However, argon-filled glazing has even the smallest gaps in it. The gas between the panes are broken and would allow the argon gas to leak out (Cuce, 2018). It would reduce the thermal performance of argon filled glazing. In order to minimise the impact of argon leakage. The design of VG-cavity 3L has been promoted. It is a hybrid vacuum glazing composed of vacuum glazing and low-e glass. The cavity is injected with air to achieve ultrahigh thermal insulation performance.



Figure 5.15 The photo of the positions of thermocouples and heat flux sensor

As with the previous insulation performance testing, the rigs needed were the same as for the investigation on the SIPs. Place 5 thermocouples on both inside and outside surfaces to record the temperature of the internal and external surfaces of a window. The thermocouples are tightly attached to the surface and fixed by aluminium tapes. In order to minimise the impact of ambient air temperature, there is another masking tape covering the aluminium tape. The heat flux sensor was placed in the centre of the glazing, as Figure 5.15 shows.

From the testing, the measured U-value of the promoted VG-Cavity 3L is about 0.42 W/(m^2K). According to Table 2.2, the maximum acceptable U-value of glazing is about 0.8 W/(m^2K) for windows in Passivhaus Standard. The performance of VG-Cavity 3L is outstanding.

Wall

Walls are the main part of the building envelope. And thermal resistance (*R*-value) of the wall has significant impacts on the capacity of heat conservation in buildings. Improving the insulation performance of building fabric is one of the most cost-effective ways to reduce energy consumption. In this section, investigations on the various thermal performances of insulated panels are provided.

Testing on VIP and SIP

The options of insulation material for the wall includes the structural insulated panel and vacuum insulated panel. The experimental investigation of insulation panels was carried out using an environmental chamber, located on the ground floor of the SRB building, the University of Nottingham, UK, to simulate the indoor and outdoor environmental condition. Half of the unit panel is positioned faced in to one chamber acting as interior temperature condition, the other half of unit was faced to the other chamber which was set as the exterior condition. The cold side is about 10 °C. The hot side is about 30 °C. The temperature difference is about 20 °C. The rigs are the same in Chapter 4.

A vacuum insulation panel (VIP), as shown in Figure 5.16, is a novel thermal insulation component for the market. VIP can give the same thermal resistance with a much thinner thickness. This part presents the evaluations of VIPs and SIPs and the factors which must be considered during the application of VIPs in buildings.



Figure 5.16 The photo of VIP

As Figure 5.17 shows, the thickness of the designed SIPs wall is about 202 mm, including three finish layers on both sides of the wall and three insulation layers. The main insulation material is rigid insulation with a thickness of about 125 mm. The expected U-value of the wall is about 0.28 W/(m^{2}K).

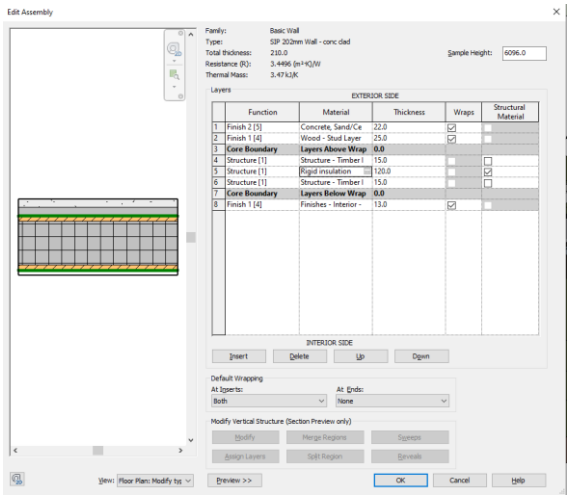


Figure 5.17 The screenshot on the structure of SIPs in Revit

The sample of the structural insulated panel was made by technicians of laboratory. It had a similar structure to designed structure in Revit but without finish layers, as shown in Figure 5.18.



Figure 5.18 The photo of SIP

The U-values of the insulated panel is measured as Table 5.7 shows. The costs of the panels are queried from a construction company in China. It can be noticed that the cost of SIPs is just about 35% of the cost of the VIPs. The gap of total cost on wall between Eco-house with VIPs and SIPs is over £16,000. Thus, the project partner selected the SIPs as the main structure of the wall for Eco-house.

Table 5.7 The measured U-value of SIP and VIP

Option	U-value-W/(m^2K)	Cost-/m^2
VIP	0.15	£100
SIP	0.29	£33

Testing the wall in Eco-house

From the above statement, the VIP enjoys higher insulation performance than SIP. As mentioned in Section 2.8, the VIP is suitable for the building with high in cost. It is not suitable for the budget Eco-house because of its high cost. The benefits with space saving are not obvious because VIPs cannot compensate extra capital cost of the SIPs as the land price in suburban. Thus, SIPs have become the most famous form of prefabricated building envelope for normal sustainable houses. SIPs can form a solid thermal envelope around the structure. The well-designed connection joint between the two panel would also reduce the heat loss and increase air tightness.

In section 2.3, various governments have proposed the regulations or guidelines for Low-carbon houses. *(Ministry of Housing and Urban-Rural Development in China, 2015)* defines the thermal transmittance should be lower than 0.35 W/(m^2K). In order to check the performance of SIPs in the Eco-house,

an investigation into the heat flux and temperature record was undertaken. Like the previous insulation performance testing, the investigation employed the Datalogger and thermocouples to record the temperature differences every 10 seconds. The internal and external temperatures were recorded over the 2 hours experimental period. The heat flux sensor, Hukeseflux HFP01 heat flux sensor, was used to record the heat flow through the wall.

It should be mentioned that the thermocouples used in Wuhan is supplied by the project partner in Wuhan. They have calibrated the thermocouples with accuracy of ±0.5°C. The datalogger and heat flux sensor is the same one used in the UK.

Based on Equation 4, the U-value of the exterior wall is about 0.278 W/(m^2K). Compared with the expected U-value stated above, it can be noticed that the SIPs of Eco-house could achieve the expected target in practice. The thermal performance of the exterior wall cannot satisfy the requirements of Passivhaus Standards and CfSH Code 4. However, the climate of Wuhan is warmer than the European countries. The performance of the SIPs has satisfied the Chinese building regulations.

5.4. Testing the overall performance of the Eco-house

There is obvious evidence to suggest the performance of some components are not as good as expected. The difference between the anticipated and real performance is the performance gap of the Eco-house. The overall testing is to locate the flaws in Eco-house, includes the airtightness test, co-heating test and thermographic image test. The airtightness test and co-heating can be used to

evaluate the overall performance gap of the Eco-house in Wuhan. Using the thermographic images can identify the area which causes the gap. As this project focuses on the long-term operation, the data from April to September of 2018 was collected from every room in the Eco-house. The results were collected every ten minutes for every sensor, including the temperature and solar irradiance. The evaluations throughout the whole house, including Co-heating test, heat flow monitoring and other assessments have been undertaken. The Retrofit Advice has been proposed based on the above-mentioned investigations.

Air Tightness testing

Air leakage testing is the methodology measuring the amount of air entering or exhausting from a building through the unwanted infiltration. Air tightness measurements on post-construction buildings are extremely important to predict the heating or cooling load and retrofit projects in the future. In addition, infiltration control has become a valuable parameter on indoor air refreshing and energy saving. An airtight building has several advantages over other normal buildings:

- Due to the less air leakage and heat loss through the building fabric, the airtight building has lower heating or cooling bills
- HVAC system has better performance under same status
- Reduced chance of unwanted moisture entering the interior environment
- Less moisture, and less chance of mould

The Passivhaus Standard requests the house to have a maximum of 0.6 air changes per hour at 50 Pascals pressure (ACH50). In China, the maximum air change rate at 50 Pascals is 0.6 for ultra-low energy houses. The ATTMA (Air Tightness Testing and Measurement Association) TSL4 standard defines the air permeability methodology. The Chinese national regulation '*Standard for determination of air permeability of buildings-Fan pressurization method GB/T 34010-201' also* states the methodology on airtightness testing.

Before the test, all the openings in the building should be temporarily sealed. The openings include the windows, openings for HVAC, and so on. Furthermore, the size of the building should be measured. As for the Eco-house in Wuhan, a single-storey house, the Blower Door Testing Method has been selected to test the airtightness. There have been several available calculation techniques for the test in the market. The project partner provided some rigs. As for the air permeability envelope area, all facades, roofs, and floors should be considered as part of the building envelope. And all internal doors should be fully opened. The air change rate volume is the volume of air inside the building. The volume for the Eco-house is 262 m^3.

Table 5.8 summarizes the new used device used during airtightness testing. The testing required the previous anemometer to measure the air flow rate of the fan.

Table 5.8 The summary of device during airtightness testing

Device Type	Statement	Accuracy
Fan	QinLao Negative Pressure fan	
Pressure Sensor	Smart Sensor AS510	±0.03hPa

The pressure fan is temporarily sealed into an exterior doorway using the door panel system. The pressure sensor should be placed inside and outside of the building to measure the indoor/outdoor pressure difference. The datalogger recorded the internal and external temperature at the same time. During the testing, the pressure fan is used to blow air into the building to create a positive pressure between internal and external areas at 50Pa. The pressure differences force air to escape through the building fabric. Once reaching the 50Pa pressure difference, the speed of the fan should be fixed. The total air volume supplied to interior space is the air leakage volume-V_{50} at 50Pa pressure difference.

As for the air change rate-n_{50}, n_{50} is the air leakage volume-V_{50} divided by the building volume V.

$$n_{50} = \frac{V_{50}}{V} \quad \text{Equation 8}$$

The airtightness testing of the Eco-house was complicated by the co-corporation of the author and project partner in Wuhan. The test was undertaken after overall construction finished in April 2018, with a result of 0.68

/h @ 50 Pa. Compared with the Chinese regulation, the performance of the Eco-house is relatively good. However, the Eco-house was built according to the Passivhaus Standards. The performance of the Eco-house cannot satisfy the requirement of the Passivhaus Standards on airtightness. Further improvements on the air infiltration are necessary if want to achieve better energy saving performance.

During the test, the smoke test would help to identify the air leakage paths. Place the lit cigarette near the well-known air leakage path, such as the wall and roof junctions. Combining the result of the airtightness and thermographic images testing, the key air leakage paths could be identified. The air leakage approaches would be sealed during retrofit period in the future.

The co-heating testing

The actual energy performance of buildings can differ significantly from its initial expectations. The Co-heating test is widely used in Europe to investigate the total heat transfer through the fabric of buildings (Jack *et al.*, 2018). The co-heating test is used to investigate the heat loss through the thermal envelope, which provides an assessment of the construction quality of the completed building. It is to calculate the heat loss coefficient-HLC by comparing the heat gain into a room against the gaps between temperatures inside and outside the building. The test investigates the heat loss or heat gain through the wall and fenestrations. During the testing period, the house should be unoccupied, and all the fenestrations should be sealed completely. However, keeping the house under the above status for almost one week is impossible, as the basic interior

decoration is undertaken during this period. The restricted precondition and long time consuming of the Co-heating test would cause a deviation of results. The Co-heating test equipment are summarized in Appendix 2.

The general framework for the Co-heating test is discussed below,

- Test temperature: For optimum testing, there should be a temperature difference of at least 10°C between interior and exterior. The common interior temperature would be about 18-22°C, which is the reason the test is often undertaken in wintertime. This helps mitigate against the impact of solar gain which requires a correction to be applied. However, the testing was undertaken in April 2018. The interior temperature was about 30°C because of high exterior temperature.
- Testing duration: 9 days
- Internal space access: Access to the building should be controllable, with minimum allowances to check the equipment.
- Building component control: fenestrations should be closed during the test. The wall voids, gaps and ventilation systems would be sealed and switched off. All the building appliances such as fridge, should be turned off. Limit all possible air exchange between external and internal areas.
- Test rigs setting: the interior room temperature should be heated to 10°C higher than external temperature. The fan heater acts as a heat source. The constant interior temperature is achieved by several 2kW fan heaters. And no ventilation device was working. The thermostat can switch on or off the fan heater automatically. Another fan assisted to ensure good air mixing to even out the temperature throughout the Eco-

house. The energy/bill metre recorded the electric consumption of fan heaters. As Figure 5.19 shows, the datalogger recorded the temperature of the inside and the outside. The Eco-house remained unoccupied during the testing period.



Figure 5.19 The photo of Co-heating testing rigs

- External temperature is measured by the weather station and DataTaker. The weather station, Oregon Scientific-Pro Weather Station WMR200, should be mounted on a mast outside the house. A pyranometer is vertically mounted on the external south facade of the building. The HLC value should consider the impact of solar gains. The value from the pyranometer should be taken into consideration to correct the final value.

All above mentioned tests took place from 8th to 15th of April 2018. The outside environment conditions were recorded via a weather station installed beside the Eco-house. Dividing the daily heat gain for the interior room by the temperature difference between internal and external indicates the HLC. The Appendix 3 shows the summary of energy use for every room. A plot of the temperature difference between inside and outside against daily energy consumption during the Co-heating test is shown in Table 5.9.

Table 5.9 The temperature difference between inside and outside against daily energy consumption

Date	Temperature Difference-°C	Total-W
08/04/2018	10.3	38,792
09/04/2018	13.8	55,166
10/04/2018	8.8	35,821
11/04/2018	13.6	52,084
12/04/2018	12.7	49,253
13/04/2018	12.3	47,045
14/04/2018	15.6	62,731
15/04/2018	9.6	34,824
16/04/2018	16.3	58,817

The equation of the slope line shows the HLC measure with and without solar corrected in the Eco-house. The equation demonstrates for every 1°C difference between internal and external corresponding about 160-Watt heat loss through the envelope. Based on the previous evaluations, the thermal performance of wall and glazing systems for Eco-house is good enough. If improving the performance of uninsulated components, the heat loss coefficient

would reduce further. In addition, the HLC is not substantially affected by the solar gain as the weather is always cloudy during the testing period, resulting in only about a 14% increase of HLC for the case. The suitable solar shading device for the Eco-house also reduces the heat gain from the fenestration.

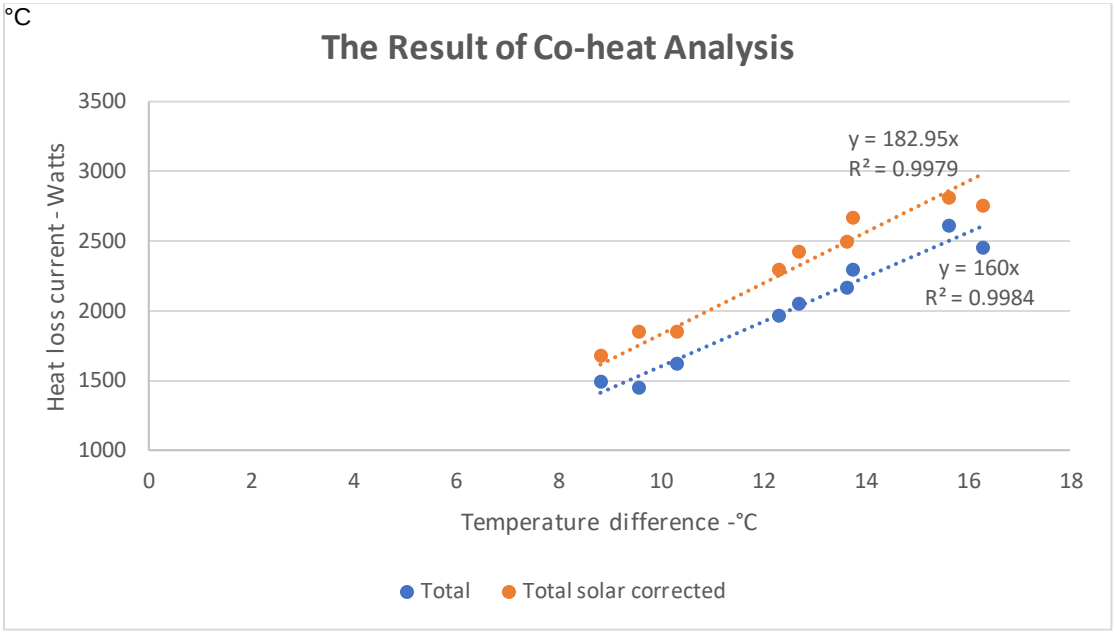


Figure 5.20 The resulting of the Co-heating testing

Several factors would cause the final HLC to be inaccurate, as shown in Figure 5.20. Further research should be conducted to identify other factors which caused the gap between the design and on-site performance.

Combining Co-heating test with other fabric tests such as airtightness and thermographic image to help to gain more insights on understanding the factors contributing to heat losses of the house. However, the testing mentioned requires more professional researchers and construction managers for the project in China, which would increase the time and cost of the construction. That is the major barrier for the evaluation on post-construction performance of sustainable house.

Thermographic image testing

The thermographic images monitoring is designed to help to distinguish the flaws in the building. The monitoring results would give the best visualization to establish the thermal bridge in Eco-house, which can help to identify the flaws during the design and construction process. The thermographic image testing is a qualitative analysis.

Innovate UK Protocol seeks to minimise the impact of these parameters by providing several guidelines:

- The temperature difference between the internal and external should be about 10°C.
- Dry building surfaces with no rain during testing period
- Wind speed less than 8 m/s
- The distance between thermal camera and target should be less than 10m

The aim of the thermographic images is to identify the heat loss approach within the building envelope. The heat loss may be caused by thermal bridges, voids in wall and air leakage within the structure. The FLIR C2 Compact Thermal Imaging System is the chosen device for this testing. The parameter of the FLIR C2 is shown in Table 5.10,

Table 5.10 Parameters for FLIR C2 Compact Thermal Imaging System

Type	Parameter	Photo
FLIR C2 Compact Thermal Imaging System	Temperature Min: -10°C Temperature Max: 150°C Thermal Sensitivity: 0.1°C	

The following thermographic images were taken on 23/04/2018 at 16:30 in Hubei University of Technology, Wuhan. The ambient environmental factors are below:

- Weather conditions: Cloudy
- External Temperature: 34-37°C
- Internal Temperature: 25°C
- Distance away from target part: 2 m – 10 m

As for this section, several external photos are taken with a suitable temperature scale set by the camera automatically. The maximum and minimum temperature value in every photo is different. The warm colour in the photo shows the area at a relatively high temperature and the dark colour represents the low temperature. The range of temperature can be indicated by

the right-hand bar of thermographic image photos. The ambient temperature is shown on the upper-left side.



Figure 5.21 The thermographic image photo of Eco-house from Front View

Figure 5.21 shows that relatively higher temperature on the southern wall and lower temperature on the roof. The temperature gap between wall and roof is up to 10°C. While the interior temperature is lower than the exterior temperature, the heat transfer through the southern wall is much less than roof. The result verified that the thermal performance of the wall is much better than the roof. Furthermore, significant heat transfer is apparent in the joints around the exterior door. This may be due to voids or gaps between the building components. This part could be retrofitted by a spray foam product.



Figure 5.22 The thermographic image photo of exterior door

The above thermographic image photo is taken from indoors. Figure 5.22 depicts obvious heat transfer from outside to inside through the door. The overall profile shows the exterior door is not well insulated compared to the walls. In addition, the heat loss through the gaps between the wall and door is very obvious. The two brightest spots are the intelligent locker system. The locker system is made of metal, which is good for thermal transfer. The photo verifies the U-value of the door is much higher than the U-value of wall. The door should be replaced in the future because of its poor thermal performance.



Figure 5.23 The thermographic image photo of window

Figure 5.23 above shows that heat transfer through the VG-Cavity 3L is a little higher than the wall. The U-value of the VG-Cavity 3L is about 0.42 W/(m^2K), which is a little higher than the U-value of the wall. However, the heat loss around door frames indicates that the main heat transfer approach is apparently through the window frame. Figure 5.23 highlights the importance of material selection as the heat transfer is apparently through the window frame. On the edge of the VG-Cavity 3L, there is a bright rectangle. The rectangle is the thermal bridge between inside and outside. It requires extra sealing material to reduce heat transfer and air infiltration. Overall, the performance of VG-Cavity 3L window is satisfactory

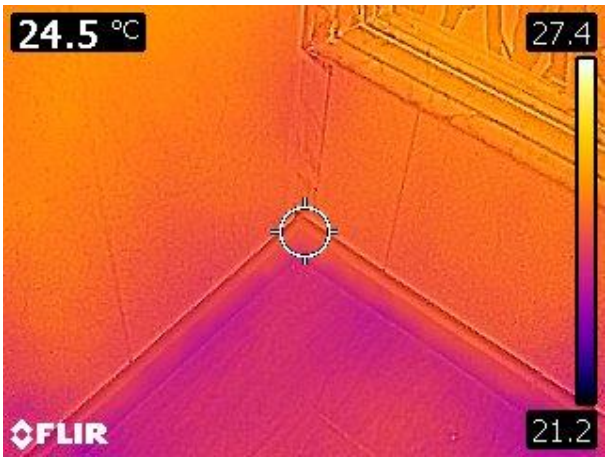


Figure 5.24 Thermographic image of the junctions between the wall and floor

The interior wall and floor are clearly visible here. However, there is no obvious sign of thermal bridging in Figure 5.24. The insulation performance of the wall panel is performing well. There is no significant heat loss in the joints between floors and walls. This may be due to the accurate prefabricated building component.

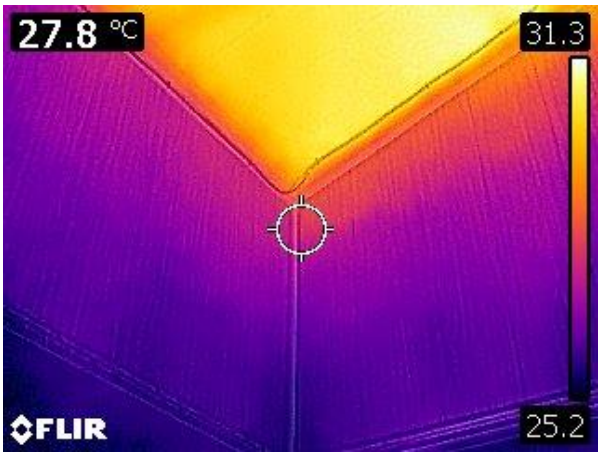


Figure 5.25 Thermographic image of the joint between wall and roof

Figure 5.25 is taken from interior space. The temperature difference between the wall and roof is about 6°C. Based on the design, the U-value of the expected roof is about 0.87 W/(m^2K). The temperature distribution suggests that the insulation performance of the roof material is much poorer than wall panels.

Furthermore, after an interview with the constructor, the actual U-value of the roof is 1.5 W/(m^2K), almost two times over the designed roof. The roof of Eco-house needs retrofits on the thermal performance in the future.

Based on the above statements, it can be summarized that the locations of thermal bridging in the Eco-house include:

- Roof and the junctions between the roof and wall
- Exterior door and junctions between door and ambient wall
- Around low-quality sealed windows and doors

Monitoring the temperature distribution of Eco-house for the long-term

Whether a given building or system is working in the energy-efficient phase depends on the different applications, climate, or other influencing factors. Thus, a long-term monitoring is necessary for the Eco-house. Once the on-site investigation finished, the Eco-house was still monitored over an extended period of time and the results were emailed to the UK for analysis every single month. The long-term testing was monitored from April 2018 to September 2018. From the end of September, the Eco-house began its first phase retrofit, which is not suitable for the long-term monitor.

As Figure 5.26 shows, the central monitor system is the DataTaker web, and the testing device is the DataTaker DT 80 serious data logger. During the monitor period, the data logger would collect the data every 10 minutes every day. The data logger collects the data from the sensor and provides the graphical for monitoring. However, there are several small construction activities during the period. The behaviour of workers would have some impacts on results. And they also reported that they would cut the power supply for the DataTaker for 1 or 2 days. Thus, there would be some flaws in monitoring the results. The monitor system included the 27-thermocouples placed in 9 different places in the Eco-house and 1 pyranometer placed on the southern wall. Two of the thermocouples are for ambient temperature. The other thermocouples are for the investigation in interior rooms.

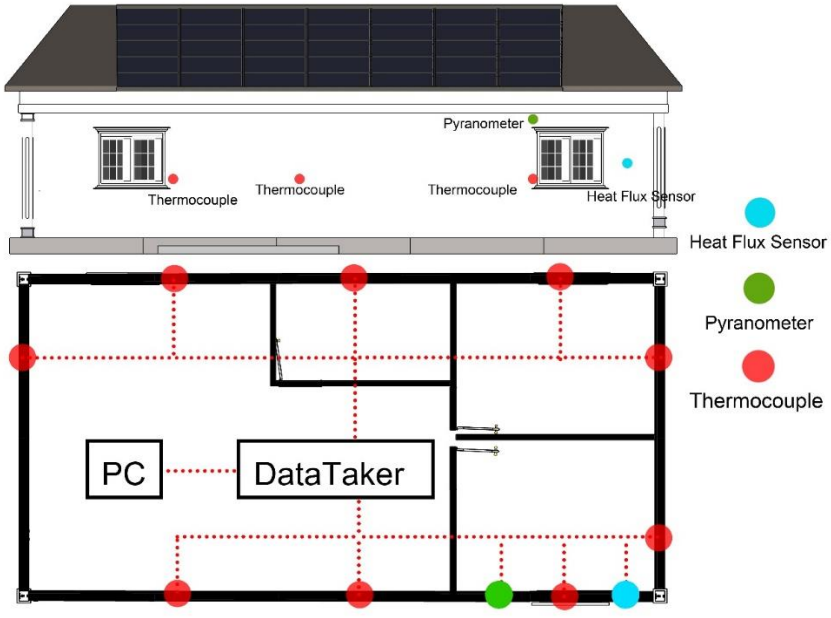


Figure 5.26 The schematic of positions of sensors

For convenience, every room has been labelled in Eco-house, the Living Room, Bedroom 1, and Bedroom 2. Bedroom 1 is the bedroom in the southeast part,

and Bedroom 2 is the room facing north. The monitoring started from 18th, April 2018 to September 2018. As for Figure 5.27, the grey line demonstrates the changes of external temperature. The temperature of the Livingroom is the blue line. The yellow line and the orange line are for Bedroom 1 and Bedroom 2, respectively.

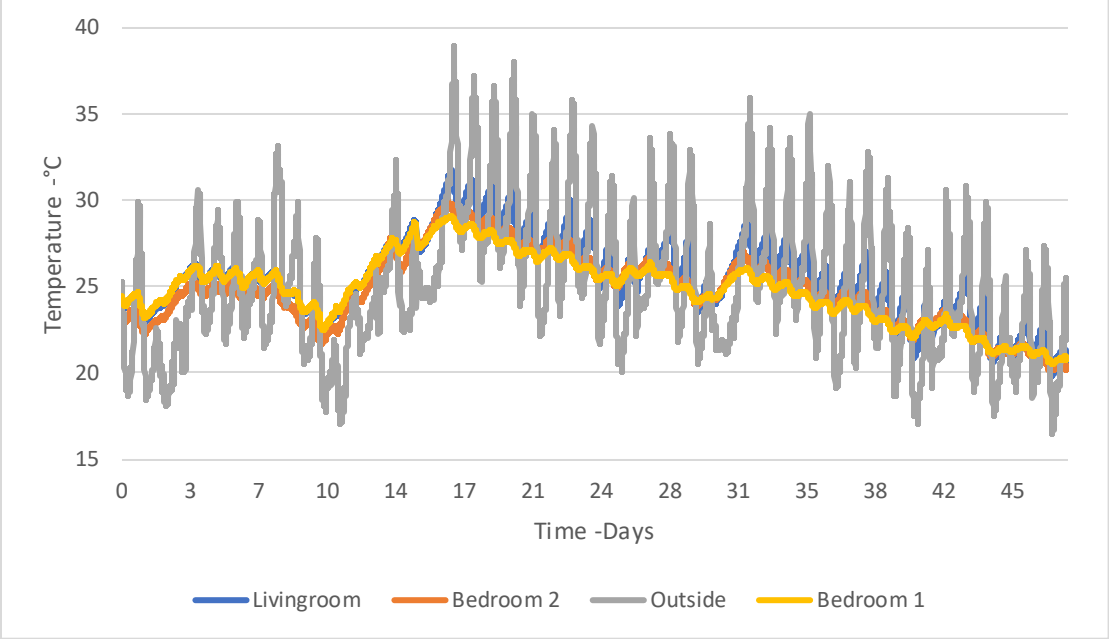


Figure 5.27 The temperature distribution for April to mid of May

Maximum and minimum external temperature in Figure 5.27 is 38.88°C and 17.11°C, respectively. The difference between the maximum and minimum external temperature values is about 21°C. On the contrary, the difference between the maximum and minimum of Bedroom 1 temperature is just about 6°C. The distribution of the external temperature is almost 4 times more than the distribution of internal temperature, which shows the Eco-house can maintain the interior temperature almost regardless of the change of external temperature.

Figure 5.28 shows the distribution of temperature in June. There are still several obvious characters. On the twelfth day of June, the external temperature reached the highest, 39.65°C. At the same time, the interior temperatures of all rooms are below 30°C. Furthermore, the orange line is almost overlapping the red line. The temperature of bedroom 1 is similar to the temperature of Bedroom 2.

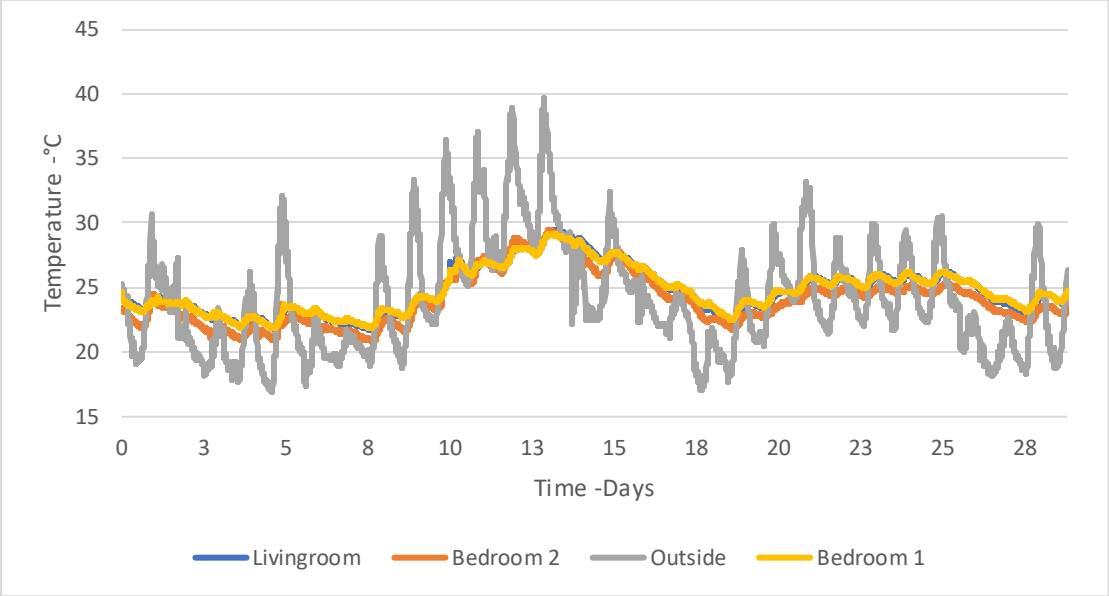


Figure 5.28 The temperature distribution for June

In July, the average external temperature is higher than in June. As Figure 5.29 shows, the average interior temperature of Livingroom is higher than the other rooms. The distribution of the Livingroom is around 11°C. The distribution of external temperature is about 18°C, which is just 1.5 times than the temperature of living room. And the distribution of Bedroom 2 is similar. From July, a new occupant began to settle in the Eco-house. Based on the interview with the occupant there, the windows of the Livingroom and Bedroom 2 are always open for ventilation, which can cause the larger distribution of temperature than June. As for Bedroom 1, the distribution is just 4-5°C, which is still a quarter of the distribution to external temperature. Based on the above monitor results, occupancy behaviours would have great impacts on the interior temperature.

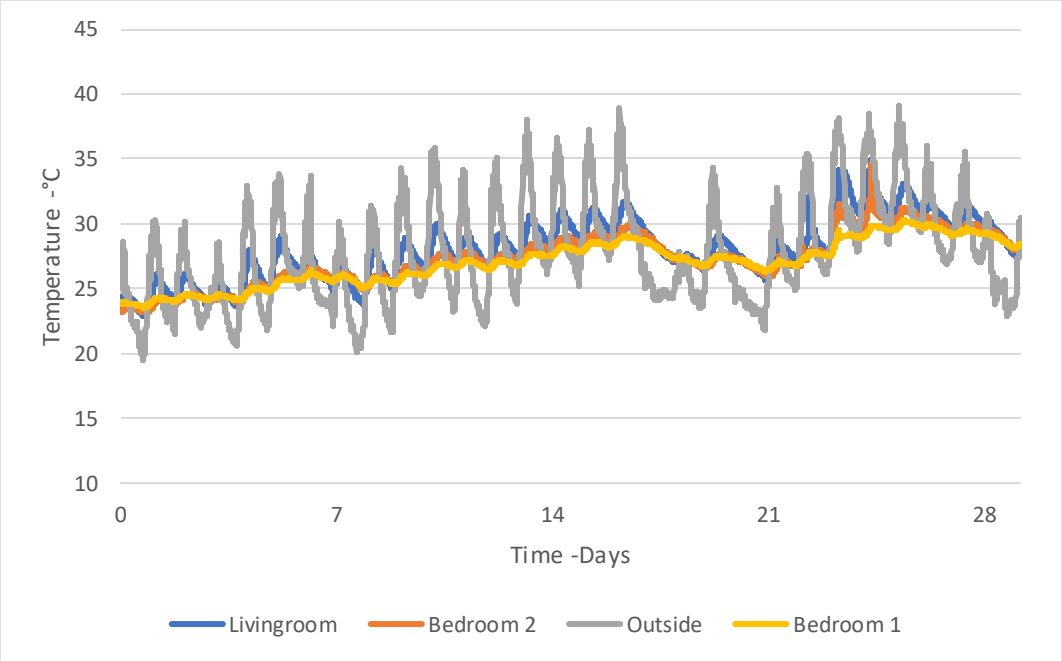


Figure 5.29 The temperature distribution of July

Figure 5.30 shows the temperature distribution in August. The average external temperature in August is the highest, about 35°C. The highest temperature reached was about 45°C, which is 20°C higher than the common thermal comfort range. But the interior temperature is much lower than the external temperature. The new applied portable air conditioning in August 2018 would be the reason. The temperature of Bedroom 1 is frequently below the external temperature, followed by Livingroom and Bedroom 2. According to the interview with the project partner, they arranged the two Bedrooms for occupants. The occupants always turned on the portable air conditioning during the daytime.

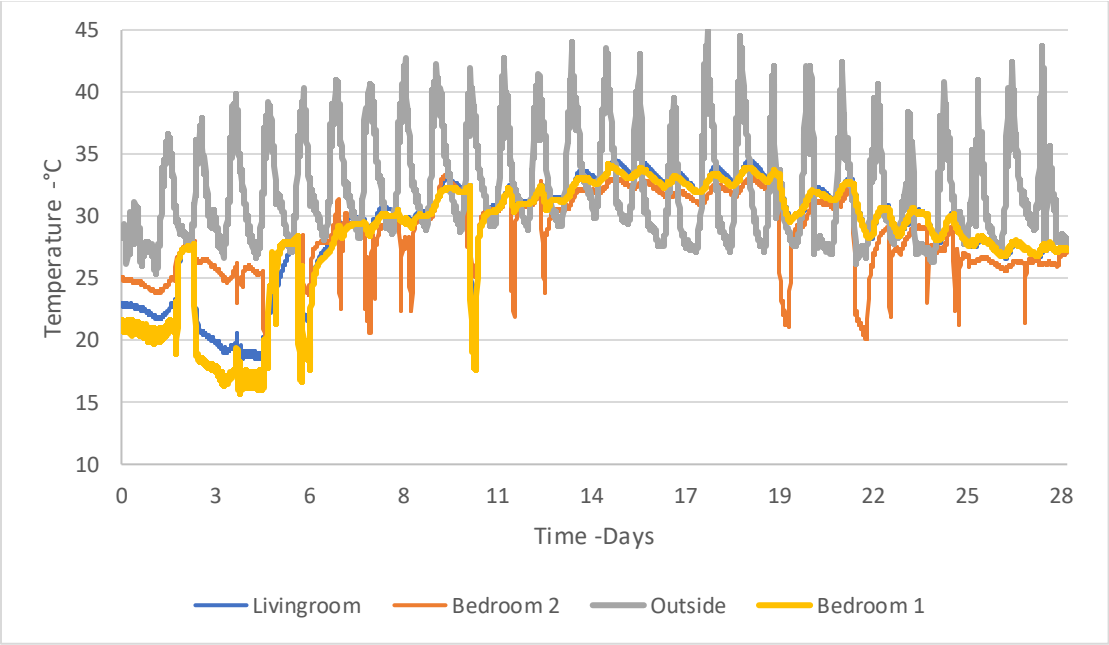


Figure 5.30 The temperature distribution of August

As shown in Figure 5.31, the external temperature in September is much lower than in August. The occupants only turned on the air-conditioning in Bedroom 2 several times at the start of September. The temperature of Bedroom 1 and Livingroom is from 23 °C to 30 °C, almost 10 °C lower than the highest external temperature at the same time. The highest interior temperature from 25th to 28th could be as low as the lowest external temperature.

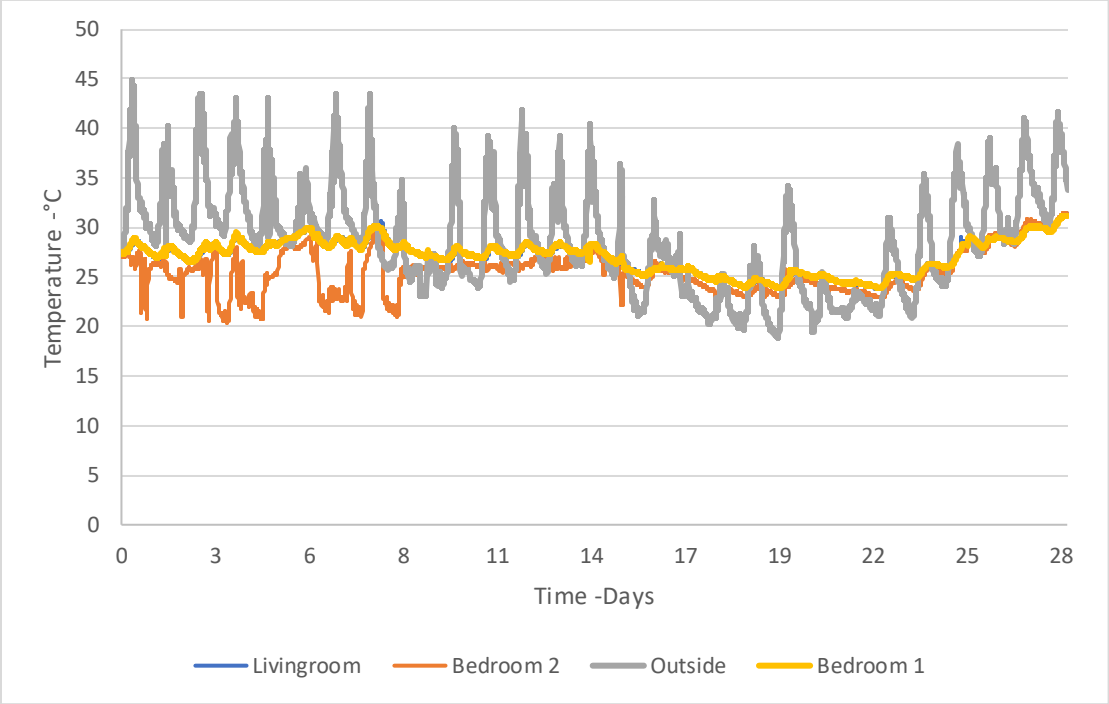


Figure 5.31 The temperature distribution of September

The long-term monitoring covered the period from April to September 2018. During the period of the hottest climate, the highest interior temperature is also over 30°C. The installation of air conditioning could help to reduce the interior temperature but increases the energy bills.

The retrofit advice

This section presents several retrofit recommendations based on the testing results above. The retrofit improvements are predicted to be undertaken in two main phases between 2019 to the end of 2021. As Table 5.11 shows, the retrofit plan includes several upgrades to both building fabric and integrated systems. With the progress of retrofit on Eco-house, the building would be more airtight. Thus, installing several more novel heat recovery ventilators above the windows becomes necessary for the occupants. However, the retrofit would be delayed because of Coronavirus in Wuhan in 2020. The end date of Phase 2 would be the end of 2021.

Table 5.11 The retrofit plan on Eco-house

Building component or system	Achieved (April 2018)	Phase 1 (2019-mid of 2020)	Phase 2 (2020-end of 2021)
External Wall	U-value: 0.278 W/(m^{2}K)	No change	No change
Roof	U-value: 1.5 W/(m^{2}K)	No change	Retrofit the roof; expected U-value 0.87 W/(m^{2}K)
Windows	U-value: 0.42 W/(m^{2}K) Triple VG-Cavity 3L	No change	No change
Doors	U-value: 3.46 W/(m^{2}K)	U-value: 2 W/(m^{2}K) Hollow core wooden door	No change
Ventilation Strategy	Natural ventilation	Novel Windows Heat recovery ventilator and natural ventilation	Installed Air Conditioner (KFR-35GW)

Airtightness Improvement Work	0.68/h @ 50 Pa	Sealing material is placed covering the edges of window and door frames	Tape and sealing material coving the junctions, Expected to 0.6/h @ 50 Pa
Photovoltaic	Inactivated 1 kW Photovoltaic Panel on roof	Applicated 1 kW Photovoltaic Panel on roof	Install extra 2 kW PV Panel
District Sewage Treatment	No	No	Install a Small-scale Sewage Treatment Tank

The previous study demonstrates that the air permeability of the Eco-house is about 0.68 /h @ 50 Pa. Following each phase of retrofit work, the airtightness test was conducted to assess the airtightness improvement. As the thesis submitting date is before the end of phase 1, the test of phase 1 just represents some of the achieved retrofit at that moment. The result tested on 05/May/2019 reduced leakage from 0.68 /h @ 50 Pa to 0.61 /h @ 50 Pa. The measured U-value of the new exterior door is about 2 W/(m^2K).

The Eco-house used to have a portable air conditioner and electric heater for workers during construction period. After construction finished, the portable air conditioner has been removed from Eco-house. According to the retrofitting plans from the project partner, a new sponsored air conditioner would be installed in Eco-house before the end of 2021. The model number of air conditioner might be KFR-35GW. The model is rated in level 1 with a cooling capacity of 3500 W and heating capacity 4500 W. (National Energy Fundamentals and Management Standardization Technical Committee, 2010)

stated the energy level for air conditioner in China. Table 5.12 summarized the Cooling Coefficient of Performance-COP for various level. The COP for an air conditioner is defined as the ratio of the heat/cool output to the power input whilst the system is in operation. Thus, the cooling COP of new installed air conditioner is about 3.6 and the heating COP is about 4.6.

Table 5.12 Air conditioning energy saving level (National Energy Fundamentals and Management Standardization Technical Committee, 2010)

Rated cooling capacity	Energy Saving level		
	1	2	3
Rated cooling capacity < 4 500 Watts	3.6	3.4	3.2
4 500 Watts < Rated cooling capacity < 7 100 Watts	3.5	3.3	3.1
7 100 Watts < Rated cooling capacity < 14 000 Watts	3.4	3.2	3.0

5.5. Computer simulation of the Eco-house

Because of the passion for low carbon buildings, architects begin to consider the thermal processes of buildings at the beginning of the design process. Building simulation software can use computer software to calculate thermal processes in a 3D digital model. Researchers have tried different software to simulate the total energy consumption. Dynamic parameters of the model are needed, including the weather details, occupancy time and so on. Thermal simulations of buildings are complex and become necessary during the design process especially for sustainable building. The simulations can help to verify if the house can meet the energy-saving targets.

Simulation target statement

This section presents the result of a simulation for the Eco-house using Autodesk Revit modelling software assisted by Ecotect. The Autodesk Revit platform could provide the simulation result based on the 3D model in software.

Several high-performance building components have been utilized in Eco-house. This section provides the simulation results of the Eco-house. The main aim is to find out the heating and cooling loads for the Eco-house. This section introduces a reference building parameter to investigate the energy saving potential of new build Eco-house in Wuhan. According to the evaluation in China, (Lu Meijun, Wang Guixiu and Fan Yi, 2009) states the common thermal properties of a house in a rural area of central China, as Table 5.13 shows.

Table 5.13 The summary of the thermal parameters and structure of 'refence house'

Building component or system	Thermal Performance and Structure
External Wall	U-value: 2 W/(m^2K) 20 mm mortar + 240 mm Brick + 20 mm mortar
Roof	U-value: 3.6 W/(m^2K) 20 mm mortar + 180 mm Cement Panel + 20 mm mortar
Windows	U-value: 6.4 W/(m^2K) Single Glazing
Doors	U-value: 3.68 W/(m^2K) Common Timber door
Ventilation Strategy	Natural ventilation
Airtightness	1.42/h @ 50 Pa
Photovoltaic	No
Heating or Cooling Method	Air Conditioning

The simulation software selection

The author had some experience with the Autodesk Ecotect. Furthermore, the model of the Eco-house is finished in the Autodesk Revit. Both of the above software is developed by the Autodesk company. The 3D model file from Revit-gbXML can be opened by the Ecotect as well without any file transfer, which can avoid unknown building information loss during file transfer. In order to use the thermal simulation software properly, a good understanding of the factors which will affect the energy saving performance is needed so as to ensure the results could be appreciated. The current simulation results largely depend on the parameter inputs. Thus, the previous on-site testing should be carefully undertaken.

Zones setting

The main parameter settings in Ecotect include annual calendar, local weather, zoning of houses, construction materials, and operation schedules. Figure 5.32 presents the 3D model of the Eco-House in Revit.

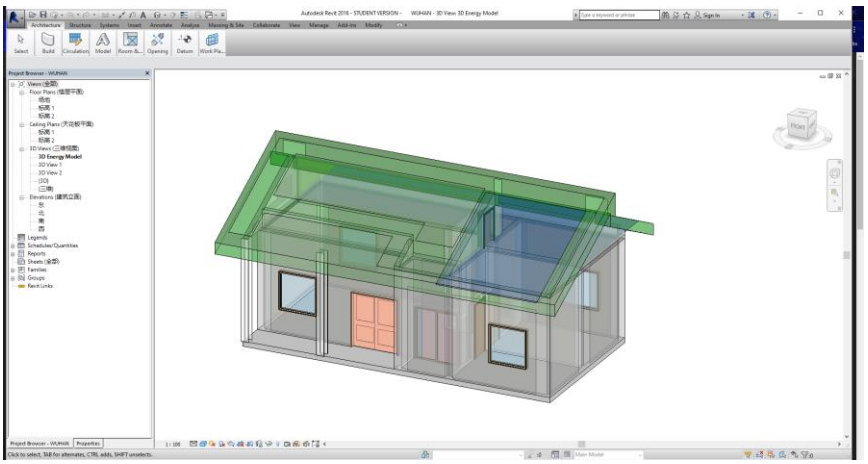


Figure 5.32 The 3D model in Revit

The zone is defined as the basic unit for building simulation. The simulation result can be represented by different zones. Figure 5.33 and Table 5.14 below shows the Eco-house zone setting. With different purposes of rooms, the whole house can be divided into Bedroom 1, Bedroom 2, Toilet, Storeroom and Livingroom.

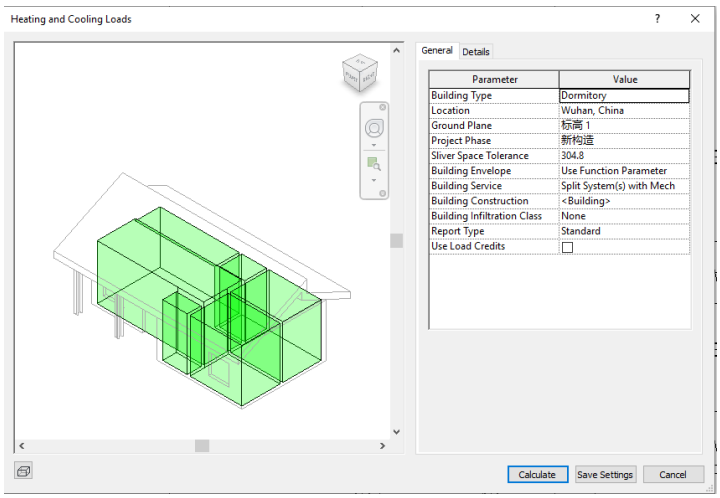


Figure 5.33 The zones of Eco-house in Revit

Table 5.14 The summary of size for different zones

Space Name	Area (m^2)	Volume (m^3)
Livingroom	32	127.5
Bedroom 1	11	41
Bedroom 2	11	41
Toilet	3	11
Storeroom	2	7

The measured parameter of the building for simulation

Heat loss through the building fabric, especially through fenestrations, takes a substantial proportion of the total heat loss. Materials with higher thermal resistance will significantly reduce unexpected heat transfer through the fabric.

The thermal parameters of the Eco-Wuhan House and 'reference house' are listed in Table 5.15.

Table 5.15 The summary of the parameters for Eco-house and 'reference house'

Building component or system	'Reference house'	Current House (April 2018)	After Retrofit in 2021
External Wall	2 W/(m^2K)	0.278 W/(m^2K)	0.278 W/(m^2K)
Roof	3.6 W/(m^2K)	1.5 W/(m^2K)	0.87 W/(m^2K)
Windows	6.4 W/(m^2K)	0.42 W/(m^2K)	0.42 W/(m^2K)
Doors	3.68 W/(m^2K)	3.46 W/(m^2K)	2 W/(m^2K)
Ventilation Strategy	Natural ventilation	Natural ventilation	Novel Windows Heat recovery ventilator
Airtightness Level	1.42/h @ 50Pa	0.68/h @ 50Pa	0. 61/h @ 50Pa
Photovoltaic	No	No	3 kW PV Panels

The calendar setting

The calendar setting is an important parameter in building energy simulation. The calendar setting would help to define the occupant's behaviours. As the weather condition varies throughout the year, the occupants would have different behaviours at different times. The behaviours would have great impacts on the internal heat gains. The occupants would not spend a long time

in houses during weekdays. During the weekend, the occupants would spend a longer time at home for entertainment. The heating and cooling system in the house would be controlled to switch on when occupied. The calendar setting for weekdays and weekends has been listed in Appendix 4.

Table 5.16 provides the expected daily energy consumption of appliances.

Table 5.16 The expected daily energy consumption of appliances

Appliances	Status	Power (kW)	Frequency	Daily Energy Consumption (kWh)
Kettle	Per 1.5L	3	4 times/Day	0.6
Cooker	When on	0.79	30 mins/Day	0.4
Fridge	When on	0.8	31 mins/Day	0.4
Microwave Oven	Per hour	0.03	All Day	0.62
	Total			2.02

Simulation results analysis and discussion

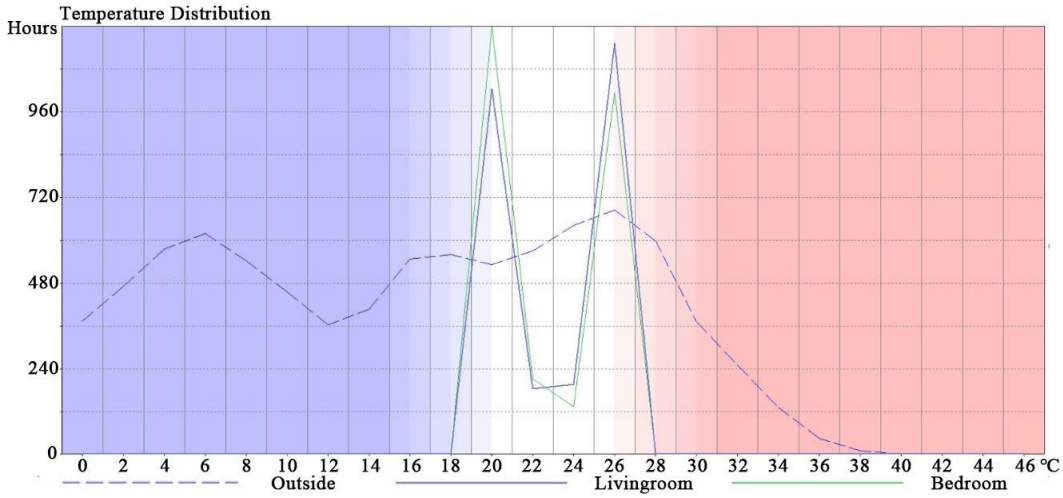


Figure 5.34 The distribution of interior and exterior temperature

Figure 5.34 above presents the comparison between the external and internal temperature distribution. The outside temperature is around 6ºC during winter and 28ºC during summer. (Ministry of Housing and Urban-Rural Development in China, 2015) required that the interior temperature should be about 20-26ºC for the ultra-low energy house. The distribution of interior temperature is much smaller compared with outside temperature due to the high thermal performance of building components.

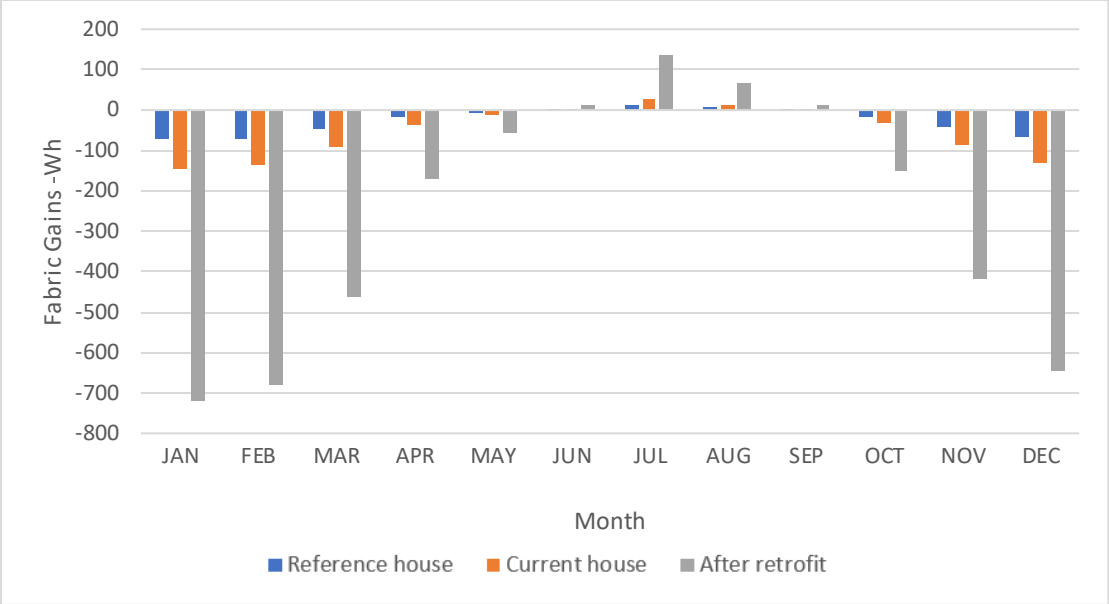


Figure 5.35 The average fabric gains for various months at 0 am

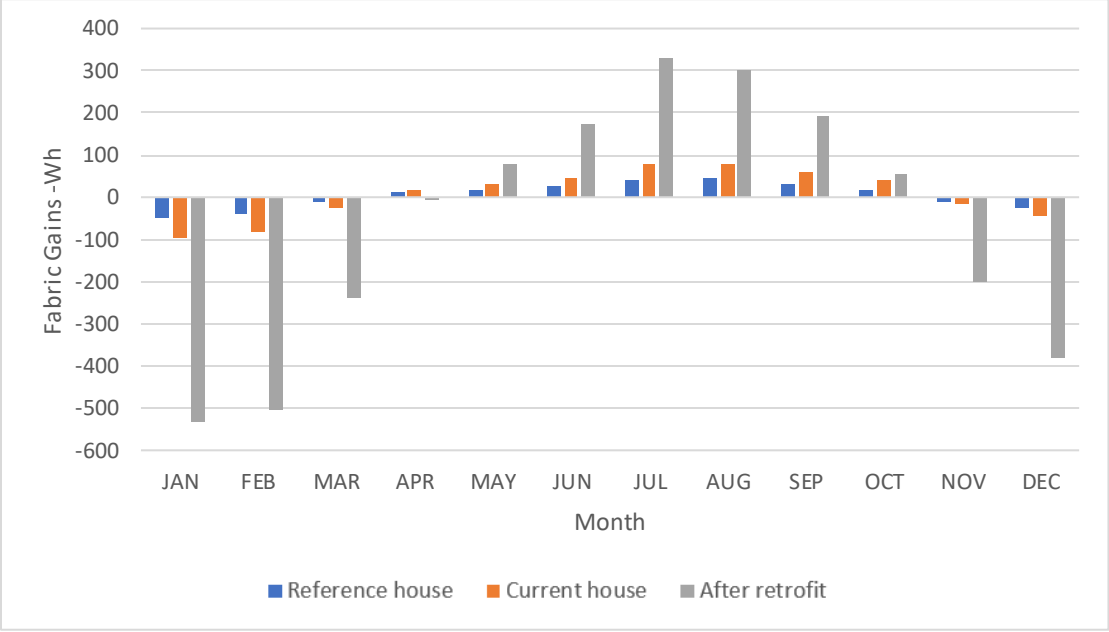


Figure 5.36 The average fabric gains for various months at 12 pm

Figure 5.35 and Figure 5.36 shows the average heat loss and heat gains through building fabric for every month at 0:00 and 12:00, respectively. It is noticed that the heat loss during the night-time is much more than in the daytime. The heat gains during the daytime are much more than during the

night-time. The fabric heat transfer of the ‘After retrofit’ house is the least because of the high thermal insulation of building components. The heat transfer through the fabric of ‘reference house’ is four times over the current house. After all the retrofit plans are finished, the fabric gains would decrease greatly, just about 15% of the fabric gains of ‘reference house’.

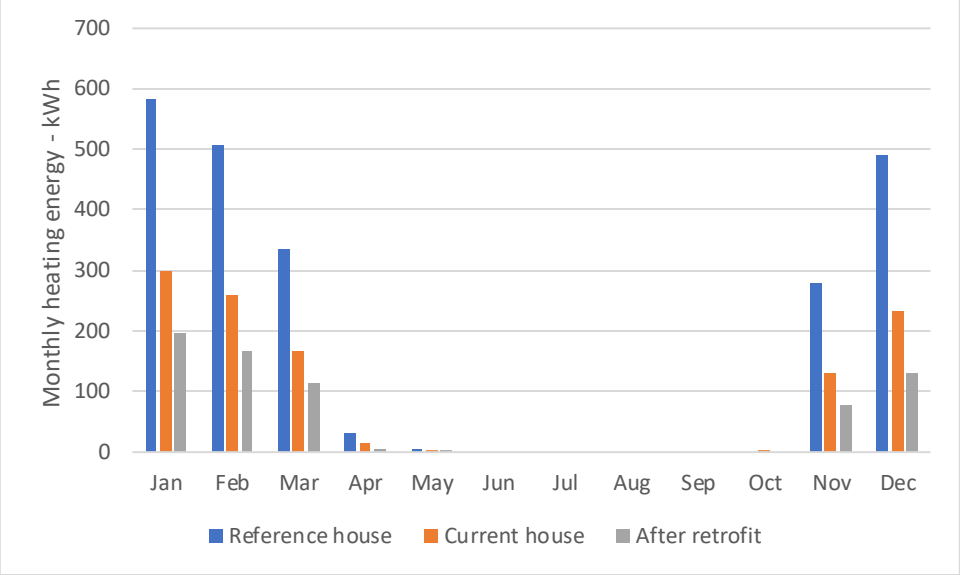


Figure 5.37 The heating loads for three cases

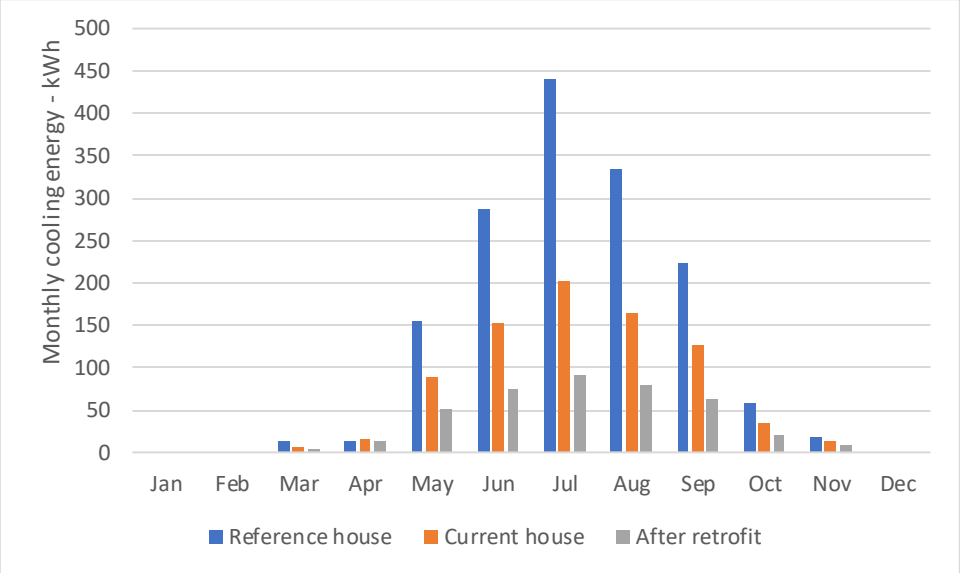


Figure 5.38 The cooling loads for three cases

As seen from Figure 5.37, Figure 5.38, and Table 5.17, the 'current house' can archive about 19 kWh/m^2 and 14 kWh/m^2 for heating and cooling load, respectively. Compared with the 'reference house' parameters, the thermal performance of the current house is much better. However, it cannot satisfy the requirement of the Passivhaus Standard, for which the annual heating or cooling loads per square meter should be less than 15 kWh/m^2. According to

the simulation results, the expected heating and cooling loads are 12 kWh/m^2 and 7 kWh/m^2, respectively, when the retrofit is finished in the future.

Table 5.17 The annual space cooling/heating of three cases

	Reference house	Current house	After retrofit
Total heating energy (Wh)	2,234,505	1,103,397	688,248
Space heating (kWh/m^2)	39	19	12
Total cooling energy (Wh)	1,547,132	809,558.2	405,507.3
Space cooling (kWh/m^2)	27	14	7

It should be noticed that there is only an electric heater and no cooling device in Eco-house currently. The energy efficiency of the cooling and heating device is set at 100% in computer simulation. The simulated results on cooling or heating energy are not the actual energy consumption for cooling or heating device. Based on the retrofitting plans mentioned in Section 5.4, there would be an air conditioner to install in Eco-house in end of 2021. If considering the COP of the air conditioner, the energy consumption for heating and cooling would be much lower. The calculated energy consumption on heating is 149 kWh. And the energy consumption on cooling is 110 kWh.

Life cycle assessment-LCA

Several models and systems for assessing environment impacts of buildings have been proposed in recent decades. As an effective tool, LCA is widely used in evaluating the environmental impacts of building construction. Life Cycle Assessment (LCA) was first proposed by the United States in 1960s. It is to quantify the impact of a specific product on the environment and find out the approaches for reducing the negative impact (Carroll, 2006). The evaluation includes the entire life cycle of the building, from processing of raw materials,

construction, operation, demolition, as well as all transportation processes involved. The activities of a building lifecycle and the relationship between the construction stage were described in Figure 5.39. LCA-based systems are based on quantitative data from life cycle database of materials or energy consumption. The BIM platform enjoys advantages over conventional design methods. It can calculate the carbon emission of material and energy consumption for specific houses.

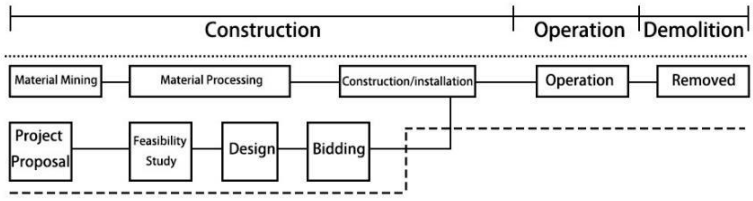


Figure 5.39 The Lifecycle of building

As for ‘current house’ case, well insulated building envelope and several low-carbon devices are applied, and carbon emission for construction accounts for 20% of the total carbon emission. On the contrary, the carbon emission of construction in ‘reference house’ just account for about 7% of total carbon emission. Comparing with ‘reference house’ case, the value of ‘current house’ case in the initial stage of construction is not much higher than that of ‘reference house’ case, but the carbon emission of operation is significantly reduced. The fenestration system requires to be replaced after 30 years later. The replacement of building components in ‘current house’ would result in more carbon emission than in ‘reference house’. In the final stage, the metal frame of ‘current house’ is worth to be recycled during demolition.

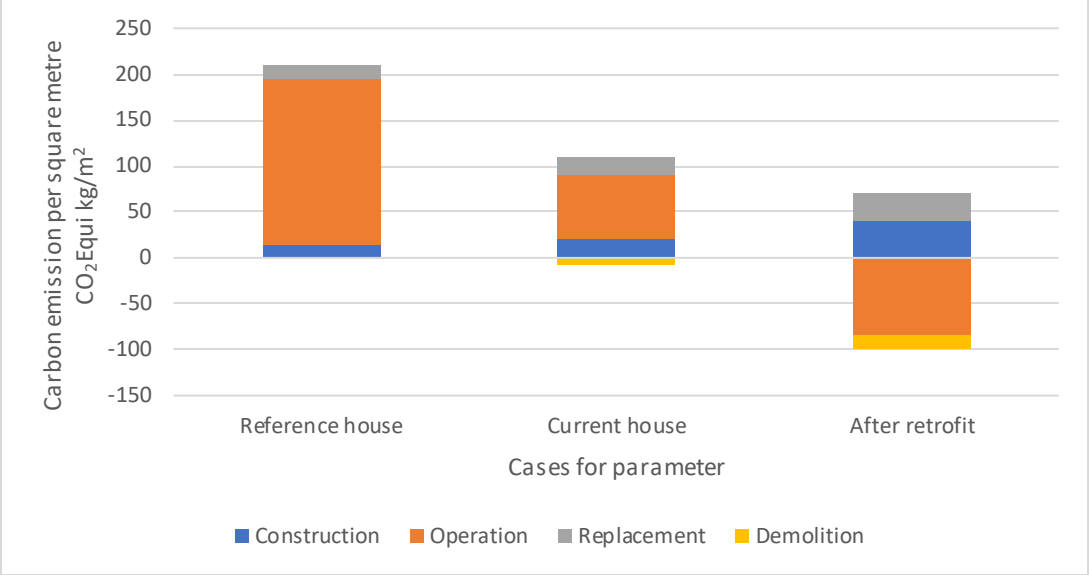


Figure 5.40 Carbon emission per square metre under various parameters

The 'After retrofit' case applied 3kW photovoltaic panels. Because photovoltaic panels have very high carbon emission value, the carbon emission in the initial construction stage is over two times than that of 'reference house' case as shown in Figure 5.40. The calculation assumes that the life of the photovoltaic panel is 20 years. And PV panels require to replaced two times during whole 60 years operation phase. Therefore, the carbon emission value of 'After retrofit' in the stage of construction and replacement is relatively high. However, the recycling of PV panel in the final stage can compensate part of the carbon emission. The 'After retrofit' case enjoys more potential on reduction of carbon emission through solar power generation.

It is worth mentioning that there were several limits on current simulation. Firstly, the simulation just covers some of the building components, excluding the decoration, water consumption and other items. In additions, the database is totally different in various regions. Furthermore, the simulation cannot consider the environmental impacts from the factory manufacture. All the above

factors would have a great impact on the actual carbon emissions of the Eco-house. Thus, the above assessment can only provide empirical evidence on the carbon emissions of various cases.

5.6. The construction experience of Eco-house in Wuhan

Before the start of this project, the project partner planned to construct the Eco-house in half a year and satisfy all requirements. From mid-2017 to now, more than 2 years later, the house is still under construction. It is worth addressing the issues causing the progress delay and unexpected performance.

The main issue was that the house project was never pursued to detail design. Before the project started, the Building Information Model (BIM) platform had been selected to let every stakeholder participate in every stage of the project. However, the BIM platform is not widely used in China, especially for budget building. The platform is too novel to consolidate the process of integration. The designer, construction companies and other partners have limited experience of the BIM platform. Thus, at the beginning of the project, learning and using the BIM platform took too much attention and time. Because of the limited knowledge of the BIM platform, the design process would not refine all the details of Eco-house. BIM platform is always the main barrier to communication.

The Eco-house is regarded as an example of a rural house in China. The construction company did not have too much experience on low-carbon prefabricated house. The benefits of prefabrication are mitigated. Many decisions were made on site by the site manager rather than communicating

with the UK part. This action not only increased capital costs, but also led to several flaws between components and technologies.

The poor-quality assembling is another issue that led to another problem, air infiltration. Air leakage accounts for 20% of heat loss. However, the air leakage identification needs extra time and labour cost. In addition, the retrofits on the air leakage are complicated for the construction company without more professional staff. The investor of Eco-house would not be eager to pay extra money for such a small and invisible flaw, as the air leakage is not directly visible to users. Thus, there would be not enough attention paid to project details.

In summary, the time spent on the detailed design and contacting can promise the basic performance of Eco-house. The construction company and project partners accumulated a lot of experience on sustainable buildings. From this house, there remain substantial concept and knowledge differences between different stakeholders. Fortunately, all the stakeholders are willing to learn new things from this project. As for future development, the construction industry should concentrate on the link between designers and construction teams.

5.7. Limitations

The main limitation of the research on Eco-house is its short duration. The current long-term monitoring just covers the period from April to September without wintertime. Further monitoring work should be done to test the performance of the Eco-house during winter. More thermocouples should be introduced into the interior space. Introducing other sensors such as an

anemometer and pyranometer would help to increase the accuracy of monitoring in the Eco-house.

The time taken for experimental testing and the number of trips to Wuhan were both limited. From 2017-2019, I went to Wuhan 5 times for testing during British holidays. The duration of testing in Wuhan is less than 40 days. There were limited opportunities to perform tests and investigations. Because of insufficient communication, the process of construction was delayed. And in the context of COVID-19, the construction plan has been delayed and postponed. Thus, the construction of the Eco-house has not been finished before the date of thesis submission. The actual energy-saving performance of Eco-house has not been tested. In addition, the Eco-house is still under construction. The total cost of the Eco-house has not been summarized.

5.8. Conclusion

The Eco-house was designed as an example building for the Chinese rural area in Wuhan. Several innovative technologies are applied to achieve a reduction in energy consumption. The house utilizes several passive and active design features for a better interior comfort environment.

Most on-site data were collected in April 2018. The analysis covers the thermal parameter tests on most of the building components. The results reveal that most building components can satisfy the initial aims and have relatively good insulation performances. And some of the building components require further retrofit in the future. From long-term testing, the interior temperature above

30°C occurs for less than 20% of the time during the summer. In addition, due to the retrofit operation in the future, the air infiltration would reduce greatly.

According to the simulation results, the ‘current house’ can achieve about 19 kWh/m^2 and 14kWh/m^2 for heating and cooling loads, respectively. Compared with the ‘reference house’, the performance of the current house is much better. The retrofit plan is essential to reduce the energy consumption of the Eco-house in Wuhan.

6. Conclusions and future work

6.1. Conclusions

This research is to investigate the potential energy-saving capability of low-carbon technologies and Eco-house. In the first half of the thesis, the contents are about the statements of prefabricated components separately. The prototype includes the novel window heat recovery ventilator system, and photovoltaic vacuum glazing. Through the investigations, the thermal performance of the prototypes has been presented. In the other half of the thesis, the contents are about the design and construction process of the Eco-house in Wuhan. Reasonable design and construction process of the Eco-house are presented. The last section is to analyse the thermal performance of the Eco-house to identify the energy saving potential of prefabricated house.

Unlike conventional heat recovery ventilator systems, the novel WHRV system enjoys advantages as following: easy manufacturing, convenient maintenance, and no cross contamination. Through experimental investigation, when the air velocities ranged from 1.24 to 2.45 m/s, the effectiveness of unit ranged from 43% to 59%. Furthermore, this unit is a compact and light device which can achieve low level in noise and could be prefabricated into a window frame.

Introducing the energy efficient window is crucial to reducing energy consumption and carbon emissions. The proposed PV VG-4L does not only have much better thermal insulation performance than conventional glazing but also has the ability to generate DC power. The U-value of the proposed glazing

system is about 0.58 W/(m^2K). At average solar irradiance of 500 W/m^2, the PV VG-4L can generate electricity at a level of 12 W/m^2.

Sustainable buildings are capable of meeting even the most stringent demands for aesthetics and architecture. Eco-house considers the sustainable design to construct and operate a building with as much as natural resources. The detailed consideration and preparation are necessary before on-site construction. The passive strategies should be considered in order to use minimum numbers of active devices. Furthermore, the monitoring devices installed in Eco-houses would be another future-oriented opportunity for the Chinese building industry. On-site analysis data was tested in April 2018. The analysis covers the thermal parameter tests on most of the building components. The results reveal that most building components of Eco-house can satisfy the initial aims and have good performance. But some of the building components require further retrofit in the future. According to the simulation results, the 'current house' can achieve about 19 kWh/m^2 and 14 kWh/m^2 for heating and cooling loads, respectively. After the retrofit, the Eco-house can satisfy the requirements of Passivhaus Standards. The retrofit plan is essential to reduce the energy consumption of the Eco-house in the future.

The analysis of the data obtained from overall tests for the Eco-house has become evidence that environmental factors and quality of construction have a great impact on energy-saving performances. The components of the Eco-house in Wuhan have better thermal performances than conventional houses in suburban areas. From long-term testing, interior temperatures above 30 °C occurs less than 20% of the time during summer. The thermographic images

verified some of the assumptions from the earlier tests. The lack of accuracy and workmanship is demonstrated by the obvious thermal bridge. The responses from this project show the pressure for greater expertise in the manufacture and construction of sustainable buildings.

6.2. Future work

The thesis has discussed several prefabricated low-carbon prototypes. Due to time constraints, there are a number of outlooks for future work to resolve the limitations of this study, including:

- The current long-term monitoring just covers the period from April to September without wintertime. Further monitoring work should be done to test the performance of the Eco-house during winter. More thermocouples should be introduced into the interior space.
- The Eco-house in Wuhan has not been occupied. It is quite difficult to evaluate the impacts from occupants. In the future, the research should introduce various tenants from different backgrounds. Through comparison, the result would be useful in assessing the impacts of living habits on building energy consumption.
- A smart home refers to a house equipped with smart technology designed to provide users with tailor-made services. Smart technologies make it possible to monitor, control and support residents, thereby improving the quality of life and promoting independent living. The building intelligent control systems can help occupants to control and manage the buildings to provide satisfying environments and energy-

saving patterns. Because the building intelligent control systems are interactive and autonomous, they are considered to be a key element to improve the coordination of zero emission building-ZEB operations and ultimately affect the overall building performance and integration. In the future, there would be several attempts in Eco-house to integrate the building intelligent control system to control the components of a house.

- The sources of data are just from the Eco-house in Wuhan. Extensive investigations are required on more sustainable buildings in China, including flats, plazas and so on.

REFERENCES

Ahmad, T., Thaheem, M. J. and Anwar, A. (2016) 'Developing a green-building design approach by selective use of systems and techniques', *Architectural Engineering and Design Management*, 12(1), pp. 29–50. doi: 10.1080/17452007.2015.1095709.

Ahuja, A. *et al.* (2010) 'Are house prices rising too fast in China?', *IMF working papers*, pp. 1–31.

Al-Waked, R. *et al.* (2013) 'CFD simulation of air to air enthalpy heat exchanger', *Energy conversion and management*. Elsevier, 74, pp. 377–385.

Alam, F. I. *et al.* (2017) 'Combining unmixing and deep feature learning for hyperspectral image classification', in *2017 International Conference on Digital Image Computing: Techniques and Applications (DICTA)*. IEEE, pp. 1–8.

ASHRAE, A. S. (2013) 'Standard 84–2013, Method of Testing Air-To-Air Heat/Energy Exchangers', *American Society of Heating, Refrigerating and Air-Conditioning Engineers Inc., Atlanta*.

ASHRAE, A. S. (2016) 'Ventilation and Acceptable Indoor Air Quality in Residential Buildings', 2016.

Asimakopoulos, D. (1996) *Passive cooling of buildings*. Earthscan.

Baehr, H. D. and Stephan, K. (2011) 'Heat and mass transfer'. Springer.

Baetens, R., Jelle, B. P., Gustavsen, A., *et al.* (2010) 'Gas-filled panels for building applications: A state-of-the-art review', *Energy and Buildings*, 42(11), pp. 1969–1975. doi: https://doi.org/10.1016/j.enbuild.2010.06.019.

Baetens, R., Jelle, B. P., Thue, J. V., *et al.* (2010) 'Vacuum insulation panels for building applications: A review and beyond', *Energy and Buildings*, 42(2), pp. 147–172. doi: https://doi.org/10.1016/j.enbuild.2009.09.005.

Balaras, C. A. and Argiriou, A. A. (2002) 'Infrared thermography for building diagnostics', *Energy and buildings*. Elsevier, 34(2), pp. 171–183.

Baldini, L., Kim, M. K. and Leibundgut, H. (2014) 'Decentralized cooling and dehumidification with a 3 stage LowEx heat exchanger for free reheating', *Energy and Buildings*. Elsevier B.V., 76, pp. 270–277. doi: 10.1016/j.enbuild.2014.02.021.

Balvers, J. *et al.* (2012) 'Mechanical ventilation in recently built Dutch homes: technical shortcomings, possibilities for improvement, perceived indoor environment and health effects', *Architectural Science Review*. Taylor &

Francis, 55(1), pp. 4–14.

Bambara, J. and Athienitis, A. K. (2019) 'Energy and economic analysis for the design of greenhouses with semi-transparent photovoltaic cladding', *Renewable Energy*, 131, pp. 1274–1287. doi: https://doi.org/10.1016/j.renene.2018.08.020.

Bauwens, G. and Roels, S. (2014) 'Co-heating test: A state-of-the-art', *Energy and Buildings*, 82, pp. 163–172. doi: https://doi.org/10.1016/j.enbuild.2014.04.039.

Bekkouche, S. M. A. *et al.* (2011) 'Introduction to control of solar gain and internal temperatures by thermal insulation, proper orientation and eaves', *Energy and buildings*. Elsevier, 43(9), pp. 2414–2421.

Berardi, U. (2016) 'A cross-country comparison of the building energy consumptions and their trends', *Resources, Conservation and Recycling*. doi: 10.1016/j.resconrec.2016.03.014.

Bhagat, R. K. *et al.* (2020) 'Effects of ventilation on the indoor spread of COVID-19', *Journal of Fluid Mechanics*. Cambridge University Press, 903.

Bodansky, D. (1993) 'The United Nations framework convention on climate change: a commentary', *Yale J. Int'l L.* HeinOnline, 18, p. 451.

Bouchlaghem, N. (2000) 'Optimising the design of building envelopes for thermal performance', *Automation in Construction*. Elsevier, 10(1), pp. 101–112.

BROWN, R., KOSSON, R. and UNGAR, E. (1991) 'Design of the SHARE II monogroove heat pipe', in *26th Thermophysics Conference*. American Institute of Aeronautics and Astronautics (Fluid Dynamics and Co-located Conferences). doi: doi:10.2514/6.1991-1359.

Bunkley, N. (2018) *Joseph Juran, 103, Pioneer in Quality Control, Dies - The New York Times*, *The New York Times Company*. Available at: https://web.archive.org/web/20170906182706/http://www.nytimes.com/2008/03/03/business/03juran.html (Accessed: 16 November 2019).

Business, D. for (2020) *UK sets ambitious new climate target ahead of UN Summit*, *Climate change international action*. Available at: https://www.gov.uk/government/news/uk-sets-ambitious-new-climate-target-ahead-of-un-summit.

Cao, X. *et al.* (2014) 'A comparative study of environmental performance between prefabricated and traditional residential buildings in China', *Journal of Cleaner Production*. Elsevier Ltd, 109, pp. 131–143. doi: 10.1016/j.jclepro.2015.04.120.

Capeluto, I. G. (2003) 'Energy performance of the self-shading building envelope', *Energy and buildings*. Elsevier, 35(3), pp. 327–336.

Capeluto, I. G., Yezioro, A. and Shaviv, E. (2003) 'Climatic aspects in urban design—a case study', *Building and environment*. Elsevier, 38(6), pp. 827–835.

Carroll, D. T. (2006) 'Using LCA Methods to Evaluate the Ability of LEED® to Compare Green buildings', (August).

Chang, Y. *et al.* (2014) 'Disaggregated I-O LCA model for building product chain energy quantification: A case from China', *Energy and Buildings*, 72, pp. 212–221. doi: 10.1016/j.enbuild.2013.12.026.

Chen, Y. (2010) *Decision Making on Prefabrication Adoption and its Environmental Impact in Residential Concrete Buildings*. Tsinghua University.

Chiesa, G., Simonetti, M. and Grosso, M. (2014) 'A 3-field earth-heat-exchange system for a school building in Imola, Italy: Monitoring results', *Renewable Energy*, 62, pp. 563–570. doi: 10.1016/j.renene.2013.08.020.

Cho, J.-S. *et al.* (2019) 'Energy harvesting performance of bifacial and semitransparent amorphous silicon thin-film solar cells with front and rear transparent conducting oxide contacts', *Solar Energy Materials and Solar Cells*. Elsevier, 202, p. 110078.

Chris Woodford (2019) *How does heat insulation trap heat? - Explain that Stuff*. Available at: https://www.explainthatstuff.com/heatinsulation.html (Accessed: 16 November 2019).

Christian, J. E. *et al.* (2006) 'Energy Efficiency, SIPS, Geothermal, and Solar PV Used in Near Zero-Energy House.', *ASHRAE transactions*, 112(2).

ClimaGuard® N: insulating glass by Guardian Glass (no date). Available at: https://www.guardianglass.com/tr/en/products/brands/climaguard/n (Accessed: 22 November 2019).

Corgnati, S. P., Perino, M. and Serra, V. (2007) 'Experimental assessment of the performance of an active transparent façade during actual operating conditions', *Solar Energy*. Elsevier, 81(8), pp. 993–1013.

Cuce, E. (2016) 'Toward multi-functional PV glazing technologies in low/zero carbon buildings: Heat insulation solar glass - Latest developments and future prospects', *Renewable and Sustainable Energy Reviews*. Pergamon, 60, pp. 1286–1301. doi: 10.1016/j.rser.2016.03.009.

Cuce, E. (2018) 'Accurate and reliable U-value assessment of argon-filled double glazed windows: A numerical and experimental investigation', *Energy and Buildings*. Elsevier, 171, pp. 100–106.

Cuce, E. and Cuce, P. M. (2016) 'Vacuum glazing for highly insulating windows: Recent developments and future prospects', *Renewable and Sustainable Energy Reviews*. Elsevier, 54, pp. 1345–1347. doi: 10.1016/j.rser.2015.10.134.

Cuce, P. M. and Cuce, E. (2017) 'Toward cost-effective and energy-efficient heat recovery systems in buildings: Thermal performance monitoring', *Energy*. Elsevier, 137, pp. 487–494.

Cuce, P. M. and Riffat, S. (2015) 'A comprehensive review of heat recovery systems for building applications', *Renewable and Sustainable Energy Reviews*. Elsevier, 47, pp. 665–682. doi: 10.1016/j.rser.2015.03.087.

Damassa, T., Ge, M. and Fransen, T. (2014) 'The US greenhouse gas reduction targets'.

DCLG (2015) 'Sustainable and Secure Buildings Act 2004 Progress towards the Sustainability of the Building Stock in England : Fifth Parliamentary Report', (March), pp. 1–22.

Department for Business, E. & I. S. (2019) 'Digest of UK Energy Statistics 2019', (July), pp. 1–11.

Department for Communities and Local Government (2010) 'Code for Sustainable Homes', *Communities*, (November), p. 296. doi: ISBN 978 1 85946 331 4.

Dhital, P., Besant, R. W. and Schoenau, G. J. (1995) *Integrating run-around heat exchanger systems into the design of large office buildings*. American Society of Heating, Refrigerating and Air-Conditioning Engineers ….

Dodoo, A., Gustavsson, L. and Sathre, R. (2011) 'Primary energy implications of ventilation heat recovery in residential buildings', *Energy and Buildings*. Elsevier, 43(7), pp. 1566–1572.

Energy, D. F. O. R. and Sources, R. E. (2009) 'LOW ENERGY BUILDINGS IN EUROPE: CURRENT STATE OF PLAY, DEFINITIONS AND BEST PRACTICE', *Central European*, (September), pp. 1–18.

European Commission (2020) *2030 climate & energy framework*. Available at: https://ec.europa.eu/clima/policies/strategies/2030_en.

Fang, Y., Hyde, T. and Hewitt, N. (2010) 'The influence of emittance of low-emittance coating on the thermal performance of triple vacuum glazing', in *The second IASTED International conference on solar energy*, pp. 921–928.

Feist, W. *et al.* (2007) 'Passive house planning package 2007', *Specifications for Quality Approved Passive Houses, Technical Information PHI-2007/1 (E), Darmstadt, Passivhaus Institut (December 2007)*.

Feist, W. (2007) ‘What is a passive house’, *Passivhaus Institute*.

Feist, W. (2009) ‘Certification as “Quality Approved Passive House” Criteria for Non-Residential Passive House Buildings’, *Passivhaus-Institut: Darmstadt, Germany*.

Frostig, Y. and Thomsen, O. T. (2011) ‘Non-linear thermo-mechanical behaviour of delaminated curved sandwich panels with a compliant core’, *International Journal of Solids and Structures*. Elsevier, 48(14–15), pp. 2218–2237.

Gaan, S. and Sun, G. (2007) ‘Effect of phosphorus and nitrogen on flame retardant cellulose: a study of phosphorus compounds’, *Journal of Analytical and Applied Pyrolysis*. Elsevier, 78(2), pp. 371–377.

Gan, G. and Riffat, S. B. (1998) ‘A numerical study of solar chimney for natural ventilation of buildings with heat recovery’, *Applied Thermal Engineering*. Elsevier, 18(12), pp. 1171–1187.

Gendebien, S., Bertagnolio, S. and Lemort, V. (2013) ‘Investigation on a ventilation heat recovery exchanger: Modeling and experimental validation in dry and partially wet conditions’, *Energy and Buildings*, 62, pp. 176–189. doi: 10.1016/j.enbuild.2013.02.025.

Gendebien, S., Parthoens, A. and Lemort, V. (2019) ‘Investigation of a single room ventilation heat recovery exchanger under frosting conditions: Modeling, experimental validation and operating strategies evaluation’, *Energy and Buildings*. Elsevier, 186, pp. 1–16.

Ghazi, S. and Ip, K. (2014) ‘The effect of weather conditions on the efficiency of PV panels in the southeast of UK’, *Renewable energy*. Elsevier, 69, pp. 50–59.

Ghiaus, C. and Inard, C. (2004) ‘2 Energy and environmental issues of smart buildings’. Citeseer.

Glass, J., Dainty, A. R. J. and Gibb, A. G. F. (2008) ‘New build: Materials, techniques, skills and innovation’, *Energy Policy*, 36(12), pp. 4534–4538. doi: 10.1016/j.enpol.2008.09.016.

Gong, Y. and Song, D. (2015) ‘Life cycle building carbon emissions assessment and driving factors decomposition analysis based on LMDI-A case study of Wuhan city in China’, *Sustainability (Switzerland)*, 7(12), pp. 16670–16686. doi: 10.3390/su71215838.

Granadeiro, V. *et al.* (2013) ‘Automation in Construction Building envelope shape design in early stages of the design process : Integrating architectural design systems and energy simulation’, *Automation in Construction*. Elsevier B.V., 32, pp. 196–209. doi: 10.1016/j.autcon.2012.12.003.

Graves, H. *et al.* (2001) *Cooling buildings in London: overcoming the heat island*. BREPress.

Haase, M. and Amato, A. (2009) 'An investigation of the potential for natural ventilation and building orientation to achieve thermal comfort in warm and humid climates', *Solar Energy*, 83(3), pp. 389–399. doi: 10.1016/j.solener.2008.08.015.

Harris, D. J. and Dudek, S.-M. (1997) 'Heat losses from suspended timber floors', *Building Research & Information*. Taylor & Francis, 25(4), pp. 226–233.

Harvie-Clark, J. *et al.* (2019) 'How loud is too loud? noise from domestic mechanical ventilation systems', *International Journal of Ventilation*. Taylor & Francis, 18(4), pp. 303–312.

Hezhev, T. A. *et al.* (2018) 'Fire resistant fibre reinforced vermiculite concrete with volcanic application.', *Magazine of Civil Engineering*, 82(6).

HM Government (2010) 'NBS 2010b The Building Regulations 2010 For England and Wales, Part F', *The Building Regulations 2010*, (October), p. 61. doi: Approved Document L1.

Hong, J. *et al.* (2018) 'Barriers to promoting prefabricated construction in China: A cost–benefit analysis', *Journal of Cleaner Production*, 172, pp. 649–660. doi: https://doi.org/10.1016/j.jclepro.2017.10.171.

Hurtado, P. L. *et al.* (2016) 'A review on the properties of cellulose fibre insulation', *Building and environment*. Elsevier, 96, pp. 170–177.

Infiltration, A. and Centre, V. (2012) 'Methods and techniques for airtight buildings Contributed Report 14'.

Institue, P. H. (2021) *Windows*, *Certified Component Database*. Available at: https://database.passivehouse.com/en/components/list/window.

Institute, P. H. (2017) *Certified Passive House component*. Available at: https://passiv.de/alte_komponentendatenbank/files/pdf/zertifikate/zd_interpane_iPlus3CE_en.pdf (Accessed: 22 November 2019).

Iyengar, K. (2015) *Sustainable Architectural Design: An Overview*. Routledge. Available at: https://books.google.com/books?hl=en&lr=&id=hbRhCQAAQBAJ&pgis=1.

Jack, R. *et al.* (2018) 'First evidence for the reliability of building co-heating tests', *Building Research & Information*. Taylor & Francis, 46(4), pp. 383–401.

Jani, D. B., Mishra, M. and Sahoo, P. K. (2016) 'Solid desiccant air conditioning - A state of the art review', *Renewable and Sustainable Energy Reviews*. Elsevier, 60, pp. 1451–1469. doi: 10.1016/j.rser.2016.03.031.

Jelle, B. P. (2011) 'Traditional, state-of-the-art and future thermal building insulation materials and solutions – Properties, requirements and possibilities', *Energy and Buildings*, 43(10), pp. 2549–2563. doi: https://doi.org/10.1016/j.enbuild.2011.05.015.

Jelle, B. P. *et al.* (2012) 'Fenestration of today and tomorrow: A state-of-the-art review and future research opportunities', *Solar Energy Materials and Solar Cells*, 96, pp. 1–28. doi: https://doi.org/10.1016/j.solmat.2011.08.010.

Jelle, B. P., Kalnæs, S. E. and Gao, T. (2015) 'Low-emissivity materials for building applications: A state-of-the-art review and future research perspectives', *Energy and Buildings*. Elsevier, 96, pp. 329–356.

Juodvalkis, J. *et al.* (2011) 'Rotary heat pump', *Mechanics*, 17(5), pp. 535–539.

Kalnæs Simen Edsjøand Jelle, B. P. (2014) 'Vacuum insulation panel products: A state-of-the-art review and future research pathways', *Applied Energy*, 116, pp. 355–375. doi: https://doi.org/10.1016/j.apenergy.2013.11.032.

Kalnæs Simen Edsjøand Jelle, B. P. (2015) 'Phase change materials and products for building applications: A state-of-the-art review and future research opportunities', *Energy and Buildings*, 94, pp. 150–176. doi: https://doi.org/10.1016/j.enbuild.2015.02.023.

Kamal, A. *et al.* (2000) 'Axonal transport of amyloid precursor protein is mediated by direct binding to the kinesin light chain subunit of kinesin-I', *Neuron*. Elsevier, 28(2), pp. 449–459.

Karamanos, A., Hadiarakou, S. and Papadopoulos, A. M. (2008) 'The impact of temperature and moisture on the thermal performance of stone wool', *Energy and Buildings*, 40(8), pp. 1402–1411. doi: https://doi.org/10.1016/j.enbuild.2008.01.004.

Khamporn, N. and Chaiyapinunt, S. (2014) 'An investigation on the human thermal comfort from a glass window', *Engineering Journal*, 18(1), pp. 25–44.

Kinmond, W. (2019) 'China Overview', in *No Dogs in China*, pp. 195–227. doi: 10.3138/9781487589264-052.

Klems, J. H. (1979) 'A CALIBRATED HOTBOX FOR TESTING WINDOW SYSTEMS? CONSTRUCTION, CALIBRATION, AND MEASUREMENTS ON PROTOTYPE HIGH-PERFORMANCE WINDOWS'.

Kontogeorgos, D. A. *et al.* (2016) 'Experimental investigation of the fire resistance of multi-layer drywall systems incorporating Vacuum Insulation Panels and Phase Change Materials', *Fire Safety Journal*. Elsevier, 81, pp. 8–16.

Kragh, J. *et al.* (2007) 'New counter flow heat exchanger designed for

ventilation systems in cold climates', *Energy and Buildings*, 39(11), pp. 1151–1158. doi: https://doi.org/10.1016/j.enbuild.2006.12.008.

Kragh, J., Rose, J. and Svendsen, S. (2005) 'Mechanical ventilation with heat recovery in cold climates', in *Proceedings of the 7th Symposium on Building Physics in the Nordic Countries. Vol. Bind*.

Li, B., Wild, P. and Rowe, A. (2019) 'Performance of a heat recovery ventilator coupled with an air-to-air heat pump for residential suites in Canadian cities', *Journal of Building Engineering*. Elsevier, 21, pp. 343–354.

Liu, X. (2012) 'Benefits of vacuum insulation panels in building envelopes for warm-keeping'.

Liu, Z. and Ying, H. (2009) 'Prefabrication construction in residential building of Vanke real estate company China', in *Management and Service Science, 2009. MASS'09. International Conference on*. IEEE, pp. 1–4.

Lorenzati, A. *et al.* (2016) 'Experimental and numerical investigation of thermal bridging effects of jointed Vacuum Insulation Panels', *Energy and Buildings*, 111, pp. 164–175. doi: https://doi.org/10.1016/j.enbuild.2015.11.026.

Lu Meijun, Wang Guixiu and Fan Yi (2009) 'Optimized design of energy-saving renovation schemes for existing rural houses in cold regions'.

M. Taylor; L. Morgan (2011) 'Ventilation and good indoor air quality in low energy homes Finding proven good practice', p. 88.

Maderuelo-Sanz, R. *et al.* (2016) 'Influence of the microstructure in the acoustical performance of consolidated lightweight granular materials', *Acoustics Australia*. Springer, 44(1), pp. 149–157.

Manz, H. and Huber, H. (2000) 'Experimental and numerical study of a duct/heat exchanger unit for building ventilation', *Energy and Buildings*, 32(2), pp. 189–196. doi: 10.1016/S0378-7788(00)00043-8.

Mardiana-Idayu, A. and Riffat, S. B. (2012) 'Review on heat recovery technologies for building applications', *Renewable and Sustainable Energy Reviews*, 16(2), pp. 1241–1255. doi: 10.1016/j.rser.2011.09.026.

MCRMA (2006) 'CONVENTIONS FOR CALCULATING U-VALUES, f-VALUES AND -VALUES FOR METAL CLADDING SYSTEMS USING TWO- AND THREE- DIMENSIONAL THERMAL CALCULATIONS', (18).

Memon, S. (2019) 'Advancements in Smart Windows: Triple Vacuum Insulated Glazing for Sustainable Low-Carbon Buildings', *World Sustainable Energy Days 2019*. World Sustainable Energy Days.

Ministry of Housing and Urban-Rural Development in China (2015) *Technical*

Guidelines for Passive Ultra-low Energy Green Buildings (Trial).

Morrissey, J., Moore, T. and Horne, R. E. (2011) 'Affordable passive solar design in a temperate climate: An experiment in residential building orientation', *Renewable Energy*. Elsevier, 36(2), pp. 568–577.

Mujeebu, M. A., Ashraf, N. and Alsuwayigh, A. H. (2016) 'Effect of nano vacuum insulation panel and nanogel glazing on the energy performance of office building', *Applied energy*. Elsevier, 173, pp. 141–151.

Nasif, M. *et al.* (2010) 'Membrane heat exchanger in HVAC energy recovery systems, systems energy analysis', *Energy and Buildings*. Elsevier, 42(10), pp. 1833–1840.

Nasif, M. S. (2015) 'Effect of Utilizing Different Permeable Material in Air-To-Air Fixed Plate Energy Recovery Heat Exchanger on Energy Saving', *ARPN J. Eng. Appl. Sci*, 10, pp. 10153–10158.

National Energy Fundamentals and Management Standardization Technical Committee (2010) *The minimum allowable value of the energy efficiency and energy efficiency grades for room air conditioners*.

NBS (2012) *China Energy Statistical Yearbook 2011*. Beijing, China. doi: http://www.stats.gov.cn/tjsj/ndsj/2011/indexeh.htm.

Nóbrega, C. E. L. and Brum, N. C. L. (2009) 'Modeling and simulation of heat and enthalpy recovery wheels', *Energy*. Elsevier Ltd, 34(12), pp. 2063–2068. doi: 10.1016/j.energy.2008.08.016.

Ochoa, C. E. and Capeluto, I. G. (2008) 'Strategic decision-making for intelligent buildings: Comparative impact of passive design strategies and active features in a hot climate', *Building and Environment*. Elsevier, 43(11), pp. 1829–1839.

Okeil, A. (2010) 'A holistic approach to energy efficient building forms', *Energy and buildings*. Elsevier, 42(9), pp. 1437–1444.

Olgyay, V. (1967) 'Bioclimatic orientation method for buildings', *International Journal of Biometeorology*. Springer, 11(2), pp. 163–174.

Omer, A. M. (2013) 'Direct expansion ground source heat pumps for heating and cooling', *International Research Journal on Engineering*, 1(2), pp. 27–48. Available at: http://www.apexjournal.org.

Ormandy, D. and Ezratty, V. (2016) 'Thermal discomfort and health: protecting the susceptible from excess cold and excess heat in housing', *Advances in Building Energy Research*. Taylor & Francis, 10(1), pp. 84–98.

Pan, W., Gibb, A. and Dainty, A. (2005) 'Offsite modern methods of construction

in housebuilding: perspectives and practices of leading UK housebuilders', *Loughboroough: Buildoffsite*.

Panjehpour, M., Abang Ali, A. A. and Voo, Y. L. (2013) 'Structural Insulated Panels: Past, Present, and Future.', *Journal of Engineering, Project & Production Management*. Citeseer, 3(1).

Park, H. I. and Oh, C. N. (2014) 'Apparatus for controlling interior temperature of a vehicle and method thereof'. Google Patents.

Patidar, S. *et al.* (2011) 'Statistical techniques to emulate dynamic building simulations for overheating analyses in future probabilistic climates', *Journal of Building Performance Simulation*. Taylor & Francis, 4(3), pp. 271–284.

Paul, W. L. and Taylor, P. A. (2008) 'A comparison of occupant comfort and satisfaction between a green building and a conventional building', *Building and Environment*, 43(11), pp. 1858–1870. doi: https://doi.org/10.1016/j.buildenv.2007.11.006.

Pereira, D. *et al.* (2016) 'Fire performance of sandwich wall assemblies', *Composites Part B: Engineering*. Elsevier, 93, pp. 123–131.

Pilkington energiKare™ Triple (no date). Available at: https://www.pilkington.com/en-gb/uk/products/product-categories/thermal-insulation/pilkington-energikare-range/pilkington-energikare-triple (Accessed: 22 November 2019).

Pilkington Optifloat™ Clear (no date). Available at: https://www.pilkington.com/en-gb/uk/products/product-categories/thermal-insulation/pilkington-optifloat-clear (Accessed: 22 November 2019).

Pilkington Spacia™ (no date). Available at: https://www.pilkington.com/en-gb/uk/products/product-categories/thermal-insulation/pilkington-spacia#benefits (Accessed: 22 November 2019).

POINT, K. E. Y. (2015) 'Arthur Lyons with AHR Architects (formerly Aedas)'.

Qi Xu, Saffa Riffat, S. Z. (2019) 'Review of Heat Recovery Technologies for Building Applications', *Energies*. doi: 10.3390/en12071285.

Qiu, C. and Yang, H. (2020) 'Daylighting and overall energy performance of a novel semi-transparent photovoltaic vacuum glazing in different climate zones', *Applied Energy*, 276, p. 115414. doi: https://doi.org/10.1016/j.apenergy.2020.115414.

Qiu, C., Yang, H. and Zhang, W. (2019) 'Investigation on the energy performance of a novel semi-transparent BIPV system integrated with vacuum glazing', in *Building Simulation*. Springer, pp. 29–39.

Radhi, H. (2008) ‘A systematic methodology for optimising the energy performance of buildings in Bahrain’, *Energy and Buildings*. Elsevier, 40(7), pp. 1297–1303.

Remes, Z. *et al.* (2019) ‘Optoelectronic Properties of Hydrogenated Amorphous Substoichiometric Silicon Carbide with Low Carbon Content Deposited on semi-Transparent Boron-Doped Diamond’, *physica status solidi (a)*. Wiley Online Library.

Ren, Y., Xiong, C. and Yuan, Y. (2012) ‘House price bubbles in China’, *China Economic Review*. Elsevier, 23(4), pp. 786–800.

Roberts, S. (2008) ‘Altering existing buildings in the UK’, *Energy Policy*. Elsevier, 36(12), pp. 4482–4486. doi: 10.1016/J.ENPOL.2008.09.023.

Robinson, P. D. and Hutchins, M. G. (1994) ‘Advanced glazing technology for low energy buildings in the UK’, *Renewable Energy*. Elsevier, 5(1–4), pp. 298–309.

Ruivo, C. R., Angrisani, G. and Minichiello, F. (2015) ‘Influence of the rotation speed on the effectiveness parameters of a desiccant wheel: An assessment using experimental data and manufacturer software’, *Renewable Energy*. Elsevier Ltd, 76, pp. 484–493. doi: 10.1016/j.renene.2014.11.068.

Sadineni, S. B., Madala, S. and Boehm, R. F. (2011) ‘Passive building energy savings: A review of building envelope components’, *Renewable and Sustainable Energy Reviews*. Elsevier, 15(8), pp. 3617–3631.

Salimova, V., Gaan, S. and Nazarov, D. (2008) ‘Effect of chemical environment of organophosphorus compounds on thermal decomposition of cellulose’, *Cellulose*, 18, p. 0.

Sauer, H. J. and Howell, R. H. (1981) ‘Promise and potential of air-to-air energy recovery systems’, *International Journal of Refrigeration*. Elsevier, 4(4), pp. 182–194.

Schackow, A. *et al.* (2014) ‘Mechanical and thermal properties of lightweight concretes with vermiculite and EPS using air-entraining agent’, *Construction and Building Materials*, 57, pp. 190–197. doi: https://doi.org/10.1016/j.conbuildmat.2014.02.009.

Seagren, J. (2019) ‘MVHR buyers guide’, *ReNew: Technology for a Sustainable Future*. JSTOR, (147), pp. 70–73.

Seo, J. *et al.* (2011) ‘Thermal performance analysis according to wood flooring structure for energy conservation in radiant floor heating systems’, *Energy and Buildings*. Elsevier, 43(8), pp. 2039–2042.

Serajian Tehrani, R. *et al.* (2019) ‘The Influence of Tilt Angle on Heat Loss and

Solar Gain in Triple Vacuum Glazing', *International Journal of Advanced Studies in Humanities and Social Science*. Sami Publishing Company, 8(2, pp. 126-222.), pp. 187–194.

SHU, Z. and Chen, Q. (2007) 'Fire Performances of Bamboo Floor Covering Compared to Wood Floor Covering by Cone Calorimeter Test [J]', *Fire Safety Science*, 3, p. 5.

Sidanius, J. *et al.* (2000) 'Social dominance orientation, anti-egalitarianism and the political psychology of gender: an extension and cross-cultural replication', *European Journal of Social Psychology*. Wiley Online Library, 30(1), pp. 41–67.

Sinnott, D. and Dyer, M. (2012) 'Air-tightness field data for dwellings in Ireland', *Building and Environment*. Elsevier, 51, pp. 269–275.

Song, J. *et al.* (2005) 'Considering prework on industrial projects', *Journal of construction engineering and management*. American Society of Civil Engineers, 131(6), pp. 723–733.

Sotayo, A., Green, S. and Turvey, G. (2015) 'Carpet recycling: a review of recycled carpets for structural composites', *Environmental Technology & Innovation*. Elsevier, 3, pp. 97–107.

Steinhardt, D. and Manley, K. (2016) 'Exploring the beliefs of Australian prefabricated house builders', *Construction Economics and Building*. UTS ePress, 16(2), pp. 27–41.

Sutcu, M. (2015) 'Influence of expanded vermiculite on physical properties and thermal conductivity of clay bricks', *Ceramics International*, 41(2, Part B), pp. 2819–2827. doi: https://doi.org/10.1016/j.ceramint.2014.10.102.

Taleb, H. M. and Sharples, S. (2011) 'Developing sustainable residential buildings in Saudi Arabia: A case study', *Applied Energy*, 88(1), pp. 383–391. doi: 10.1016/j.apenergy.2010.07.029.

Tatematsu, K. *et al.* (2014) 'Influence of temperature and moisture on aging of glass wool', *Journal of Environmental Engineering*, 79, pp. 753–762.

Troppová, E. *et al.* (2015) 'Influence of temperature and moisture content on the thermal conductivity of wood-based fibreboards', *Materials and Structures*. Springer, 48(12), pp. 4077–4083.

Tu, R., Liu, X. H. and Jiang, Y. (2013) 'Performance comparison between enthalpy recovery wheels and dehumidification wheels', *International Journal of Refrigeration*. Elsevier Ltd and IIR, 36(8), pp. 2308–2322. doi: 10.1016/j.ijrefrig.2013.07.014.

Tzikopoulos, A. F., Karatza, M. C. and Paravantis, J. A. (2005) 'Modeling energy efficiency of bioclimatic buildings', *Energy and buildings*. Elsevier, 37(5),

pp. 529–544.

UKGBC (2019) *Net Zero Carbon Buildings: A Framework Definition*, *Advancing Net Zero*. Available at: https://goodhomes.org.uk/resource/guidance/net-zero-carbon-buildings-a-framework-definition (Accessed: 16 November 2019).

Villasmil, W., Fischer, L. J. and Worlitschek, J. (2019) 'A review and evaluation of thermal insulation materials and methods for thermal energy storage systems', *Renewable and Sustainable Energy Reviews*, 103, pp. 71–84. doi: https://doi.org/10.1016/j.rser.2018.12.040.

Waichal, P. (2018) 'HFP01 - fluxmeter, any experiences with sensitivity of the sensors to different outdoor consitions such as direct sun, rain, wind??'

Wang, S. *et al.* (2019) 'Urban-biased land development policy and the urban-rural income gap: Evidence from Hubei Province, China', *Land Use Policy*. Elsevier, 87, p. 104066.

White, J. A. (2014) 'An Investigation into the Parameters That Contribute to the Gap Between the Designed and As-Built Thermal Performance of British Housing', *PhD Thesis of University of Nottingham*, (April).

Whitmore II, S. M. (2015) 'LEGACY and DWELLING: The Role of Manufactured Housing in Central Appalachia'.

Xu, Q., Riffat, S. and Zhang, S. (2019) 'Review of Heat Recovery Technologies for Building Applications', *Energies*. Multidisciplinary Digital Publishing Institute, 12(7), p. 1285.

Yang, X. *et al.* (2010) 'A Comprehensive Review on the Development of Sustainable Energy Strategy and Implementation in China', *Sustainable Energy, IEEE Transactions on*. IEEE, 1(2), pp. 57–65. doi: 10.1109/TSTE.2010.2051464.

Zach, J. *et al.* (2013) 'Development of Thermal Insulating Materials on Natural Base for Thermal Insulation Systems', *Procedia Engineering*, 57, pp. 1288–1294. doi: https://doi.org/10.1016/j.proeng.2013.04.162.

Zea Escamilla, E. *et al.* (2018) 'Industrial or traditional bamboo construction? Comparative life cycle assessment (LCA) of bamboo-based buildings', *Sustainability*. Multidisciplinary Digital Publishing Institute, 10(9), p. 3096.

Zeng, C., Liu, S. and Shukla, A. (2017) 'A review on the air-to-air heat and mass exchanger technologies for building applications', *Renewable and Sustainable Energy Reviews*. Elsevier Ltd, 75(December 2016), pp. 753–774. doi: 10.1016/j.rser.2016.11.052.

Zero Carbon Hub (2016) *VENTILATION IN NEW HOMES*. Available at: https://www.zerocarbonhub.org/sites/default/files/resources/reports/ZCH_Vent

ilation.pdf.

Zhang, K. and Liao, P.-C. (2015) ‘Ontology of ground source heat pump’, *Renewable and Sustainable Energy Reviews*, 49, pp. 51–59. doi: 10.1016/j.rser.2015.04.021.

Zhang, X. *et al.* (2019) ‘Characterization of thermal decomposition and combustion for commercial flame-retardant rubber floor cloth in TG–FTIR and FPA’, *Journal of Thermal Analysis and Calorimetry*. Springer, 135(6), pp. 3453–3461.

Zhang, X., Platten, A. and Shen, L. (2011) ‘Green property development practice in China: Costs and barriers’, *Building and Environment*, 46(11), pp. 2153–2160. doi: 10.1016/j.buildenv.2011.04.031.

Zhang, X. and Skitmore, M. (2012) ‘Industrialized housing in China: a coin with two sides’, *International Journal of Strategic Property Management*. Vilnius Gediminas Technical University, 16(2), pp. 143–157.

Zhang, X., Skitmore, M. and Peng, Y. (2014) ‘Exploring the challenges to industrialized residential building in China’, *Habitat International*, 41, pp. 176–184. doi: 10.1016/j.habitatint.2013.08.005.

Zhang, X., Wu, Y. and Shen, L. (2012) ‘Application of low waste technologies for design and construction: A case study in Hong Kong’, *Renewable and Sustainable Energy Reviews*, 16(5), pp. 2973–2979. doi: 10.1016/j.rser.2012.02.020.

Zhang, Y. *et al.* (2017) ‘Impact of fiberizing method on physical properties of glass wool fibers’, *Journal of Non-Crystalline Solids*. Elsevier, 476, pp. 122–127.

ZHANG, Y., MO, J. and CHENG, R. (2015) ‘Developing a sustainable indoor air environment: Problems, considerations and suggestions’, *Chinese Science Bulletin*. Science China Press, 60(18), pp. 1651–1660.

Zhao, D.-X. *et al.* (2015) ‘Social problems of green buildings: From the humanistic needs to social acceptance’, *Renewable and Sustainable Energy Reviews*, 51, pp. 1594–1609. doi: https://doi.org/10.1016/j.rser.2015.07.072.

Zhong, K. and Kang, Y. (2009) ‘Applicability of air-to-air heat recovery ventilators in China’, *Applied Thermal Engineering*. Elsevier, 29(5), pp. 830–840.

Zhou, N. *et al.* (2019) ‘A roadmap for China to peak carbon dioxide emissions and achieve a 20% share of non-fossil fuels in primary energy by 2030’, *Applied Energy*, 239, pp. 793–819. doi: https://doi.org/10.1016/j.apenergy.2019.01.154.

Zuo, J. and Zhao, Z. Y. (2014) ‘Green building research-current status and future agenda: A review’, *Renewable and Sustainable Energy Reviews*. Elsevier, 30, pp. 271–281. doi: 10.1016/j.rser.2013.10.021.

APPENDIX

Appendix 1

Thermocouple	0 °C	100 °C
1	0.1	100.0
2	0.1	99.8
3	0.0	100.2
4	0.2	100.4
5	0.1	100.2
6	0.1	99.9
7	0.0	99.6
8	0.2	100.3
9	0.1	100.1
10	-0.1	100.3
11	0.0	99.8
12	0.1	100.1
13	0.2	100.1
14	0.0	100.1
15	-0.1	100.3
16	0.2	99.6
17	0.1	99.9
18	0.2	100.1

Appendix 2

Component	Equipment Used	Accuracy
Datalogger	DataTaker DT 85 with K-type thermocouples	±1.5°C
Thermostat	Timeguard ET05 Plug-In Electronic Thermostat	Temperature Range Control 0°C to 35°C
Electric consumption metre	Pinyi Electrical consumption and bill metre	-3.5% to +2.5%
Fan heater	2kW fan Heater	
Weather Station	Oregon Scientific -Pro Weather Station WMR200	< 15 mm/hr: +/-1 mm 15 mm to 9999 mm: +/-7%
Pyranometer Sensor	Kipp & Zonen SMP3 Pyranometer	Zero offset A: < 15 W/m² Zero offset B: < 5 W/m²

Appendix 3

		Date	14/04/2018	13/04/2018	12/04/2018	11/04/2018	10/04/2018	09/04/2018	08/04/2018
Temperature (K)	Mean interior temperature	Livingroom	30.28643	28.86253	29.03555	31.34054	28.26438	30.28049	28.07581
		Bedroom 1	31.59807	31.64099	28.10712	31.55754	29.25722	28.93942	28.33114
		Bedroom 2	28.86050	28.32729	29.96093	28.11195	29.48789	30.17041	29.29034
		Toilet	29.33790	31.15574	29.05233	29.86888	28.90115	31.89074	29.56074
	Mean interior temperature		30.02073	29.99664	29.03898	30.21973	28.97766	30.32026	28.81451
	Mean external temperature		14.37397	17.68162	16.33431	16.57555	20.15485	16.56828	18.49860
	Temperature Difference		15.64675	12.31502	12.70468	13.64418	8.82281	13.75198	10.31591
Power Usage (W)	Energy Usage (Wh)	Livingroom	31365	23522	24627	26042	17911	27583	19396
		Bedroom 1	14637	10977	11492	12153	8358	12872	9052
		Bedroom 2	12546	9409	9851	10417	7164	11033	7758
		Toilet	4182	3136	3284	3472	2388	3678	2586
		Total	62731	47045	49253	52084	35821	55166	38792
	Total		2614	1960	2052	2170	1493	2299	1616
	Solar Gain		191	337	367	319	178	365	232
	Total solar corrected		2804	2297	2419	2489	1671	2664	1848
	HLC (W/K)		167	159	162	159	169	167	157
	HLC Corrected (W/K)		179	187	190	182	189	194	179

15/04/2018	16/04/2018
30.05702	31.96523
30.32693	29.99940
30.46103	31.22963
28.97476	31.89197
29.95494	31.27156
20.37722	14.95861
9.57771	16.31294
17412	29409
8126	13724
6965	11763
2322	3921
34824	58817
1451	2451
393	304
1844	2754
151	150
193	169

Appendix 4

The calendar setting for weekdays (1-occupied; 0-unoccupied)

Kitchen Appliances	Livingroom Appliances	Livingroom Occupancy	Bedroom Appliances	Bedroom Occupancy	Heating or Cooling	Room Type
0	0	0	0	1	1	1
0	0	0	0	1	1	2
0	0	0	0	1	1	3
0	0	0	0	1	1	4
0	0	0	0	1	1	5
0	0	0	0	1	0	6
0	0	0	0	1	0	7
1	0	0	1	1	0	8
0	0	0	0	0	0	9
0	0	0	0	0	0	10
0	0	0	0	0	0	11
0	0	0	0	0	0	12
0	0	0	0	0	0	13
0	0	0	0	0	0	14
0	0	0	0	0	0	15
0	0	0	0	0	0	16
0	1	1	0	0	0	17
0	1	1	0	0	1	18
0	1	1	0	0	1	19
1	1	1	0	0	1	20
1	1	1	0	0	1	21
0	1	1	0	0	1	22
0	0	0	0	0	1	23
0	0	0	1	1	1	24
3h	5h	5h	2h	9h	12h	Total

The calendar setting for weekends (1-occupied; 0-unoccupied)

Kitchen Appliances	Livingroom Appliances	Livingroom Occupancy	Bedroom Appliances	Bedroom Occupancy	Heating or Cooling	Room Type
0	0	0	0	1	1	**1**
0	0	0	0	1	1	**2**
0	0	0	0	1	1	**3**
0	0	0	0	1	1	**4**
0	0	0	0	1	1	**5**
0	0	0	0	1	0	**6**
0	0	0	0	1	0	**7**
1	0	0	1	1	0	**8**
0	0	0	0	0	0	**9**
0	0	0	0	0	0	**10**
1	0	0	0	0	0	**11**
0	0	0	1	1	0	**12**
0	0	0	1	1	0	**13**
0	0	0	0	0	0	**14**
0	0	0	0	0	0	**15**
0	0	0	0	0	0	**16**
0	1	1	0	0	0	**17**
0	1	1	0	0	1	**18**
0	1	1	0	0	1	**19**
1	1	1	0	0	1	**20**
1	1	1	0	0	1	**21**
0	1	1	0	0	1	**22**
0	1	1	0	0	1	**23**
0	0	0	1	1	1	**24**
4h	6h	6h	4h	11h	12h	**Total**